

A Paleoclimatic and Paleooceano-
graphic Study in a Portion of the
Southern Ocean

A Senior Thesis submit-
ted by Michael A. Rosen
as partial requirement
for a Bachelor of Science
Degree in Geology/Miner-
alogy, Ohio State Univer-
sity.

May 29, 1980

Abstract

Nine deep-sea piston cores recovered along a north-south track from 58 S to 52 30'S at about 10 E were dated using Weaver's (1976) modification of McCollum's (1975) high latitude diatom zonation and paleomagnetic data. Deduced climatic fluctuations during the past five million years are based on Weaver's (1973) model for climatically related marine sedimentation and on the distribution of sediment types and unconformities in the nine piston cores.

Conditions during part of the interval from the Pliocene/Miocene transition (about 5.0 m.y. B.P.) were cool and are represented by unconformities, which resulted from the increased production of Antarctic Bottom Water. Climates that began warming before the Gilbert "b" event (4.14 m.y. to 3.97 m.y. B.P.) is represented by siliceous sediment, which continued accumulating until late Gilbert. Sometime after the beginning of the Gauss magnetic epoch (3.32 - 2.43m.y. B.P.) climate deteriorated and led to one or more episodes of regional scouring or nondeposition. By the end of the Olduvai magnetic event (1.86 - 1.71 m.y. B.P.) sediment began accumulating again.

From the end of the Olduvai until the present, climate and oceanographic conditions fluctuated but not as drastically as earlier and sediment accumulated throughout most of the area. The locus of erosion/nondeposition also shifted geographically to areas in the north and south of the study region in the Holocene and possibly the Pleistocene. The two

positions of erosion /nondeposition suggest the action of two bottom water masses, Antarctic Bottom Water and Circumpolar Deep Water.

Acknowledgments

I sincerely thank Paul Ciesielski for providing me with the opportunity to "get my feet wet" in the field of marine geology and for his constant and excellent efforts to teach me the tools of the trade. I also thank Michael Ledbetter for his professional assistance in providing the magnetic information for the study cores. Very special thanks are extended to David Elliot for suggestions and what must have often seemed an undue amount of patience during discussions and editing sessions. I thank Dr. Walter Sweet for valuable lessons in geology and learning opportunities; neither will soon be forgotten. In addition, I thank especially Ross Powell, William Zinsmeister and Tom DeVries, but also other members of the Institute of Polar Studies and the Department of Geology and Mineralogy at Ohio State for their helpful comments and suggestions. Special thanks are given to Fred Myers who often endured hardships along with me. Also I would like to thank my other friends, above all Anne, who tolerated my "ill humor" during some of the lower points of this research effort.

Finally, I would like to thank the Honors Committee of the College of Arts and Sciences, especially Dean C. Grey Austin. Without their financial support the completion of this project would not have been possible.

List of Figures

Figure 1	Southern Ocean silicoflagellate paleotemperature curve formed by plotting ratios of the genera <i>Dictyocha</i> and <i>Distephanus</i> against surfact water temperatures (after Ciesielski, 1974).....	3
Figure 2	Model explaining the spatial and temporal distribution of IRD in sediments from the Southern Ocean (after Watkins, 1974).....	5
Figure 3	Case I of a model to explain the spatial and temporal occurrence of IRD in the vicinity of the Ross Sea (after Fillon, 1977).....	7
Figure 4	Case II of a model to explain the spatial and temporal occurrence of IRD in the vicinity of the Ross Sea (after Fillon, 1977).....	8
Figure 5	Circulation patterns in the Southern Ocean today (after Treshenikov, 1964).....	10
Figure 6	Generalized cross-section of the Southern Ocean showing relative position with depth of dominant water masses (after Gordon, 1967).....	11
Figure 7	Generalized recent sediment distribution of the Southern Ocean (after, Goodell, 1973).	14
Figure 8	Map of Antarctica and the surrounding Southern Ocean. The heavy lines on the right side of the map include the general region of study. The line A-A' represents the approximate position of the core track.....	19
Figure 9	Map of the study region which includes a number of cores not considered in this investigation. Cores in this study occur along the northern section of the western core track and are numbered.....	24
Figure 10	A portion of the cruise 11 course of the <u>Islas Orcadas</u> which includes the study cores.....	25
Figure 11a - 11e	Cruise profiles showing the relationship of cores (excluding I01176-67) to the immediate topography. Vertical scale is given on the left as depth in fathoms. Horizontal scale varies.....	26-28
Figure 12	Generalized representation of contemporary surface circulation in the study region (after Treshinikov, 1964).....	29
Figure 13	Generalized recent sediment distribution in the study area (after Goodell, 1973).....	31

List of Figures (cont.)

Figure 14	Standard Magnetic Time Scale used in this study (after Opdyke, 1972).....	34
Figure 15	Regional Magnetic correlations and lithologies of the nine cores along the cruise track.....	42
Figure 30	Graphic plot of tops (+) and bases (0) of fossils in a SRS and a sedimentary section.....	73
Figure 31	Illustration of the graphic solution to motion problems.....	74
Figure 32	Graphic plot of tops and bases of fossils with a LOC.....	77
Figure 34	Graphic plot of stratigraphic events and a LOC exhibiting the "plateau" effect due to omission of strata or inadequacy of the sampling coverage.....	85

List of Tables

Table I	Latitude, longitude and depth of study cores.....	21
Table II	Bottom Topography in the vicinity of the cores.....	22
Table III	Biostratigraphic zone positions.....	37
Table IV	Magnetic polarity changes.....	82
Table V	Biostratigraphic ranges.....	83

Table of Contents

i.	Abstract.....	ii
ii.	Acknowlegments.....	iv
I.	Introduction.....	1
II.	Introduction to Study Area.....	20
III.	Methods.....	32
IV.	Biostratigraphic Results and Problems.....	36
V.	Interpretation and Discussion.....	43
VI.	Summary.....	55
VII.	Appendix I.....	57
VIII.	Appendix II.....	72
IX.	Bibliography.....	102

INTRODUCTION

That the marine sedimentary record of the Southern Ocean contains some historical evidence of paleoclimatic conditions has long been recognized. From the findings of Murray (1876), made possible by the pioneering voyage of the H.M.S. Challenger, to the information gathered by the Soviet vessel Ob and finally to the data collected on numerous American cruises, principally the USNS Eltanin and others, evidence has accumulated that points to pronounced effects on marine sedimentary characteristics resulting from climatic change. The diversity of these effects has been demonstrated.

Biologic components of deep sea sediments, particularly the preserved tests of siliceous and calcareous microorganisms, provide one such means of inferring paleoclimatic conditions. Blair (1965) has shown that provincialism among foraminifera assemblages corresponds to major oceanographic boundaries, the geographic distributions of which are partially controlled by climatic conditions. Ciesielski (1974) found similar climatic control over the distribution of recent silicoflagellate genera and demonstrated the application of this distribution as a

paleoclimatic indicator (Ciesielski and Weaver, 1973; Weaver and Ciesielski, 1974) (Figure 1). Hays and Opdyke (1967) and Bandy et al. (1971) similarly used radiolarian and diatom provincialism to infer paleoclimatic fluctuations. Also it has been suggested the O^{18}/O^{16} ratios derived from the tests of calcareous plankton are influenced by climatic conditions and therefore are paleoclimatic indicators (for example, Chaput, 1974).

Aspects of ferromanganese nodule formation have also been attributed to climatically induced conditions. Watkins and Kennett (1972) pointed out that formation of manganese pavements to the scouring action of bottom currents that removed sediments through winnowing and provided the low sedimentation rates that are often regarded as optimum for nodule formation. Ledbetter and Watkins (1978) attempted to relate lag accumulation and nodule accretion in order to separate the former from deposits of ice-rafted detritus. Kennett and Thunell (1975) attributed increased manganese nodule formation to increased submarine volcanism. Greater volcanic activity might enhance climatic cooling and promote higher bottom current velocities that would scour the ocean floor. Craig (1975) proposed that changes in the Carbonate Compensation Depth may also influence manganese-nodule formation indirectly by affecting sedimentation rates (Glasby, 1978).

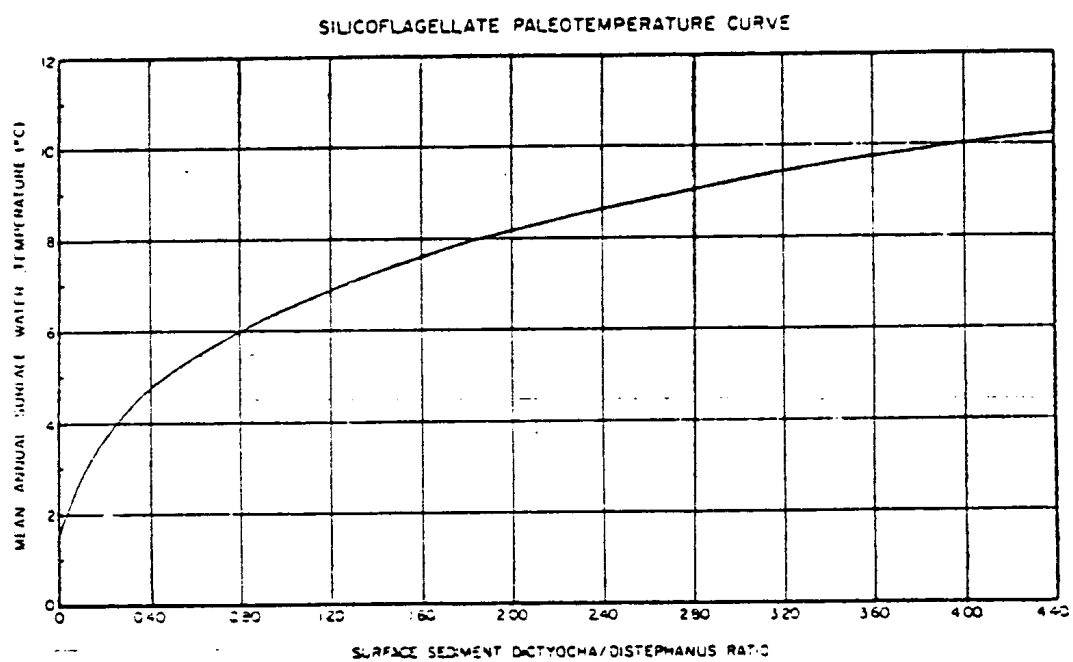


Figure 1. Southern Ocean silicoflagellate paleotemperature curve formed by plotting ratios of the genera Dictyocha and Distephanus against surface water temperatures (after Ciesielski, 1974.)

Although attributing paleoclimatic significance to ice-rafted components of Southern Ocean sediments remains controversial, it is generally acknowledged that these deposits originate from melting of sediment-laden icebergs. Whether increased ice-rafted detritus (IRD) represents cooler or warmer climatic conditions and how spatial occurrence of the IRD maxima vary with time are key questions of the controversy. Watkins et al. (1974) claimed that IRD horizons may be diachronous and constructed an explanatory model (Figure 2). During glacial periods the IRD-maxima zone occurred relatively north as surface water temperatures capable of melting icebergs migrated north and expanding ice shelves protected larger areas of sea floor from IRD deposition. During interglacial conditions the southern waters were warmer relative to glacial periods. Increased calving of continental glaciers and reduced sea ice occurred, as IRD maxima were closer to the continent and the volume of debris decreased rapidly northward (Watkins et al., 1974). Fillon (1977) developed another method of explaining IRD deposits. In the first part of a two-case model IRD deposition occurred in the presence of an ice shelf. Fillon uses this case ("Case I") to describe ice rafting in the Ross

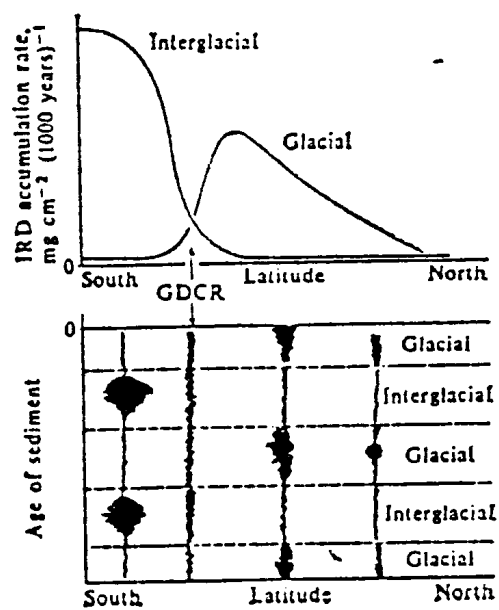


Figure 2. Model explaining the spatial and temporal distribution of IRD in sediments from the Southern Ocean (after Watkins, 1974.)

Sea vicinity after about 2.6 m.y. B.P. (Figure 3).

Case II provided an explanation of deposition in the absence of an ice shelf as is thought to fit IRD accumulation for the same area from about 3.2 m.y. to 2.6 m.y. B.P. (Figure 4). The Watkins model and both cases of Fillon's model include a latitudinal region where climatically induced variation in amounts of IRD should not be significant. This zone was termed the Glacial Debris Conjugate Region (GDCR) by Watkins et al. (ibid.).

In contrast to these examples of IRD used as a paleoclimatic indicator, Warnke (1970) attributed ice rafting to erosional characteristics of glaciers through time and indicated climatic interpretations are not necessarily exclusive of other explanations. He postulated that a "heightened erosional efficiency" early in Antarctic glacial history gave way to decreased glacial erosion as pre-glacial chemically weathered unconsolidated material was exhausted (ibid., p. 276). Because of the influence and variation with time of geomorphic processes, such as changing erosional efficiency, interpretation of IRD depositional patterns through long temporal core intervals was questioned.

Patterns of sediment distribution and stratigraphic relationships of lithologic variations have also been

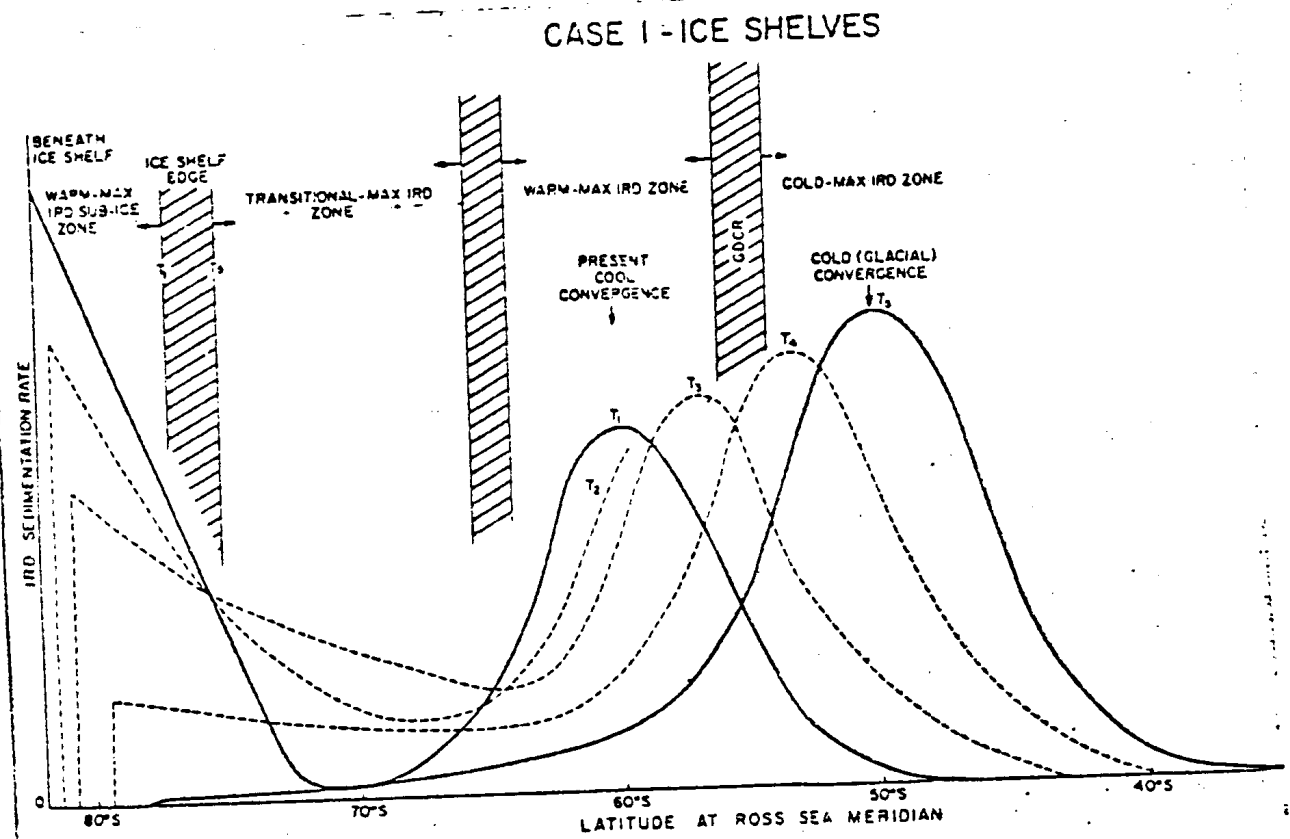


Figure 3. Case I of a model to explain the spatial and temporal occurrence of IRD in the vicinity of the Ross Sea (after Fillon, 1977.)

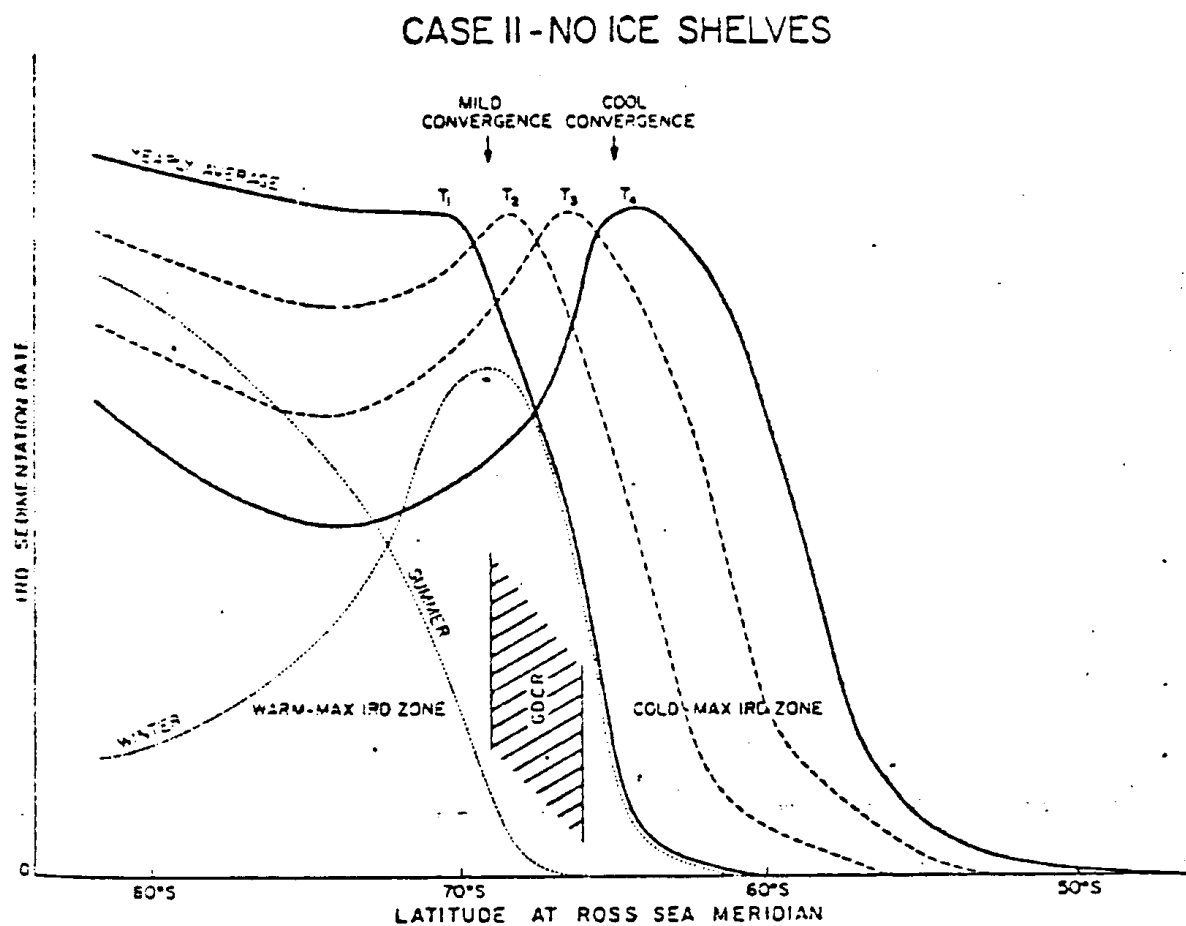


Figure 4. Case II of a model to explain the spatial and temporal occurrence of IRD in the vicinity of the Ross Sea (after Fillion, 1977.)

inferred as products of paleoclimatic fluctuations (Phillippi, 1910; Schott, 1939; Lisitzin, 1962; Hays, 1965, 1967; Goodell et al., 1968; and Weaver, 1973).

Goodell (1973) identified circulation, topography and structure, and terrigenous-sediment contribution as the three parameters controlling sediment deposition around Antarctica.

Circulation in the Southern Ocean is principally east or clockwise around the continent with a minor northerly component of flow (Figures 5 and 6). At depth the current is deflected north at bathymetric highs (ridges, seamounts, etc.), south at bathymetric lows (basins, for example) and increases velocity where it passes through channels and fractures in the ridge system. Otherwise this current, the Antarctic Circumpolar Current (ACC), has little attenuation with depth (Gordon, 1971). Closer to the continent than the east-flowing ACC is the East-Wind Drift. Deviations from a west-flowing circumpolar current entirely encircling the continent are manifested as clockwise gyres with northern and southern components often associated with the flanks of embayments such as the Weddell, Ross and Bellingshausen seas. The oceanic front between the East-Wind Drift and the ACC is the Antarctic Divergence (Kort, 1968).

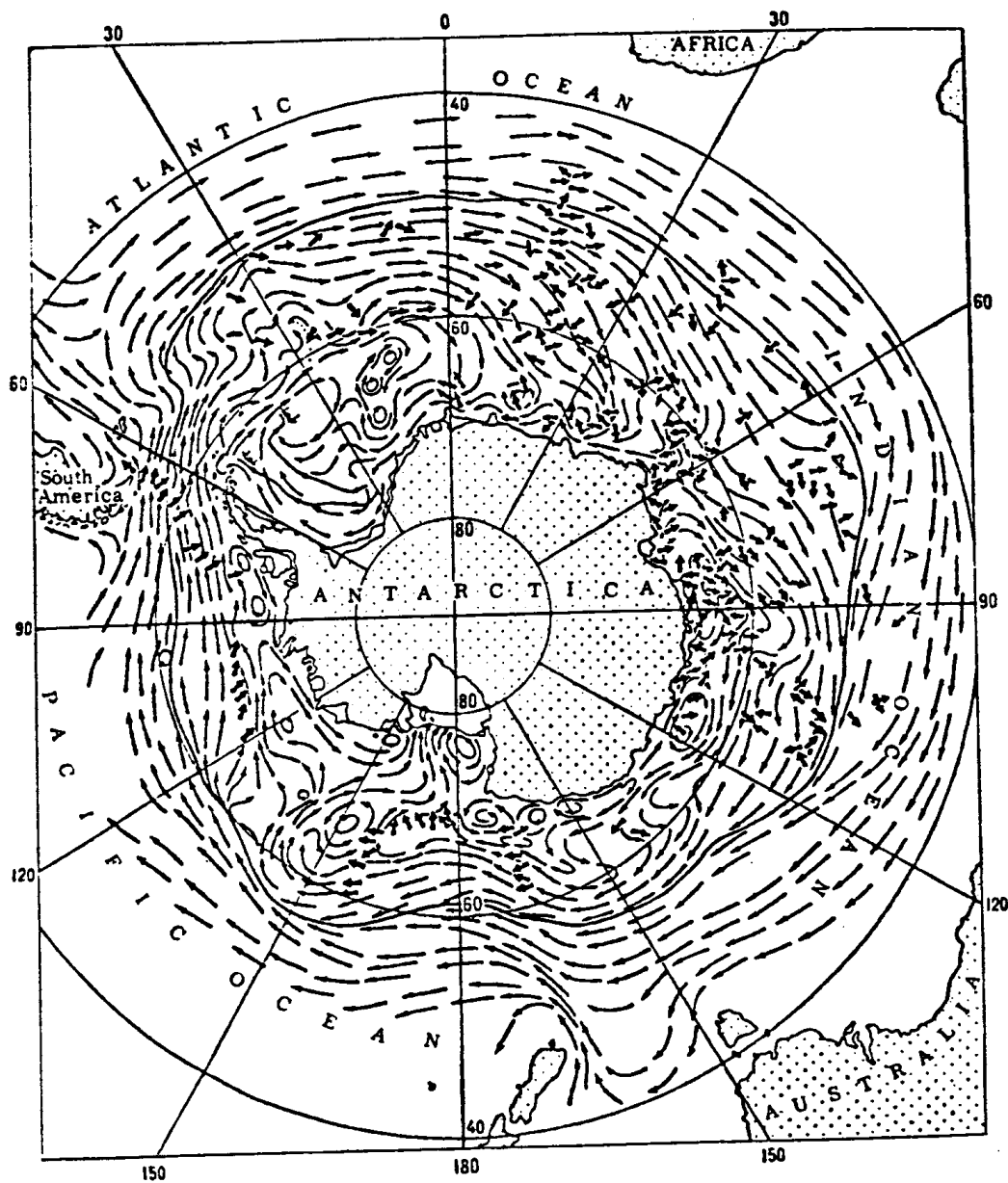


Figure 5. Circulation patterns in the Southern Ocean today
(after Treshnikov, 1964.)

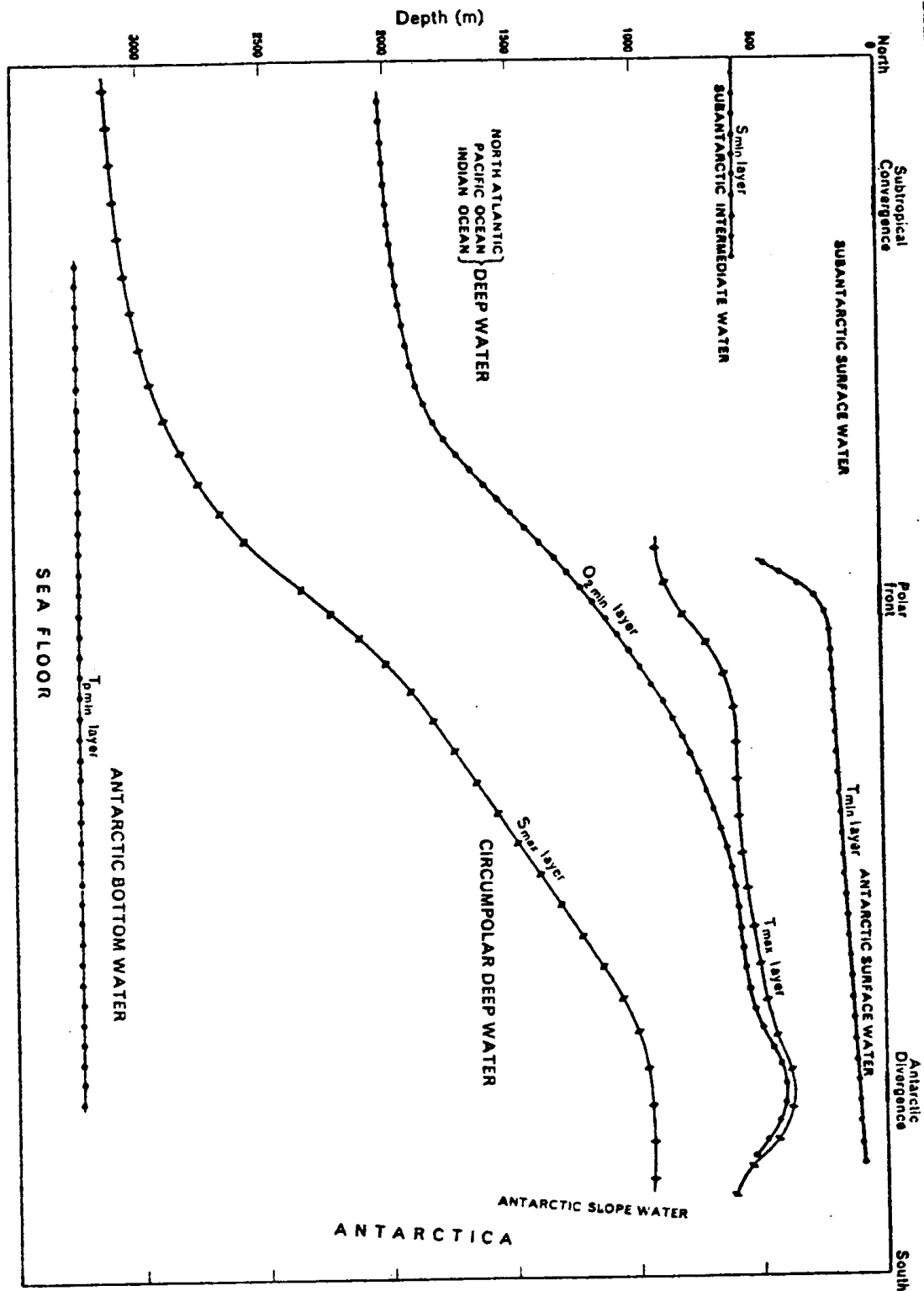


Figure 6. Generalized cross-section of the Southern Ocean showing relative position with depth of dominant water masses (after Gordon, 1967.)

An important part of the ACC is the Circumpolar Deep Water (CPDW), which is defined by a salinity maximum. The CPDW, a high-salinity, warm nutrient-rich water mass, flows south and east, and eventually rises to form two other major water masses: the Antarctic Surface Water (AASW), defined by a temperature minimum/oxygen maximum, and the Antarctic Bottom Water (AABW).

The AASW is a fresher, colder, highly oxygenated alteration product of CPDW that flows northeast before meeting the less dense Subantarctic Surface Water at the Polar Front Zone (Gordon, 1971) or Antarctic Convergence (Deacon, 1933, 1937; MacIntosh, 1946, for examples). Here AASW sinks to form Antarctic Intermediate Water, continues north, sinks farther and in northerly latitudes begins a return southward as reconverted CPDW.

AABW, also produced partially by conversion of upwelling CPDW, can be formed in three different ways (Gordon, 1971). First, freezing sea water at the ice shelves leaves a residual dense highly saline water mass that mixes with CPDW to become (AABW I), which is more dense than either parent. This method may be important in the Weddell Sea. Second, in a process attributed to Ross Sea AABW (II) production, freezing of water to or melting from ice shelves produces "supercooled" highly saline water. Third, AABW (III) could be produced through intense

cooling by katabatic winds.

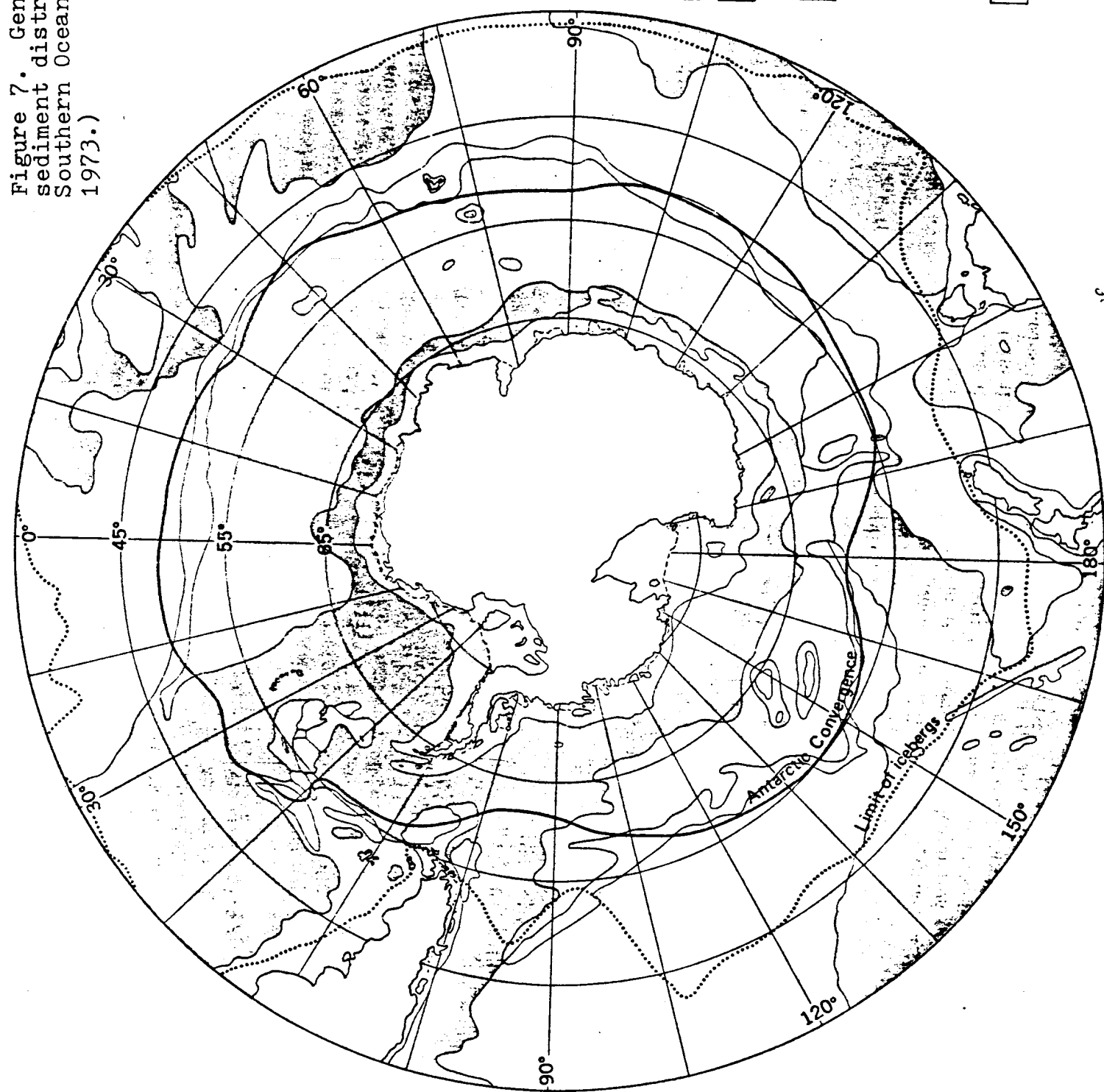
In all three cases AABW sinks to become a major influence on sediment distribution and erosion in the Southern Ocean. During cooling and glacial maxima increased AABW production may lead to regional unconformities resulting from bottom water scouring and removal or nondeposition of sediment. The hiatuses so formed have been interpreted in paleoclimatic terms.

The classification of Southern Ocean sediments includes four types of particular importance in this paleoclimatic interpretation: (1) Glacial-marine sediments, (2) Siliceous Oozes, (3) Calcareous Oozes, and (4) Pelagic Clays (Figure 7).

Glacial-marine deposits, those proximal to the continent, were first described by Phillippi (1910) as having "almost no CaCO_3 , few other organic constituents, poor sorting and an abundant silt fraction composed of rock flour" (Goodell, 1973, p.4.) Although subsequent investigators have redefined the essential characteristics of glacial-marine deposits (Pirie, 1913; Hough, 1950; and Goodell, 1965) acceptance of their primarily terrigenous nature has not been questioned.

North of the Glacial-Marine Zone is an area 900 to 2000 kilometers wide characterized by upwelling of nutrient-rich CPDW and the production of nearly three

Figure 7. Generalized re it
sediment distribution of
Southern Ocean (after Goodell,
1973.)



- ☐ Calcareous ooze
Mostly foraminiferal
- ☐ Calcareous-siliceous ooze
Both types of test exceed 30%
- ☐ Siliceous ooze
Mostly diatoms, often with radiolarians
- ☐ Clayey silts and silty clays
Red, brown, gray and olive; often high in volcanic debris; calcareous near calcareous oozes and in the vicinity of New Zealand and Australia; siliceous adjacent to siliceous oozes; sandy adjacent to continent shelves
- ☐ Shelf and coastal deposits
Submarine tills and glacial-marine sediments adjacent to Antarctica; calcareous sands and gravels adjacent to New Zealand, Australia, Africa, and South America

Fig. 6. Antarctic sediments, generalized from Plate 2.

quarters of all oceanic silica (Lisitzin, 1972). This region is the Siliceous Ooze Zone. The boundary between the two sediment regimes is approximately coincident with the Winter (August) 0 °C surface isotherm (Goodell, 1973). Unlike sediments of the Glacial-Marine Zone, major constituents of which are allochthonous and derived from ice rafting and transport by marine current (Anderson, 1977), siliceous-ooze sediments consist mainly of radiolarian, diatom and silico-flagellate tests. The northern boundary of the Siliceous Ooze Zone occurs at about the positions of the Antarctic Convergence. Sediments to the north are calcareous foraminiferal oozes or pelagic clays. Goodell (1973) has defined glacial-marine deposits as the sediments with "...30% and larger grain sizes and silt:clay ratio exceeding 1.0 and often exceeding 2.0..." He has also classified the sediments with 30% or more biogenically originating siliceous and calcareous components as biogenic oozes (ibid.). Goodell does not discuss what has been referred to above as "pelagic clay." Other investigators, such as Anderson (1977, for example), have developed their own classifications in addition to having utilized and modified preexisting ones. Many of these investigators have developed classifications that include compositional/textural parameters also characteristic of sediments such as mode of transportation and environment of deposition.

In this paper mode of transportation, composition, spatial relationship to other sediment types and texture will be used to classify sediments. The compositional and textural characteristics of sediments in the cores of this study were obtained from the Islas Orcadas cruise 11 core descriptions (Kaharoeddin, 1978).

Glacial-marine sediments refer in this text to deposits that exhibit a variety of textures and compositions, are located south of the zone of siliceous ooze accumulation, are largely terrigenous, probably originating in Antarctica and were deposited from a variety of transport media. Close to the continent these sediments may accumulate by ice shelved settling from submarine streams. Ice-rafting, below floating sea-ice and farther north by icebergs, is another important mode of transportation. Included in this group is sediment with a large fine fraction, which represents material reworked by bottom water. These "fine-bearing" deposits probably include Goodell's (1973) "clayey silts" and "silty clays". Such deposits are generally the glacial-marine sediments closest to the siliceous ooze zone and are the only glacial-marine sediments in the cores of this study.

Siliceous oozes are those sediments with 30 percent biogenic silica that accumulate south of the calcareous oozes and pelagic clays. ~~Calcareous~~ oozes are sediments

that contain 30 percent or more biogenic calcareous components. Both ooze types, since they are mainly allochthonous, that is, originating in the area, are transported largely by oceanic currents.

The pelagic clays referred to in this investigation include deposits accumulating north of the siliceous ooze belt. Most of these deposits are derived from the Antarctic continent and are transported primarily by bottom currents. The pelagic clay in the cores of this study represents sediment that accumulated in the zone of calcareous ooze deposition but received a relatively large enough volume of inorganic material large enough to keep biogenic fraction below 30 percent. Accumulation below the CCD is one means of accomplishing this.

The mixtures of sediment types, such as siliceous/calcareous oozes, siliceous muds and calcareous muds, were identifications provided in the Islas Orcadas cruise 11 core descriptions as were siliceous and calcareous oozes. Clays in the cores were described as pelagic clays and differentiation between what has been referred to here as glacial-marine and pelagic clays was made as part of this investigation.

Because the distribution of these sediment regimes is controlled by oceanographic conditions, which, themselves, are influenced by climatic conditions, the migration of regime boundaries identified in cores as changes

from one sediment type to another, reflects fluctuations in paleoclimate. Hays (1965, 1967) attributed changes from red clay to diatomaceous ooze in cores from the Southern Pacific to climatic cooling. Goodell et al. (1968) proposed similar explanations for sediment changes recorded in cores from the Drake Passage. Anderson (1972) and Weaver (1973) developed models to explain the fluctuation of sediment with oceanographic and climatic changes.

This study will apply some of the above methods to identify paleoclimatic changes recorded in nine Islas Orcadas cruise 11 cores from the area shown in Figure 8.

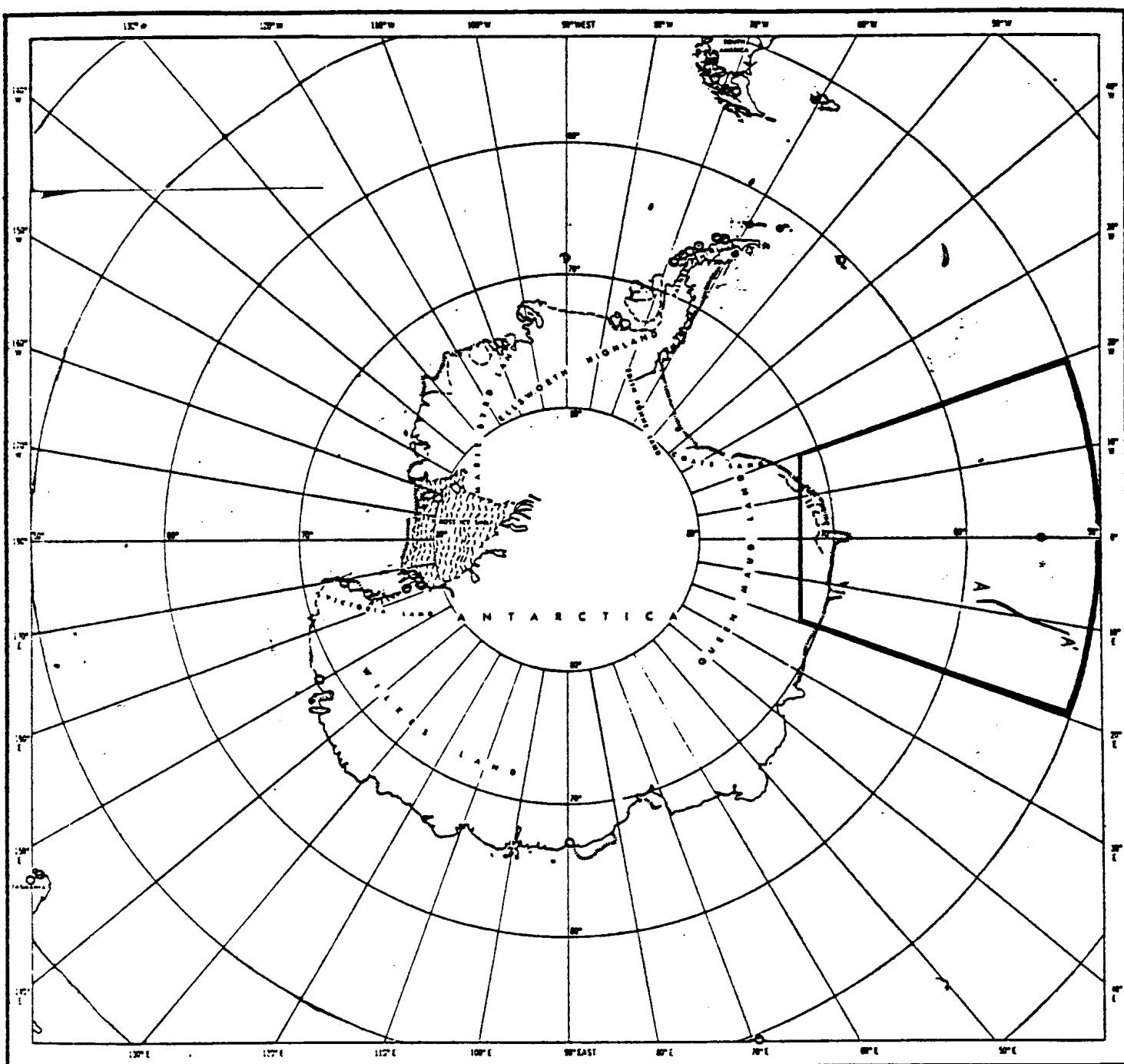


Figure 8. Map of Antarctica and the surrounding Southern Ocean. The heavy lines on the right side of the map include the general region of study. The line A - A' represents the approximate position of the core track.

INTRODUCTION TO THE STUDY AREA

The general area of the Southern Ocean included in this study is bounded to the south by the Antarctic continent, north by the 50° S latitude and east and west by the 20° meridians although the cores themselves come from a track in the northwest portion of this region extends approximately N30E from $57^{\circ} 55.3'S$, $08^{\circ} 59.0' E$ to $52^{\circ} 31.6' S$, $11^{\circ} 34.3' E$. Specifically the study is concerned with changes from 0° to 20° E and $50^{\circ}S$ to $60^{\circ}S$ as recorded in the cores. Table I gives the latitude and longitude of the core recovery sites and the depth in meters at these locations. Table II describes the relation of each core to immediate topography.

Topography and Structure

The area from 0° to 20° E, 50° S to 60° S includes a portion of the Antarctic-Indian Basin and isolated areas below 6000 meters depth. Shallower depths characterize waters over the Atlantic-Indian Ridge (also called the Africa-Antarctic Ridge and Antarctic-African Ridge), which crosses the region at about 52° to 55° (from a figure in Goddell, 1973). Near the core locations the ridge

TABLE I*

Core Number	Latitude	Longitude	Depth (m.)
IØ 1176-66	57°55.3'S	08°59.0'E	4513
IØ 1176-64	57°13.8'S	08°12.1'E	5479
IØ 1176-67	57°02.6S	09°14.9'E	5274
IØ 1176-68	56°11.2'S	09°35.3'E	4830
IØ 1176-70	55°09.0'S	09°58.0'E	4521
IØ 1176-71	54°31.2'S	10°17.9'E	3809
IØ 1176-52	53°42.7'S	10°24.0'E	3815
IØ 1176-73	53°31.2'S	10°49.1'E	3167
IØ 1176-76	52°31.6'S	11°34.3'E	3127

* Data for this table taken from Islas Orcadas
Cruise 11 Core descriptions (1979).

TABLE II^{*}

Core Number	Relation to Topography
IØ 1176-66	Gently sloping; at apex of broad abyssal rise, 400-500 fathoms (732-914 m) relief.
IØ 1176-64	Fairly flat sediment pocket between two abyssal hills, 80-100 fms. (146-183 m) in relief.
IØ 1176-67	Very gently sloping; sediment pond between abyssal hills.
IØ 1176-68	Moderately sloping; small basin in a trough between two abyssal hills, 200-300 fm (366-549 m) relief, approximately 360 Km south-southwest of the crest of an offset portion of the African-Antarctic Ridge.
IØ 1176-70	Very gently sloping; sediment pocket between two 300 fm (549 m) relief hills, approximately 240 Km southwest of an offset of the African-Antarctic Ridge.
IØ 1176-71	Gently sloping; apex of an abyssal hill.
IØ 1176-52	Gently sloping; approximately 400 Km northwest of Bouvet Island. Core located on a 400 fm (732 m) rise; approximately 100 Km southwest of an offset of the Antarctic-African Ridge crest.
IØ 1176-73	Moderately sloping; approximately 46 Km southwest of an apex of the African-Antarctic Ridge.
IØ 1176-76	Cored on a minor promontory, in a trough, in a region of very rough topography located just 20 Km north of the axis of an offset portion of the African-Antarctic Ridge.

* Data for this table taken from Islas Orcadas
Cruise 11 Core descriptions (1979).

spreading axis is interrupted by four transform faults, which offset the ridge up to 300 km each and are marked by depths of up to three kilometers or less deeper than the surrounding topography (Sclater et al., 1977). Bouvet Island (about 03° E, 55° S) is the structural high of the region (Figures 9, 10 and 11).

Circulation

Surface circulation in the study area is dominated by the west to east flow of the ACC and by part of a gyre in the East-Wind Drift influenced by the Weddell Sea. The East-Wind Drift is principally a west flowing current close to the continent. At depth, the major current influence is from AABW produced in the Weddell Sea partially from CPDW. Islas Orcadas cruise 11 oceanographic observations "revealed a variety of deep water mixing between CPDW and Weddell deep waters" (Sclater et al., 1977, p. 64). The location of the Divergence in the area is poorly defined because of the Weddell gyre but ranges from about 62° S at 10° E to 68° S at 20° W. The Convergence of Polar Front Zone occurs at or near the northern boundary of the study area in a narrow range from about 49° S to 50° S (Sclater et al., *ibid*) (Figure 12).

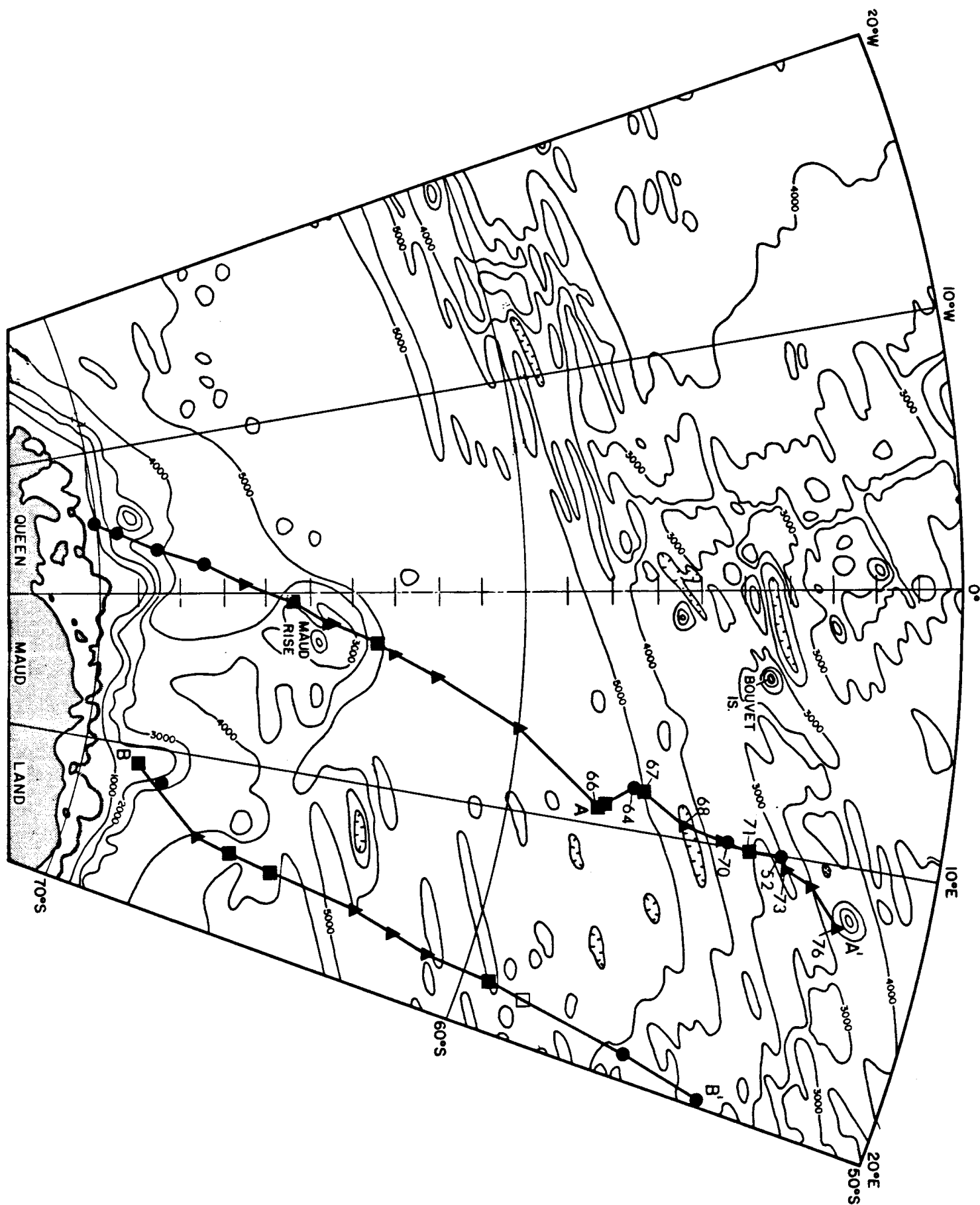


Figure 9. Map of the study region that includes a number of cores not considered in this investigation. Cores in this study occur along the northern section of the western core track and are numbered.

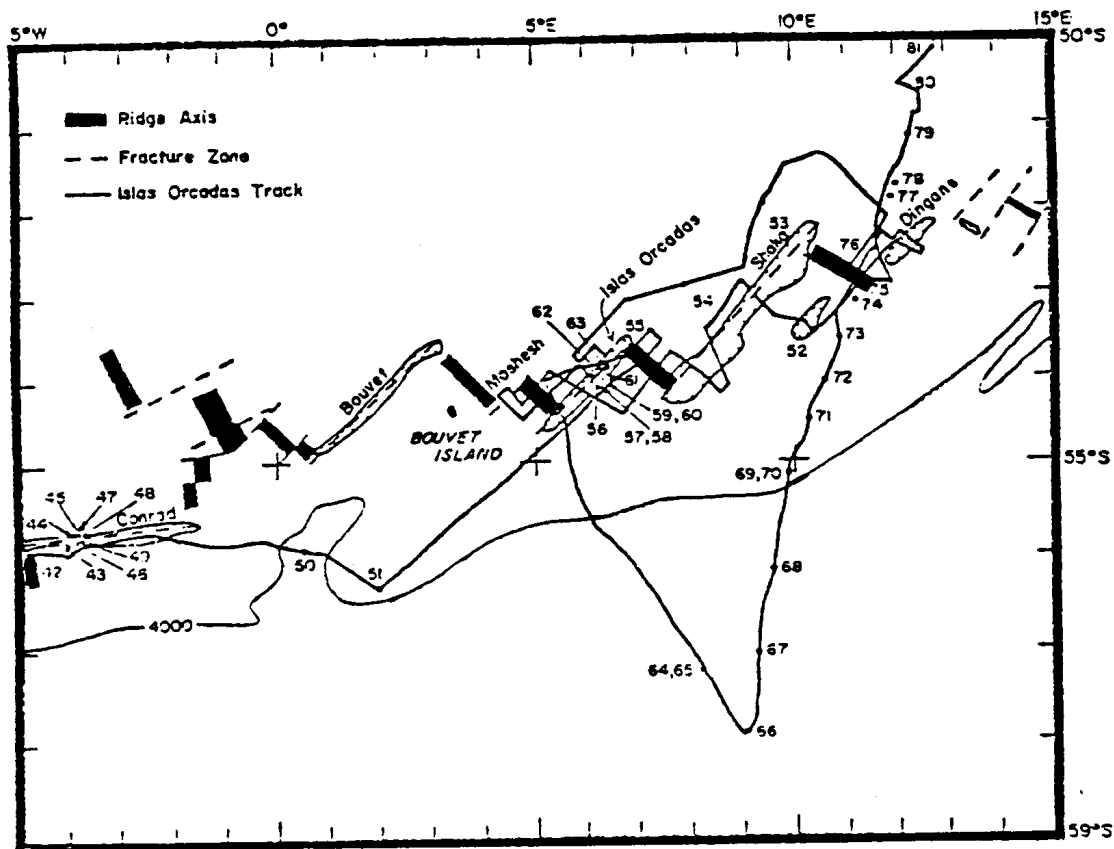
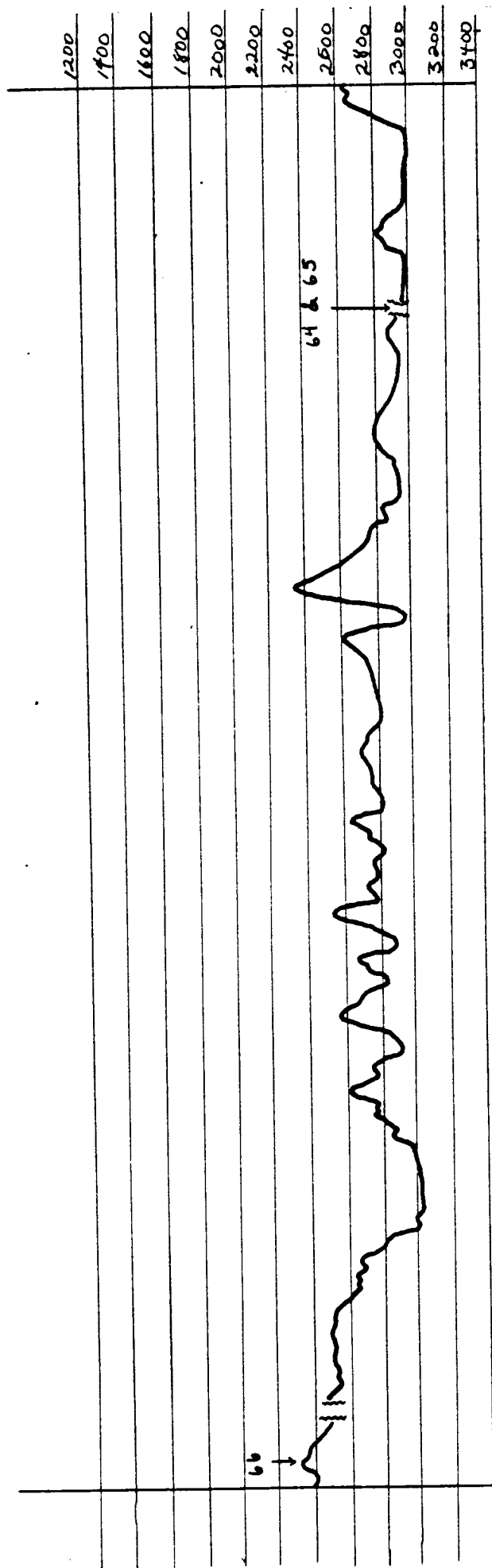


Figure 10. A portion of the cruise 11 course of the Islas Orcadas, which includes the study cores (Slater, 1977.)

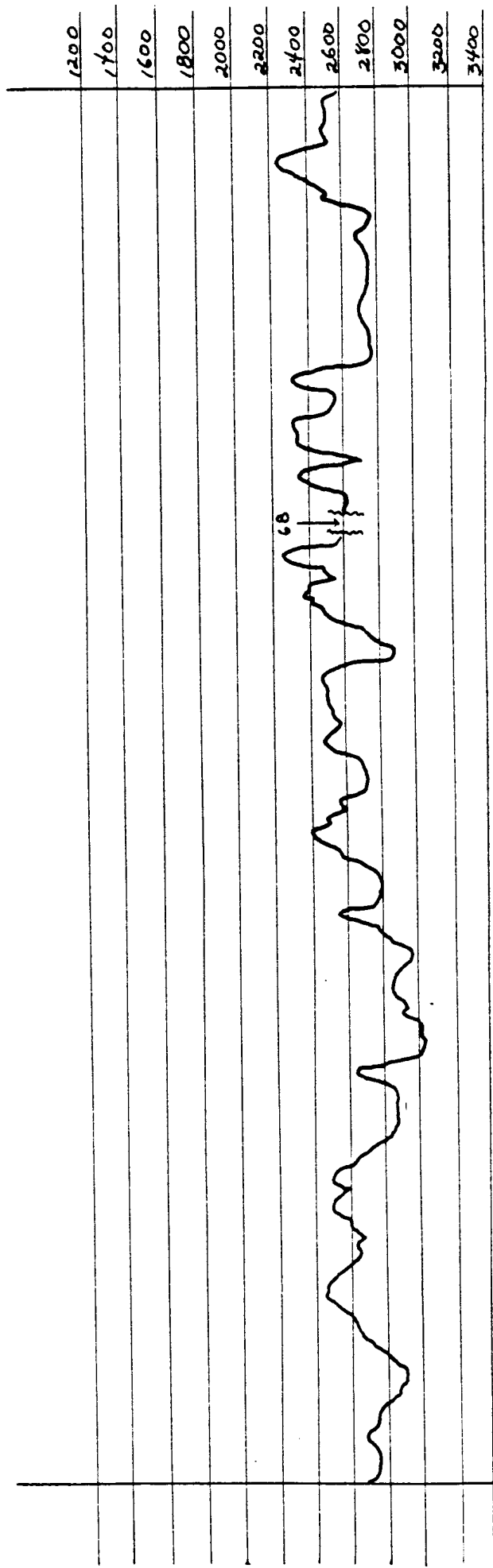
Figure 11a - 11e. Cruise profiles showing the relationship of cores (excluding I01176-67) to the immediate topography. Vertical scale is given on the right as depth in fathoms. Horizontal scale varies.

A'

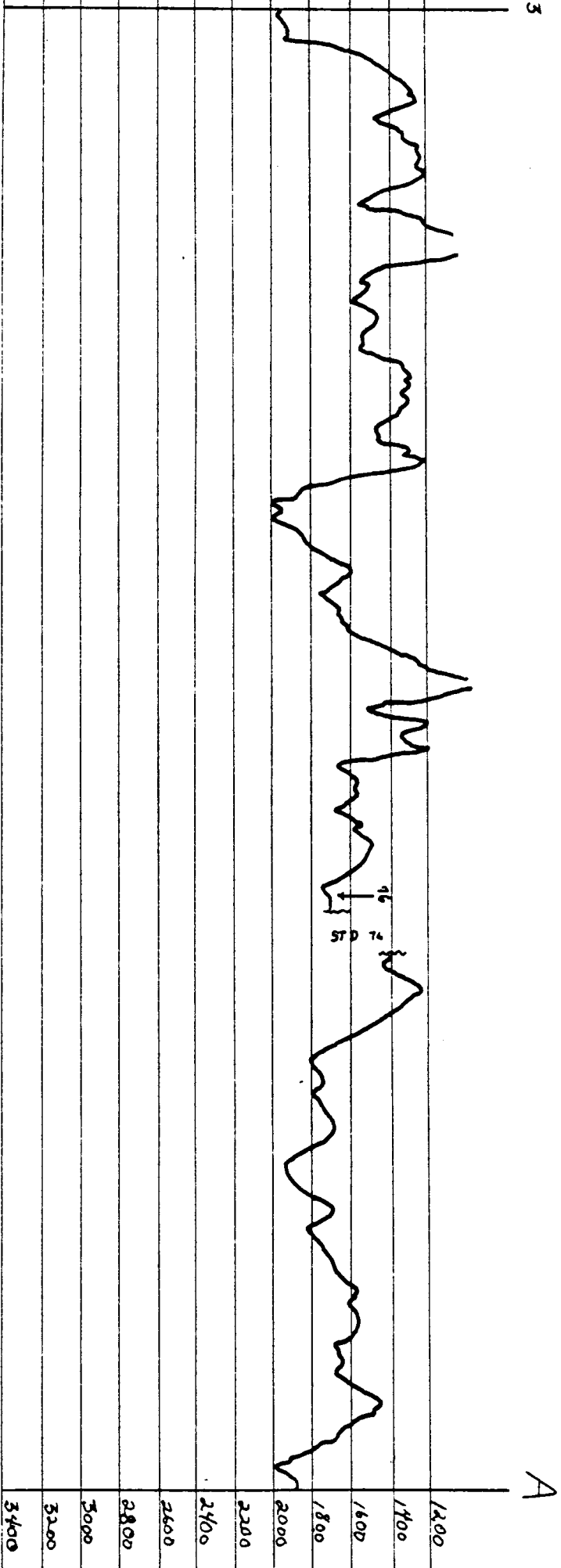
1



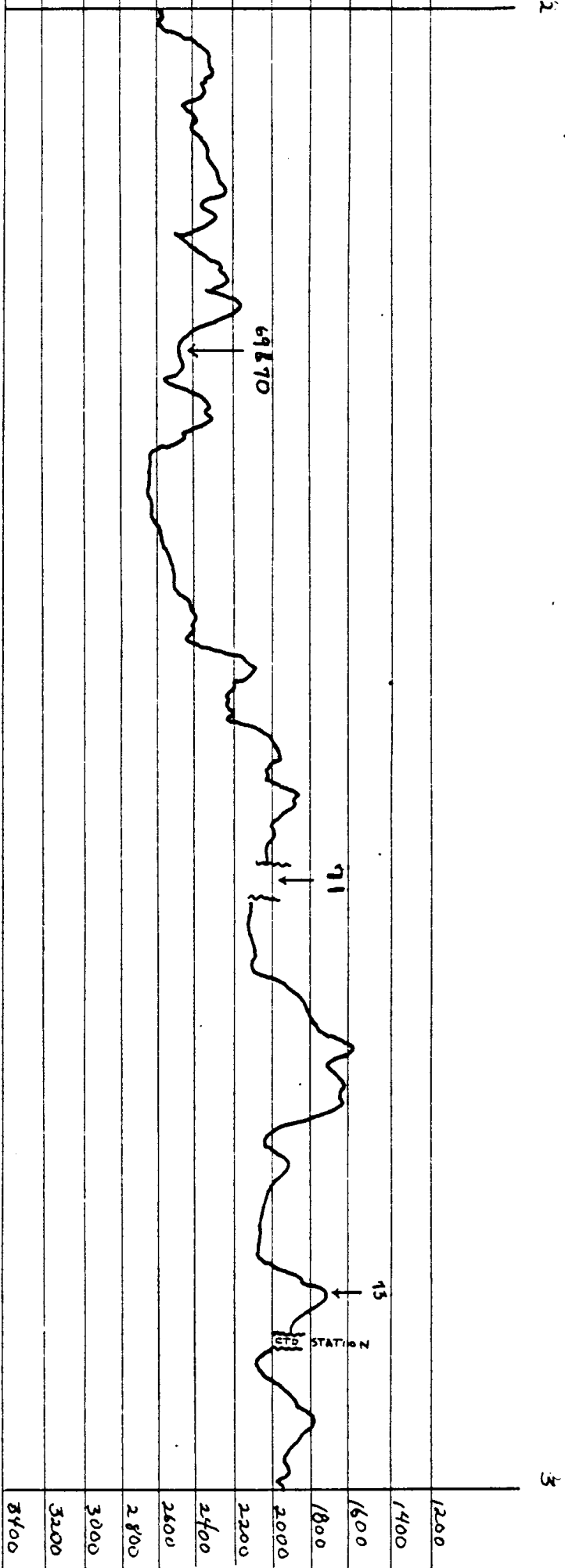
2



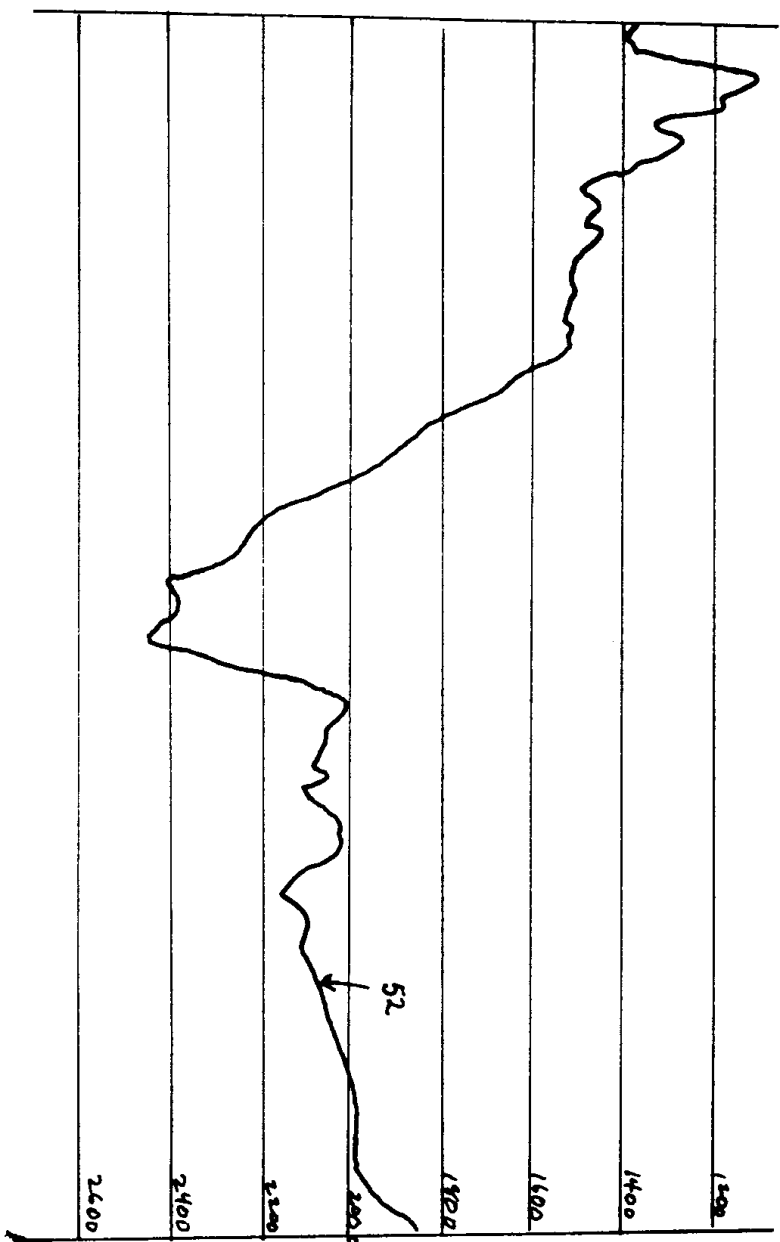
3



2



c.



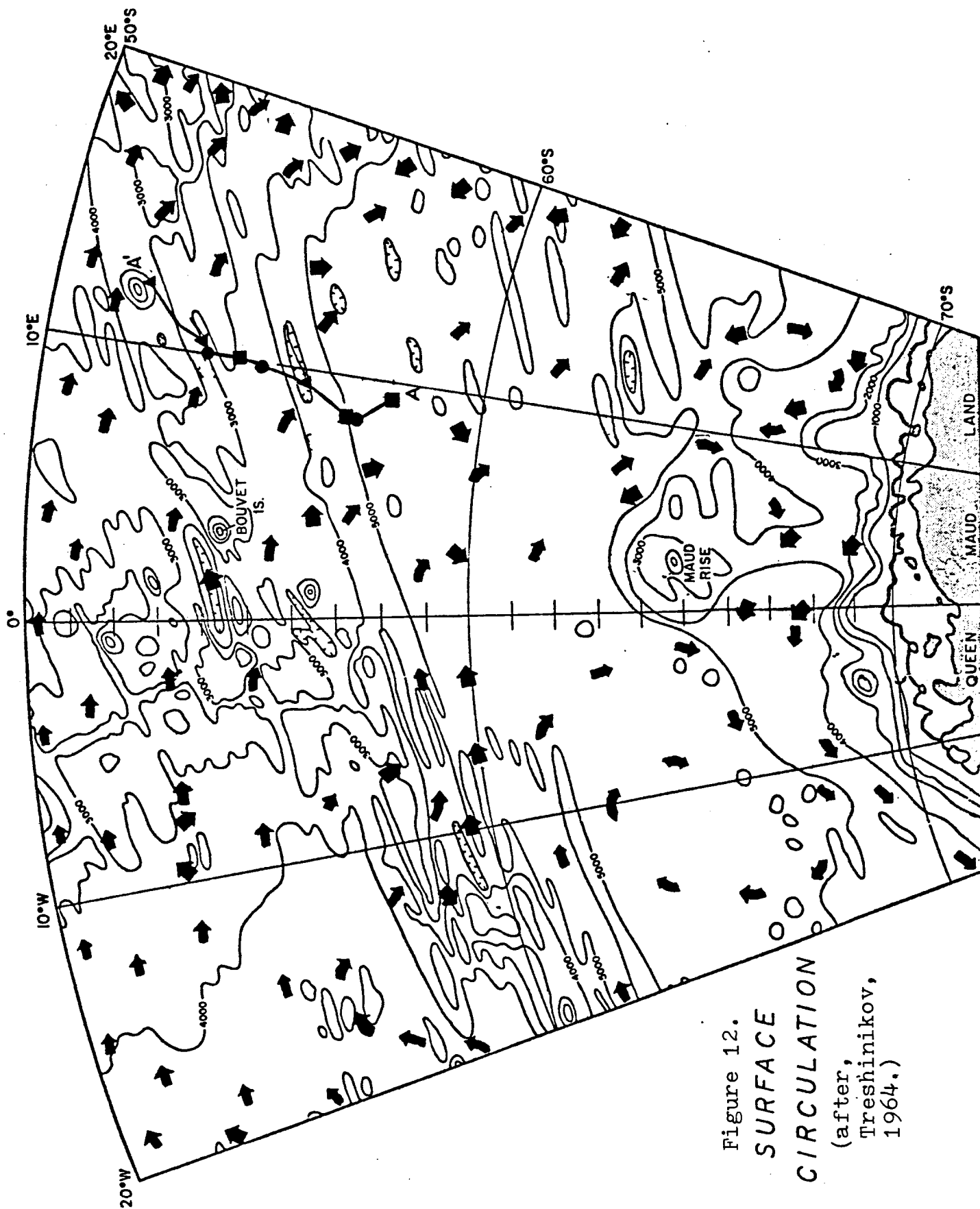
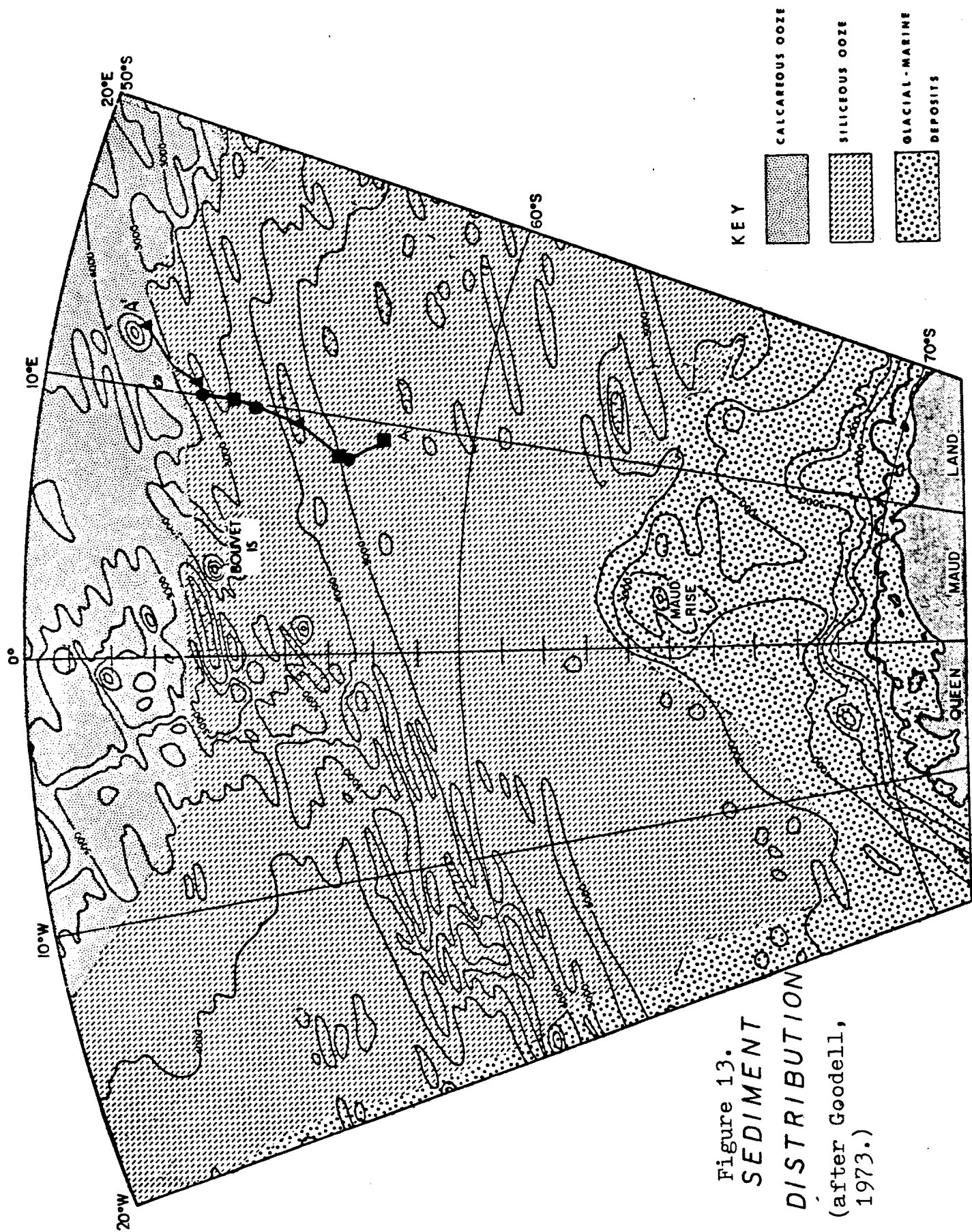


Figure 12.
SURFACE
CIRCULATION
 (after,
 Treshnikov,
 1964.)

The Sediments

Although most of that portion of the cruise track that includes the study cores occurs within the zone of Recent siliceous-ooze accumulation, the general study area (20° E to 20° W) contains examples of nearly all major sediment types recognized by Goode11 (1973) (Figures 7 and 13). These include glacial-marine gravels, sands, silts and clays, which occur south of 65° S and on the Maud Rise; siliceous and calcareous siliceous oozes covering the abyssal depths and south flank of the ridge system, respectively; and calcareous ooze and calcareous/siliceous ooze mixtures north of the siliceous ooze at depths at which carbonate can accumulate. Volcanic ash is also present, probably contributed from Bouvet Island (Ciesielski and Ledbetter, personal communications).



METHODS

Nine deep sea cores (numbers IØ11-52, -64, -66-68, -67, -73, 70, 71, and 76) from Islas Orcadas cruise 1176 were sampled at 10 and 20 cm. intervals for paleomagnetic and biostratigraphic investigation. Magnetostratigraphic information provided by Dr. Michael T. Ledbetter (University of Georgia) made possible more efficient use of samples for the biostratigraphic investigation. Sampling of the cores was conducted at the National Science Foundation Antarctic Research Facility at Florida State University in Tallahassee by various facility staff members, Dr. Paul Ciesielski and Dr. Ledbetter and his students from the University of Georgia. Two hundred seventy-five samples for the biostratigraphic study were obtained.

During December 1979 I visited the facility to become acquainted with sampling procedures (none of the cores sampled during this visit is included in this study). The sediment is collected intact by inserting a clear plastic box, one cubic centimeter in volume, into the center of the core at a known stratigraphic position. Care is taken to avoid collecting sediment from the core

margins, which are often deformed during coring.

Smear slides for this study were made using Piccolyte as a mounting medium and were examined, using a Leitz stereoscope, for diatom content.

Biostratigraphic relative ages based on Weaver's (1976) revision of McCollum's (1975) high-latitude diatom zonation were assigned to the cores. The basis of these assignments is the observed stratigraphic ranges in the cores of index fossils used in the Weaver and McCollum schemes.

The resulting biostratigraphic zonation of the cores was then compared with the stratigraphic record of paleomagnetic reversals as determined for these cores by Dr. Ledbetter. Because McCollum and Weaver have indicated an approximate correlation of the biostratigraphic zones to a standard magnetic time-scale, such as presented in Figure 14, tentative identification of magnetic events preserved in the cores could be made.

Using the stratigraphic locations of the tops and bases of both the tentatively identified magnetic events and the ranges of the index fossils, a graphic comparison was made of the time-significant events recorded in the cores. The graphic correlation provided a means of checking the tentative assignment of the magnetic events. The principle utilized in this correlative

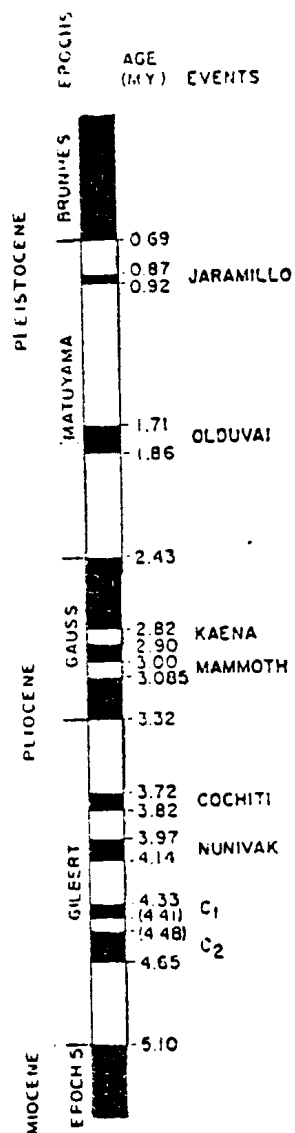


Figure 14. Standard Magnetic Time Scale used in this study (after Opdyke, 1972.)

procedure is discussed in Miller's (1977) modification of the method that first was demonstrated by Shaw (1964); the method has been illustrated by other workers (Sweet, 1979, for example).

Biostratigraphic range charts, magnetostratigraphic data, biozone/magnetic correlations and lithologic information for the cores are included in Appendix I. Appendix II contains the results of the graphic correlation and a brief explanation of the principles involved.

BIOSTRATIGRAPHIC RESULTS AND PROBLEMS

Results of the biostratigraphic investigation of the cores, that is, the location in the cores of the zones defined by McCollum (1975) and Weaver (1976), are given in Table III. The ranges of index fossils characterizing these zones and their boundaries have been correlated to the magnetic time scale in both diatom zonal schemes. Discrepancies were found between those correlations and the stratigraphic occurrence of the fossil ranges relative to the magnetic events preserved in the study cores.

In particular the ranges of Actinocyclus ingens Rattray and Nitzschia angulata (O'Meara) deviated from those defined by McCollum and Weaver. A. ingens Cosinodiscus whose latest occurrence defines the base of ~~the~~ ^{the} lentigenosis ^{Zone} was observed in certain cores (101176-66, -68, -70, -76) above the base of the Brunhes magnetic normal event. However, the base of both the biostratigraphic zone and the magnetic event are described by McCollum as "approximately" coincident (McCollum, 1975, p. 519.)

TABLE III
BIOSTRATIGRAPHIC ZONE POSITIONS

Biostratigraphic Zones	IØ11-	Position (cm.) of Index Fossil Ranges										Core No.'s
		66	-64	-67	-68	-70	-71	-72	-73	-76		
Coscinodiscus lentigenosis	Top Base		0 1128	0 208	0 200	0 1068					0 20	
Coscinodiscus elliptipora/ Actinocyclus ingens	Top Base	1148 1309	228 1148	300 870	1088 1528	0 388	0 920	0 71	28 118			
Rhizosolenia barboi/nitzschia kerguelensis	Top Base		1168 1228	870 950			920 969		128			
R. barbei/ Cosc. Kolbei	Top Base			1000 1400								
Cosc. insignis	Top Base			1500 1767?								
N. interfrigidaria	Top Base	0? 24?	1248 1428		1538 1608	408 428		84 388	138 178?			
N. angulata	Top Base	24(0?) 188	1448 1588			448 590		428 629	178? 278?			
N. reinholdii	Top Base	208 454				600 758			278? 308			
Denticula husted- tii	Top Base	454 ?				778 ?			318 ?			

The first common occurrence of Nitzchia angulata defines base of the Nitzchia angulata Zone. Weaver has said this base "correlates between the Gilbert events 'a' and 'b' ($t = 3.90$ m.y. B.P.)." However, in cores I01176-71 and I01176-76 the base of the N. angulata Zone, located on the basis of the first common occurrence of N. angulata, is within the Gilbert "b" event ($t = 4.14-3.97$ m.y. B.P.). This observed diachroncity in the first occurrence of N. angulata could be a depositional feature or may be attributable to diachronous first appearances of the specie in different areas of the ancient Southern Ocean.

Haituses

A number of unconformities were discovered in the cores. In core I71176-66, the southernmost core recovery site, a minor disconformity is inferred to exist at about 454 cm. The inference is based on an anomolous rate of sedimentation in the suspected interval and on the presence of a sharp contact separating clay from superjacent diatomaceous ooze. The unconformity would occur within the Nitzchia reinholdii Zone so no biostratigraphic confirmation of its existence could be made.

In the same core the youngest sediments record the Gilbert 'a' magnetic event, and indicate either nondeposition since the Gilbert "a" ($t = 3.82 - 3.72$ m.t. B.P.) or post-Gilbert "a" deposition and subsequent erosion. In either case, the lack of sediment younger than Gilbert "a" indicates an unconformable surface in existence today in the

vicinity of the 101176-76 core recovery sites.

In core 101176-64, the next core north along the track, a regional gap in the sedimentary record, observed in many of the cores, has its most pronounced temporal extent. Sediments with an Upper Pleistocene flora from the Coscinodiscus elliptipora/A. ingens Zone overlie upper Miocene deposits. This stratigraphic relationship indicates a minimum temporal hiatus of 4.2 m.y.

Core 101176-67 contains part of the same disconformity, which separates sediment deposited during the early Gauss (N. interfrigidaria Zone) from overlying deposits containing assemblages characteristic of the Rhizosolenia barboi/N. Keuguelensis Zone (approximately correlative with the Olduvai magnetic event).

101176-70 contains a biostratigraphic gap with Coscinodiscus elliptipora/A. ingens Zone assemblages in siliceous mud overlying clay with fossils of the N. angulata Zone.

101176-71 contains an unconformity at 409 cm., with covering lower Gauss sediment of the N. interfrigidaria Zone covered by Matuyama Cosc. elliptipora/A. ingens Zone deposits. A second unconformity in the core is suggested by a very low sedimentation rate (0.05cm/1000 yr.) between the recorded lower Gauss normal event (base: 439 cm.) and the Gilbert "a" magnetic normal (top: 459 cm.).

Core -71 also contains an unconformity at about 759 cm., which is recognized by an absence of sediment deposited during the Gilbert " c_1 " and " c_2 " events. Because the unconformity would be at the boundary between two biostratigraphic zones adjacent to one another in conformable relationship no biostratigraphic control substantiates the existence of this second unconformity.

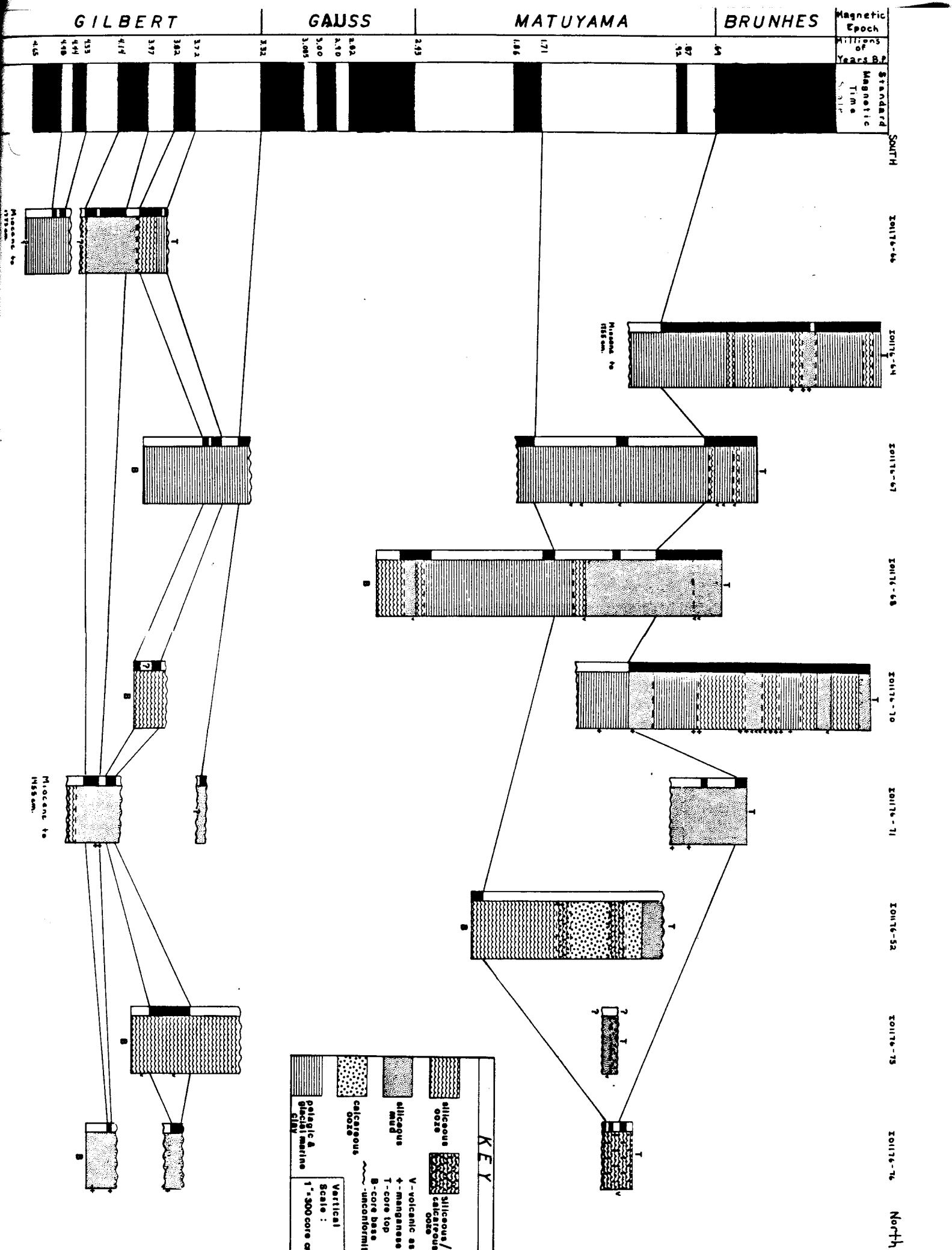
IØ1176-52, which is the next core north but lies off the main track, has no disconformities. Its youngest sediments contain assemblages of diatoms found in the Cosc. elliptipora/A. ingens Zone and not recent assemblages, this toward the presence of an erosional/nondepositional surface.

Core IØ1176-73, north of IØ1176-71 on the core track contains a layer of reworked sediment from about 52 cm. to 71 cm. No time significance could be given the sediment within this lithologic unit; however, in superjacent sediment Coscinodiscus elliptipora/Actinocyclus ingens Zone fossils were identified and below the reworked zone. Deposits were assigned the N. interfrigidaria Zone.

The northernmost core, IØ1176-76, contains two unconformities. The first at 128-138 cm. is substantiated by a biostratigraphic hiatus between the R. barboi/N. ker-guelensis Zone and the N. interfrigidaria Zone below. The second disconformity is inferred by the existence of

manganese encrusted detritus (possibly lag deposits) at 211-230 cm. and relatively low sedimentation rates between 220-230 cm. The unconformity occurs within the N. angulata zone precluding substantiation, using diatom zonation, of its existence. Similar layers of manganese encrusted gravel are located at 200-203 cm. and 343-351 cm. These may also be lag deposits.

Figure 15. Regional Magnetic correlations and lithologies of the nine cores along the cruise track.



Interpretation and Discussion*

If the general climatic model for AABW production, summarized by Gordon (1971) is correct, then unconformities in the sedimentary record indicate climatic deterioration. As yearly average temperatures decrease, sea ice cover would begin to expand partially through freezing of sea water. Residual highly saline water produced by freezing would sink due to the increased density relative to the underlying water. This model has been applied particularly to the formation of AABW originating in the Weddell Sea area where scouring of sediments on the surrounding ocean floor is attributed to AABW. The study area lies within the influence of AABW originating in the Weddell Sea.

Similarly, if the proposed model of sediment regime migrations is correct, then changes in sediment lithology in a core represent the response of sediment distribution to fluctuating climatic conditions. Glacial-marine deposits closest to the continent are replaced northward by siliceous ooze that, in turn, is replaced by calcareous ooze or pelagic clay deposits. The deposition of calcareous ooze versus pelagic clay depends, in this study area, on the depth of sediment accumulation relative to the CCD. The regimes are thought to migrate over one another as oceanographic conditions controlling their distribution respond to climatic change.

The models proposed to account for the formation of

*Figure 15 should be referred to as often as necessary during the reading of this section.

unconformities and lithology changes in the cores, were the two used in this study to make climatic interpretations. The actual utility of these general models depends upon the regional extent of both stratigraphic features and the degree of resolution with which they are defined. An unconformity or lithology change observed in one core might represent only a change in local conditions with no climatic implications. Locally, sediments on bathymetric highs may be winnowed of their finer fractions, like clay, leaving behind the coarser components, which are often biogenic. Or, in an area within the belt of siliceous ooze accumulation, for example, sediment with unusually high percentages of fine material, representing the material transported during winnowing, may accumulate in basins or other areas of lower energy. Should such a depositional event be recorded in a core, anomalous stratigraphic relationships might appear. For reasons such as these, much of the interpretation that follows is proposed as one possibility; in some instances sedimentary evidence may just as easily reflect local conditions as regional paleoclimatic changes.

Miocene-Pliocene Boundary and Gilbert Magnetic Event Conditions

The Miocene-Pliocene boundary is contained in three cores (I01176-66, -64, -71) within an unconformity (core -66 may contain a conformable boundary). In core -66, sediment deposited during magnetic Epoch 7 (tentatively identified by Dr. Ciesielski) of the Miocene is truncated and overlain by

deposits of the early Gilbert magnetic Epoch prior to the "c₁" and "c₂" events, which are also recorded in this core. In core -71, the unconformity separates sediment of Epoch 5 (identified by Dr. Ciesielski) from deposits of the Gilbert "b" event. The unconformity in -64 is shown by Miocene sediment overlain by Pleistocene deposits but probably does not represent a continuous erosional event. This will become more evident later.

Also in core -66 is a possible unconformity between the Gilbert "b" and "c₁" events. Because the sediment above this unconformity closely resembles the earliest Pliocene sediment in core -71, the erosional events resulting in those hiatuses possibly had regional extent and ended similarly in both locations with the deposition of siliceous ooze between 4.14 and 4.33 m.y. B.P. It cannot be determined whether the erosion that ended after the Gilbert "c₁" in core -71 was the same erosional event that caused the unconformity between Miocene and Pliocene sediments in core -66 or whether it was equivalent only to the erosion that produced later unconformity in core -66 but managed to erode more deeply. All that can be said is that erosion (or only nondeposition), possibly diachronous and probably of varied magnitude along the spatial extent, ended just prior to the Gilbert "b" event with the deposition of siliceous ooze. This ooze represents climatic warming. A short intense climatic cooling at that time has been suggested by previous investigators (Ciesielski, personnel communication.)

The gradational contact between the ooze and the siliceous mud above becomes slightly younger to the south

supporting an argument for continued climatic warming with accompanying sediment boundary migrations toward the continent. The same siliceous mud seems to have dominated deposition in the study area during the Gilbert "b" event ($t = 4.14$ to 3.97 m.y. B.P.) as seen in cores -66, -71, and -76. Although the absence of age equivalent sediment between core -66 and -71 may exclude deposits of ooze, the sediment probably represents transitional deposits between siliceous ooze and pelagic clay. These could have been deposited below the CCD in a zone in which calcareous ooze might otherwise accumulate.

An alternative hypothesis must be proposed to account for the lack of carbonate in core -76 not only in deposits that record the Gilbert "b" event, but also in those deposited during the Gilbert "a". In the same core Pleistocene and Holocene deposits containing calcareous components are mixed with siliceous ooze. This probably represents sediment that is the equivalent of the transitional environment mixture proposed above for the Gilbert "b" deposits. However, the younger sediment must have accumulated above the CCD. To explain the lack of calcareous components in the Gilbert "b" (and "a") deposits of core -76 would require one or more of the following:

- 1) the position of the CCD fluctuated independently of the factors controlling sediment distribution,
- 2) calcareous components of the older portions of core -76 deposits were removed post-depositionally, or
- 3) the Gilbert "b" deposits did not occur in an environment receiving any carbonate and do not therefore represent siliceous/calcareous ooze admixtures deposited below the paleo CCD.

In the last case, the siliceous muds might represent sediment accumulated during an episode of decreased primary production and/or increased northward extent or volume of clastic sediments derived from the Antarctic continent. Either of these could have caused an increase in the clay fraction relative to the biogenic fraction sufficient for deposition of siliceous muds. The older (Gilbert "a") sediment of core -73 also lacks carbonate and the younger (Matuyama) sediment bears carbonate.

One other general observation is that no clay deposits occur in cores recovered north of I01176-70. This may represent the control of bottom topography, and bottom-current velocity on sediment distribution. Cores -71, -73, -52 and -76 were at least 200 fathoms above those from the other sites. The location of the recovery sites of these northern four cores along the flank and top of the ridge system, may coincide with a zone of increased bottom current velocity, which has winnowed away considerable amounts of clay. Volume of sediment deposited since the Gauss Magnetic Epoch in the northern four cores compared to contemporaneous deposits at the other core sites supports the winnowing hypothesis.

The lack of clay may also represent the control of depth over sediment distribution. Not only could glacial-marine clays accumulate in the area between cores -66 and -70, but during climatic warming the calcareous ooze depositional zone might have migrated across this area in which the sediment-water interface

was probably always below the CCD. As no carbonate can then accumulate and the belt of siliceous ooze lies to the south, pelagic clays representing the northern fringes of significant deposition of Antarctic continental detritus occurs at great depths. If this were true, however, contemporaneous carbonate-bearing sediment should occur in the cores from shallower water (-71, -52, -73, and -76.) At least in sediment older than about 3.0 m.y.B.P. this is not evident indicating that clays older than 3.0 m.y. B.P. are probably glacial-marine muds. Dissolution of silica may also have occurred at depth and is supported in some cores by poor preservation of diatoms.

Deposition between the Gilbert "b" and "a" events was interrupted in core I01176-76, and is represented by an unconformity. To the south, other cores provide no evidence to suggest regional continuity of the feature, and cores -71 and -76 show continuous accumulation of siliceous mud, which indicates no substantial change in existing climatic conditions.

During the Gilbert "a" core -66 records a change from siliceous mud to ooze. Providing the siliceous mud is the transitional deposit between siliceous and calcareous ooze zone deposits below the CCD proposed earlier this indicates climatic cooling. However, the siliceous ooze seen here could also be partially attributable to other conditions such as (locally?) increased winnowing. In the Islas Orcadas cruise II-core descriptions (Kaharoeddin, 1978) lithologic descriptions of the siliceous ooze layer mention decreasing radiolarian

content with depth and smear analysis from two intervals shows both an increase with depth of the clay fraction and decrease of diatom percentages (Kaharoeddin, 1978). Because the diatom and radiolarian constituents of these sediments are often the coarser fraction of deep sea Southern Ocean sediments, this indicates coarsening upward. If the increased winnowing suggested by the coarsening-upward has climatic significance (which it may not; again, local conditions may be controlling the observed pattern) it would be that cooling occurred; this idea is supported by the presence of clays, probably glacial marine above the siliceous ooze.

Northward, deposition during the Gilbert "a" was dominated by siliceous deposits except in core -67. This core contains clay that would be bounded laterally by siliceous ooze accumulation as indicated from cores -66 and -70. The only explanation for this is local control over sediment accumulation in core -67. If winnowing of sediment and removal of fine fractions occurs on topographic highs as Kurtz (1979) has suggested, then topographic lows, as areas of lower energy, should receive more clay relative to the highs. The local topography of the core -67 recovery site is a "...sediment pond between two abyssal hills" (Kaharoeddin, 1978). The high clay percentage in sediment of this core supports the general model for bathymetry related winnowing. Cores -70, -71, -73, and -76 are the others containing Gilbert "a" deposits that are all either siliceous mud or ooze.

Post Gilbert Pre Brunhes
Conditions

The sedimentary record shows a post-Gilbert "a" gap in deposition that encompassed most of the Gauss and part of the Matuyama Magnetic epoch. Even the three cores that do contain portions of the Gauss (-67, -68 and -71) do not recorded both of the Gauss reversed magnetic events. These cores were recovered from areas that probably were sheltered from increased bottom-water velocity, which caused formation of the hiatus through sediment removal or nondeposition.

In other cores the unconformity above Gilbert "a" deposits has a variety of temporal ranges. In core -64 the unconformity shows its greatest temporal extent. Miocene clays in this core are overlain by Pleistocene sediments hence, the unconformity a maximum time of formation of about four million years (5.0 m.y. B.P. to .7+ m.y. B.P.). I01176-76 shows the shortest temporal extent of the hiatus other than in core -67. In -76 it is bounded below by sediment that record the Gilbert "a" event and above by sediment deposited during the Olduvai. This indicates the duration for a non-depositional event would have been about 2.11 m.y. that it occurred between 3.82 and 1.71 m.y. B.P. If the unconformity is partially attributable to erosion rather than completely to nondeposition the period of formation of the unconformity was probably shorter and occurred during the same time interval.

Other cores containing the unconformity (-66, -70, -71 and -73) have a variety of hiatus lengths. In general, though, these are no

continuous nor of equal magnitude everywhere. The early Gauss sediment of core -71 and the Matuyama sediment of -73 are bounded stratigraphically by unconformities. Furthermore these two layers of sediment were deposited during temporal intervals encompassed in other cores by the regional unconformity. This indicates that possibly at some core sites the record of separate erosional events became superimposed and produced a single unconformity as sediment that accumulated during intermittent periods of deposition was subsequently eroded. In this case, the magnitude of erosion at sites -71 and -73 was relatively lower. Another explanation is that the sites of cores -71 and -73 underwent deposition while at other core sites, erosion or nondeposition was occurring. Again, the magnitude of erosion at -71 and -73 recovery sites had to be less than elsewhere. These sorts of fluctuations between deposition and nondeposition/erosion are likely to have continued throughout the study area, during the formation of the regional unconformity in particular.

The regional unconformity, whether or not it is diachronous or represents continuous erosion/nondeposition suggests at least one major cooling episode between 3.32 and 1.71 m.y. B.P. that must have influenced paleoceanographic conditions to cause widespread scouring. The same regional scouring could have continued longer in the vicinity of cores -64, -70 and -71. However, the Pleistocene hiatuses in these cores may represent different erosional/nondepositional episodes than those that caused the regional unconformity.

Also suggested by the distribution of unconformities in the cores is a shift in the geographic location of nondeposition events. Scouring indicated during the Gauss and early Matuyama appears to have influenced sedimentary conditions throughout the core track; whereas more recent (late Matuyama?) scouring is situated in the northern (cf. cores -52 and -73) and southern (cf. cores -66 and -64) portions of the track area. It is not possible, however, to determine whether or not scouring/nondeposition was actually occurring during the late Matuyama. It may also be erroneous to term the changes in distribution of unconformities a "shift" in scouring/nondeposition, which implies a continuous and migrating erosional zone. The appearance of two areas of erosion may correspond to nondeposition induced by both AABW (in the south) and CPDW (north).

Brunhes and Late Matuyama Changes

The observed fluctuation in sediment types suggests alternating climate deterioration and amelioration during this interval but cooling was possibly not as dramatic as during the Gauss to late Matuyama when a regional unconformity developed.

The post-Olduvai sediment of core -52 alternates between siliceous and siliceous/calcareous ooze. If the record of this core has more than local significance, two explanations, or a combination of these, could account for the alternations. First, the observed fluctuations may represent sediment deposited as the Polar Front Zone (PFZ) migrated north and south over the core-recovery site. The PFZ is the oceanographic

boundary that roughly corresponds to the boundary between siliceous and calcareous-ooze deposits. When this oceanographic boundary was south of the core -52 recovery site, siliceous/calcareous ooze accumulated. When the PFZ was relatively north, siliceous ooze was deposited. The PFZ, like sediment-regime boundaries, is thought to migrate south during climatic cooling and north during warming. As seen in the oceanographic observations of the Islas Orcadas cruise 11 the PFZ corresponds approximately to the position of the ridge axis in this area (Ciesielski, personnel communications) today. This indicates that the position of the PFZ during the late Matuyama was very similar to the present location. High rates of sediment accumulation, characteristic of deposits near the PFZ and also exhibited in core -52, support the argument for close proximity to, and fluctuation of, the PFZ position.

A second explanation of the sediment alternations is a fluctuation in the position of the CCD. Although the CCD might migrate to a shallower position during climatic cooling, other conditions could also influence such a shift. For example, increased productivity of calcareous microorganisms could "leach" oceanic water of much dissolved calcium carbonate. The position of sediment types in core -52 could represent either or both of the above explanations.

As in core -52, fluctuations of sediment occur in core -70. The Brunhes deposits of this core exhibit a variety of lithologic types including siliceous mud and ooze and, probably pelagic, clay. If these fluctuations represent more than local variation in oceanographic conditions, such as episodic

winnowing, climatic fluctuations are suggested. Core -64 exhibits similar fluctuations in lithology during the Grunhes, but these are uncorrelative with the fluctuations in core -70.

The absence of changes in the biostratigraphic and magnetostratigraphic record of the past 0.7 m.y. has prevented correlations of contemporaneous layers of sediment and sediment of like depositional conditions. For this reason it was not possible to formulate a more definitive statement on Pleistocene and Holocene climatic changes.

Summary

The formation of an unconformity during the transition from the Miocene to Pliocene (about 5 m.y. B.P.) recorded in core -66 and -71 suggests climatic deterioration sufficient to have initiated bottom scouring or nondeposition. Unconformities in cores -64 and -71 together with clay deposits and an unconformity in core -66, may indicate either persistent cooling climatic conditions or alternations between warmer depositional episodes and cooler erosional/nondepositional episodes during the early Gilbert.

Deposits of older siliceous ooze, which accumulated before the middle Gilbert "b" magnetic event in the area of cores -66 and -71, represent a climatic amelioration. The diachroneity of the contact between this siliceous ooze and the siliceous mud above indicated continued climatic warming; the widespread deposition of siliceous mud throughout the Gilbert "b" in cores -66, -71 and -76 also reflects continued warm conditions. Unconformities in cores -71 and -76 in late Gilbert age sediment may represent deviations from a stable climate or only variation in local conditions.

Sometime subsequent to the Gilbert "a" a regional unconformity developed. The shortest temporal extent of this hiatus suggests one or more episodes of at least nondeposition between the early Gauss (3.32 m.y. B.P.) and the end of the Olduvai event (1.71 m.y. B.P.). Such a regional unconformity could be formed during drastic climatic deterioration as a result of either nondeposition or scouring of sediment.

Renewed deposition after the Olduvai, including the first accumulations of calcareous sediments in the study region, suggests eventual climatic warming. The diachronous nature of the contact formed by the unconformity may indicate that either the position of scouring/nondeposition migrated or warming was not continuous and, instead, climatic conditions indirectly caused sporadic erosion/nondeposition during this period. Fluctuations could have prolonged nondeposition or caused more than one scouring event. Alternating lithologic types in the Pleistocene portions of core -70 and -52 may reflect migration of the Polar Front Zone and accompanying shifts in sediment regimes as a response to fluctuating climatic conditions.

In the pre-Matuyama record of the cores the location of scouring is represented by an unconformity throughout the area. Scouring seems to have shifted in the late Matuyama or Brunhes to locations both in the south and north of the core track. These two zones of scouring probably reflect the position of scouring by two water masses, the AABW and CPDW. Since the production of CPDW is influenced more by climatic conditions in the northern hemisphere than conditions in the southern hemisphere, unconformities that develop as a result of CPDW may be misleading to determining the paleoclimatic history of the southern hemisphere.

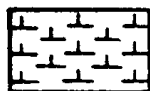
Finally, this study notes a number of instances where local topography may have influenced sedimentation enough to limit the utility of general sedimentation models. It is therefore a conclusion that local conditions, particularly topography, exert a profound influence on sediment distribution.

Appendix I

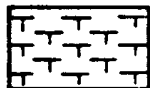
Figures 16-29 represent detailed descriptions of sediment lithology in the cores and corresponding magnetic and biostratigraphic information. Also shown are the sampled intervals, deformation that occurred during coring, and the ages of the sediment as defined biostratigraphically.

KEY

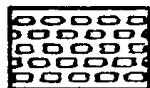
SYMBOLS USED FOR CORE DESCRIPTIONS



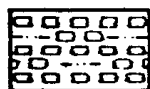
Nannofossil ooze



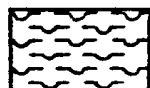
Foraminiferal ooze



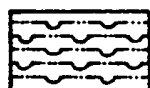
Calcareous ooze



Marly, calcareous ooze



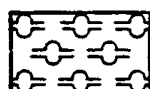
Diatomaceous ooze



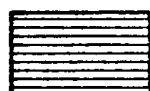
Muddy, diatomaceous ooze



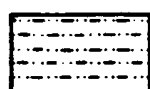
Radiolarian ooze



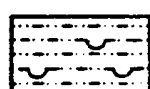
Siliceous ooze



Pelagic clay



Mud



Diatomaceous mud



Sand



Volcanic ash



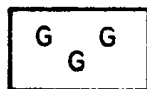
Breccia



Lapilli, pumice



Gravel, rocks, rock fragments



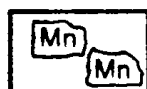
Glauconite



Sedimentary clasts



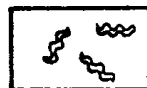
Sedimentary casts



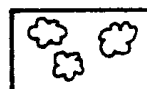
Manganese nodules



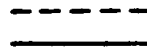
Disseminated manganese oxides



Bioturbation



Mottling



Gradational contact



Sharp contact

303

Core section "breaks"



Scale change



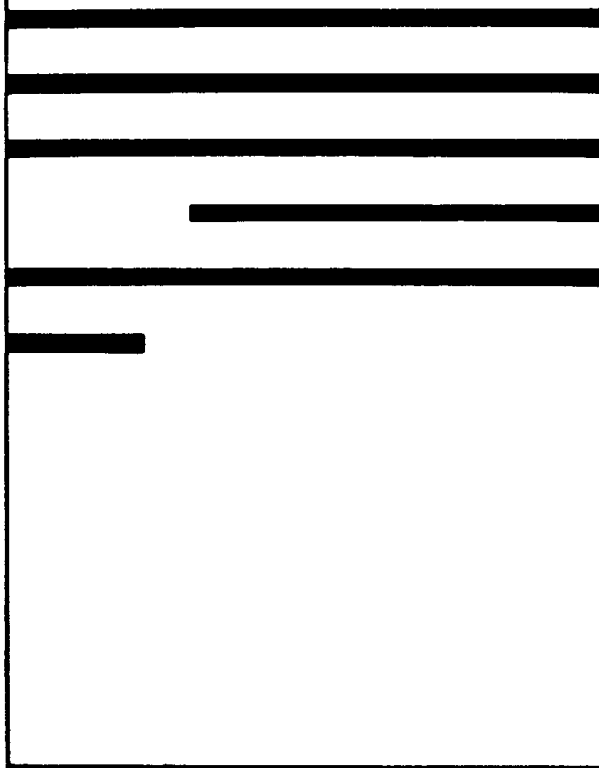


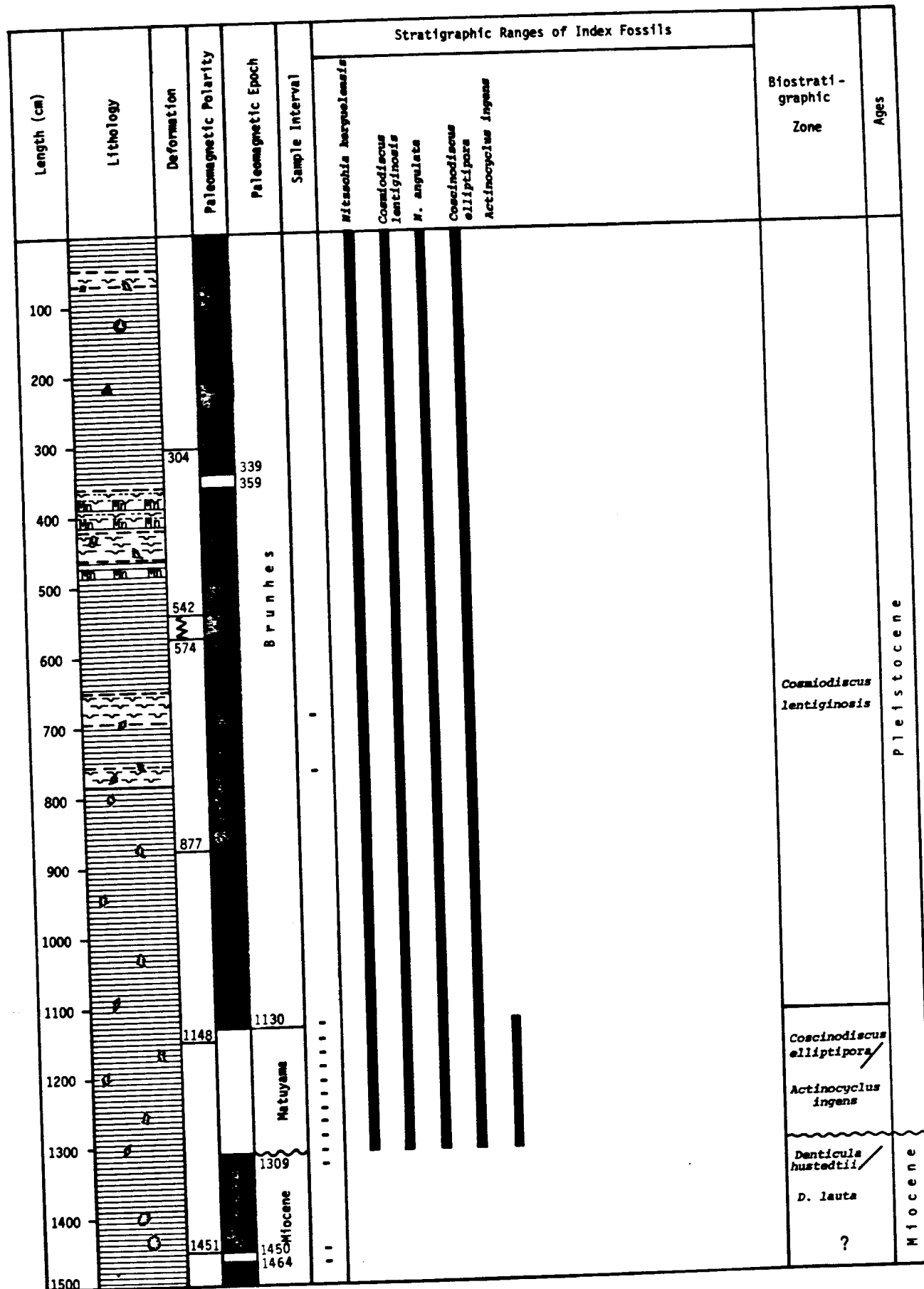
Slightly disturbed



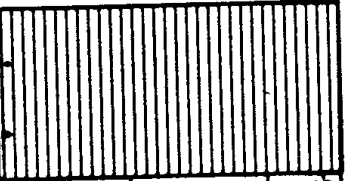

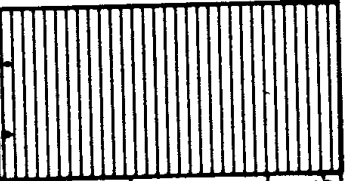

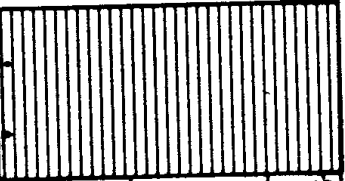

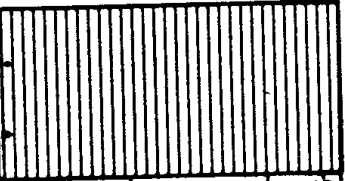

Very disturbed

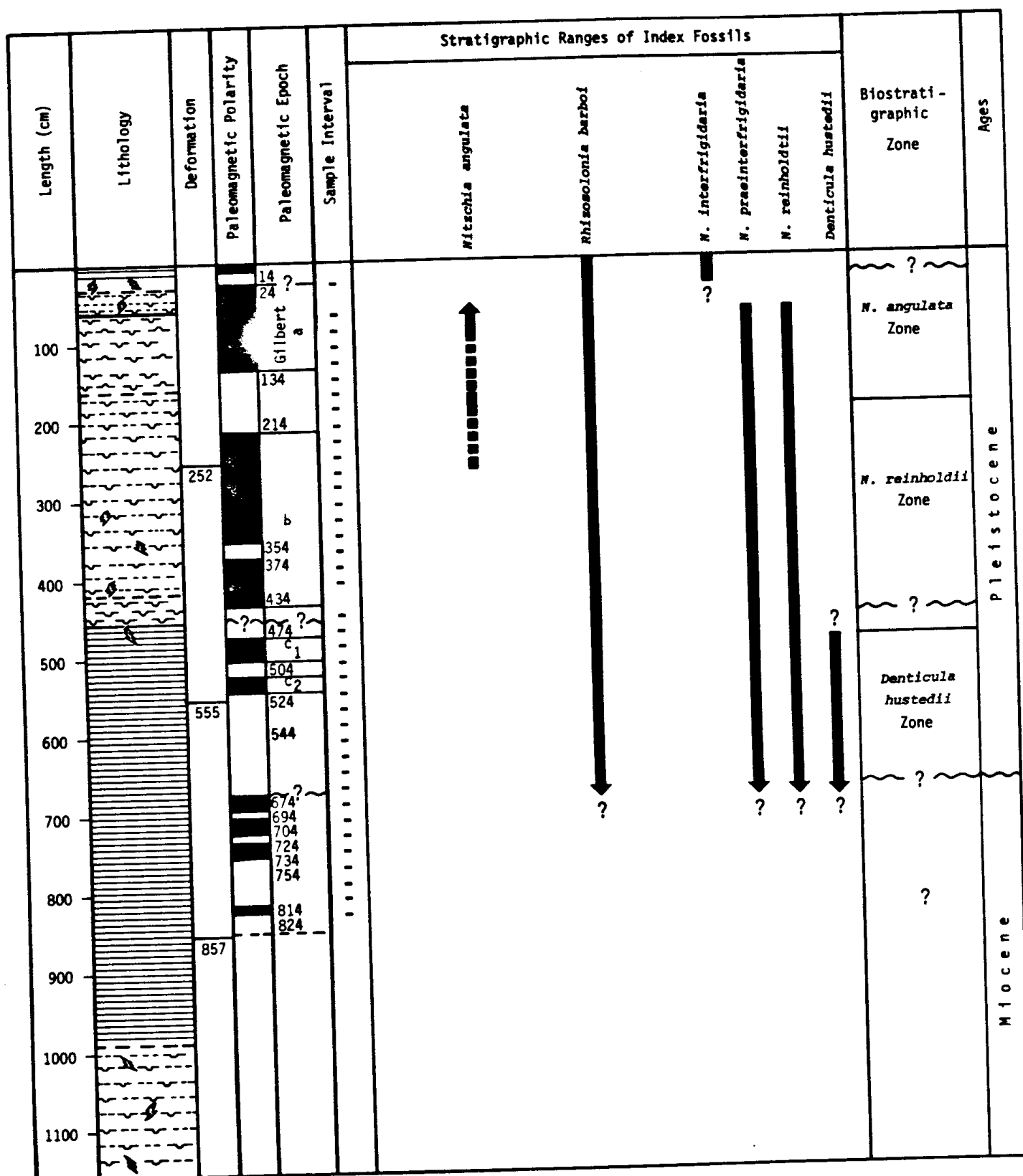
Length (cm)	Lithology	Deformation	Paleomagnetic Polarity	Paleomagnetic Epoch	Sample Interval	Stratigraphic Ranges of Index Fossils					Biostratigraphic Zone	Ages
						<i>Nitacinthis baryuensis</i>	<i>Coscinodiscus lentiginosus</i>	<i>N. angulata</i>	<i>Coscinodiscus elliptipora</i>	<i>Actinocyclus ingens</i>		
100			58								
200												
300			359							<i>Coscinodiscus elliptipora</i> <i>Actinocyclus ingens</i> Zone	Pleistocene
400												
500			664								
600												
700											
750												

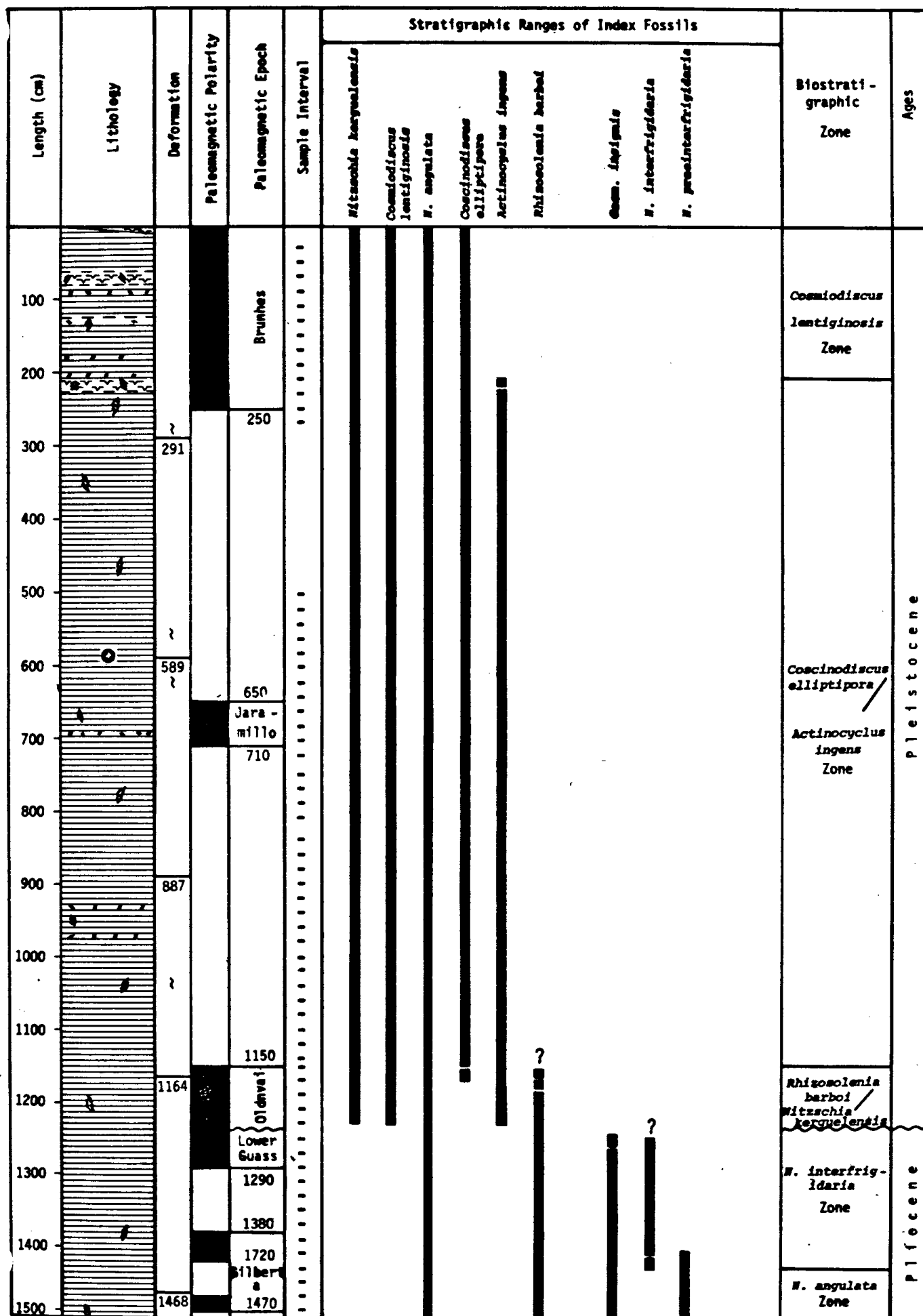
969	900	800	Length (cm)	
			Lithology	
			Deformation	
			Paleomagnetic Polarity	
Olduvai 920			Paleomagnetic Epoch	
• • • • •			Sample Interval	
			Stratigraphic Ranges of Index Fossils	
Rhizosolenia barboi / Nitzschia kerguelensis		Actinocyclus ingens Zone		Biostratigraphic Zone
Coscinodiscus elliptipora /				
Pleistocene			Ages	



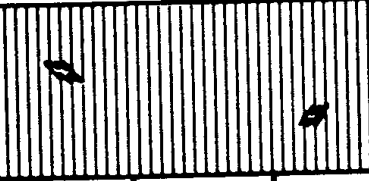
ISLAS ORCADAS 11-64

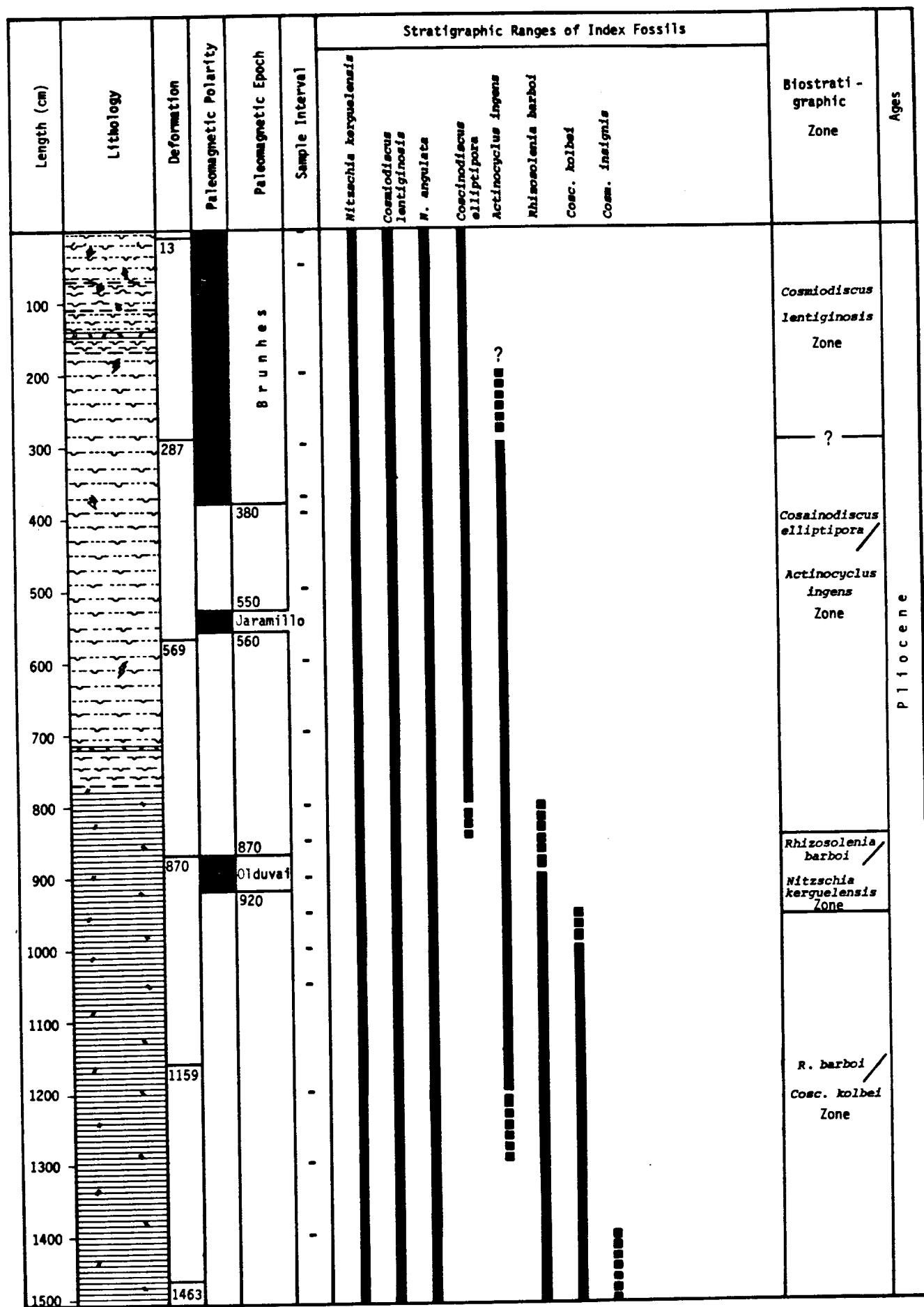
MIOCENE		Ages		Stratigraphic Ranges of Index Fossils		Biostratigraphic Zone	
Length (cm)	Lithology	Deformation	Paleomagnetic Polarity	Paleomagnetic Epoch	Sample Interval		
1600				1534		
				1554			
				1564			
				1574			
				1584			
				1614			
				1634			
				1644			
				1684			
				1714			
1700							
1756							



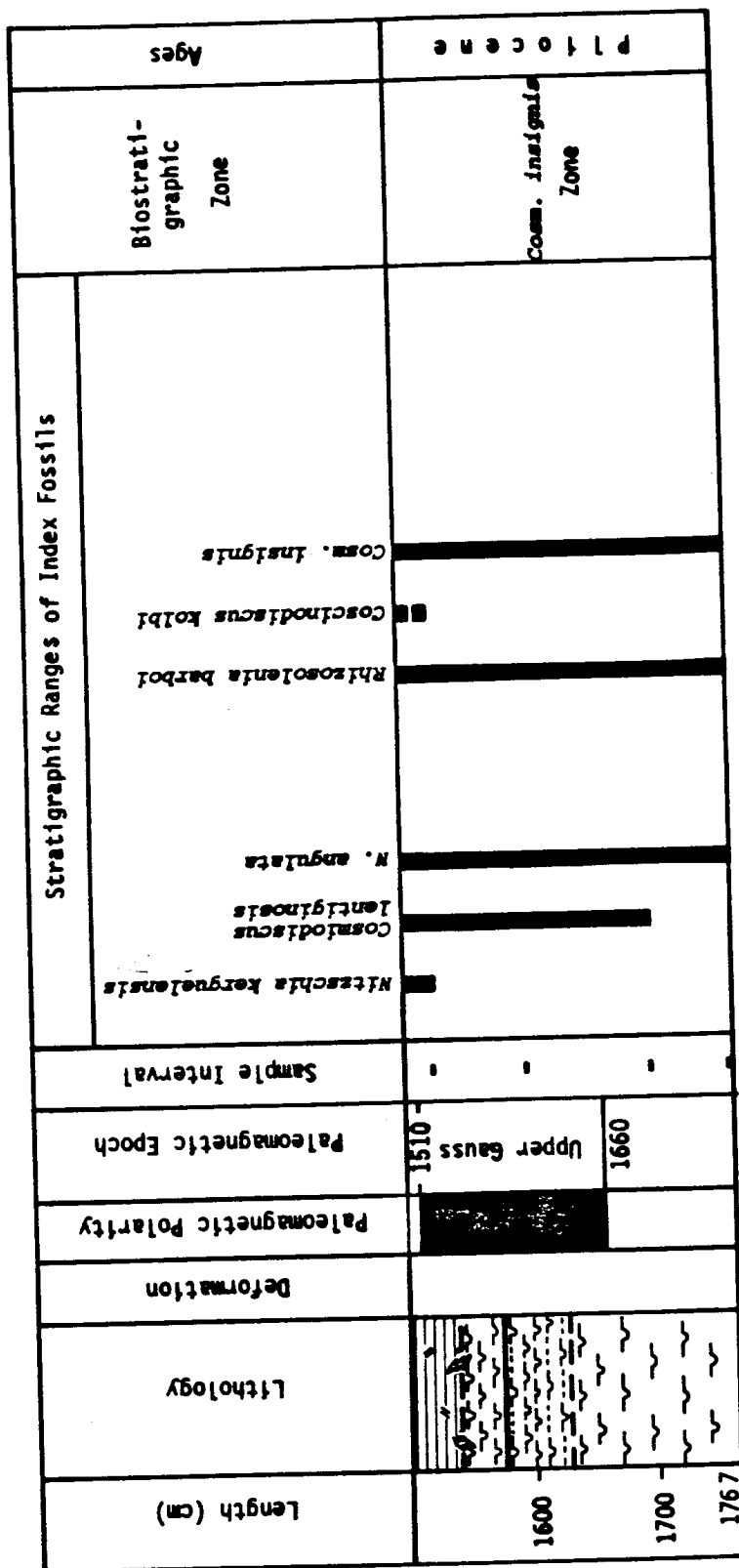


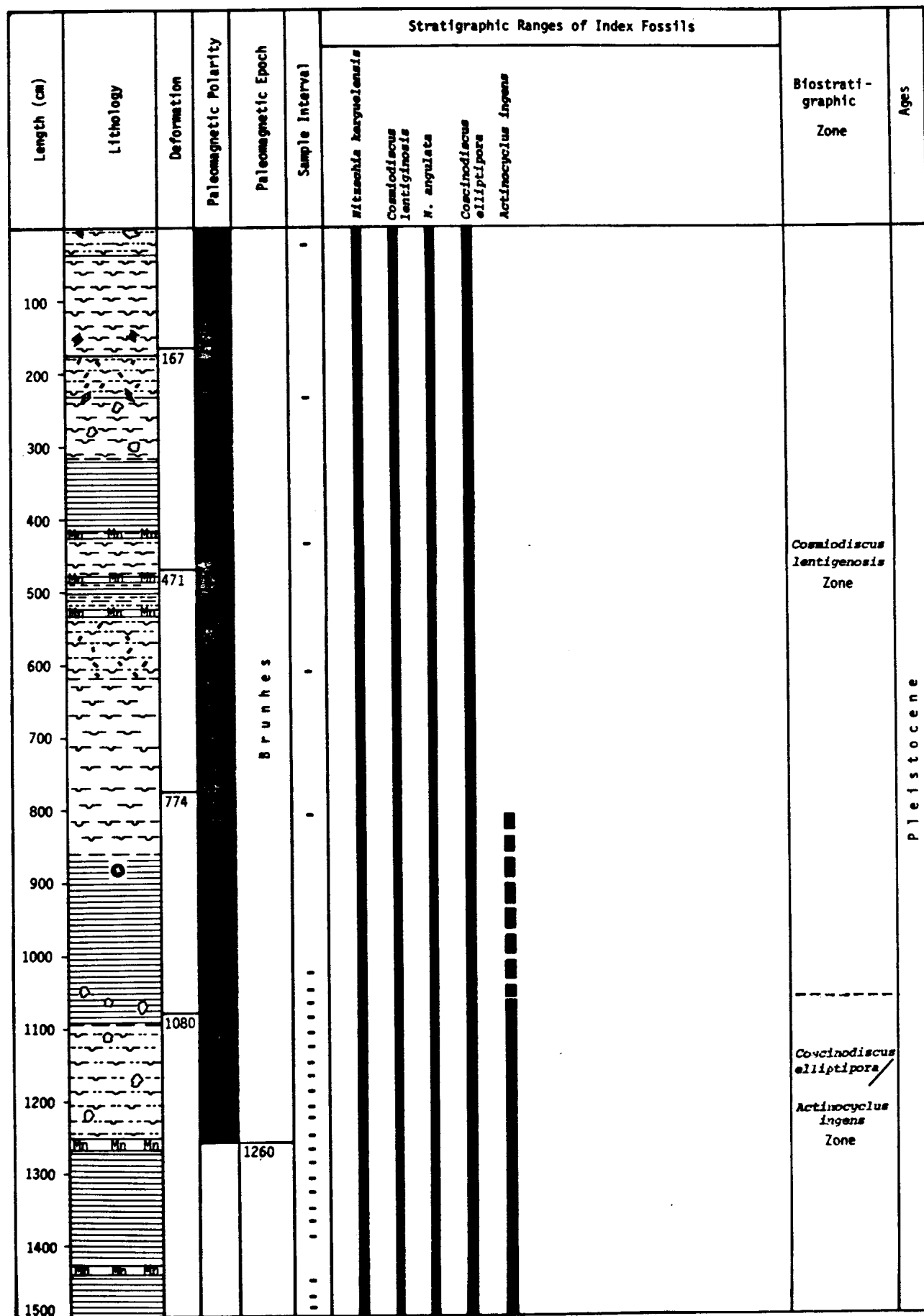
ISLAS ORCADAS 11-67

Length (cm)	Lithology	Deformation	Paleomagnetic Polarity	Paleomagnetic Epoch	Sample Interval	Stratigraphic Ranges of Index Fossils	Biostratigraphic Zone	Ages
1600 1700		Flow In 1640			<div> <div>N. angulata</div> <div>Rhizosolenia barboi</div> <div>Cosm. insignis</div> <div>N. praeteritrigidaria</div> </div>	N. angulata Zone	Pliocene



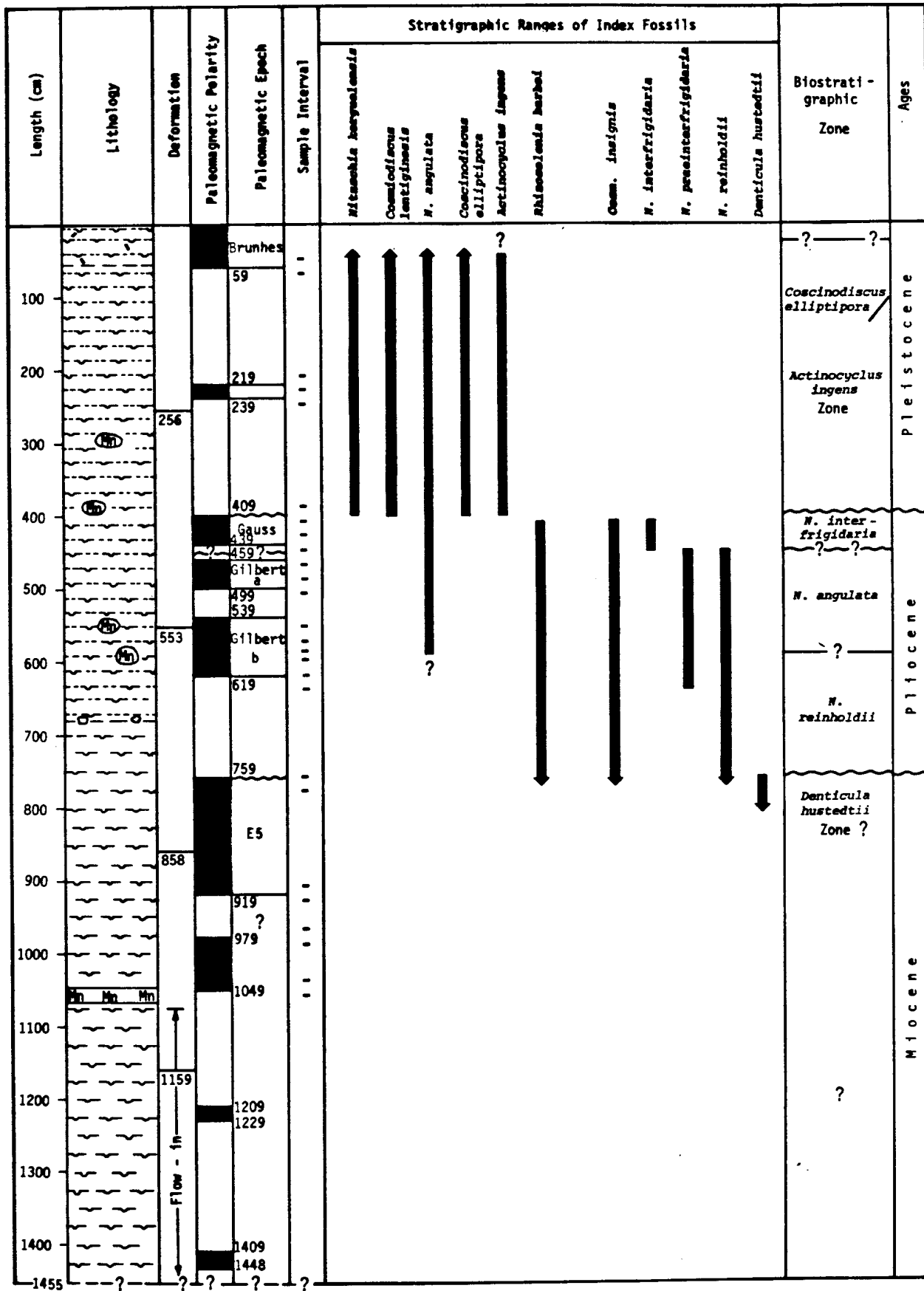
ISLAS ORCADAS 1176-68

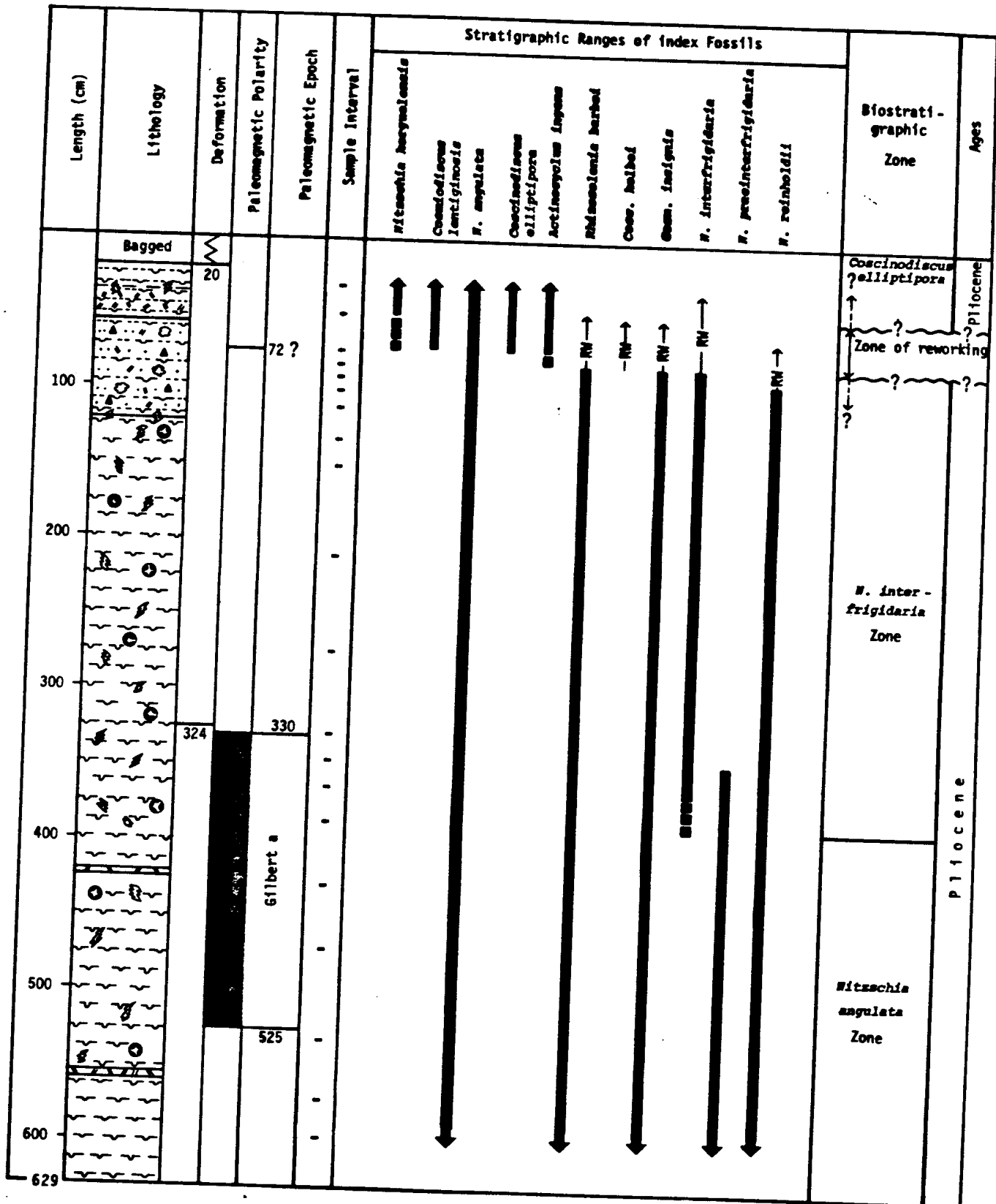




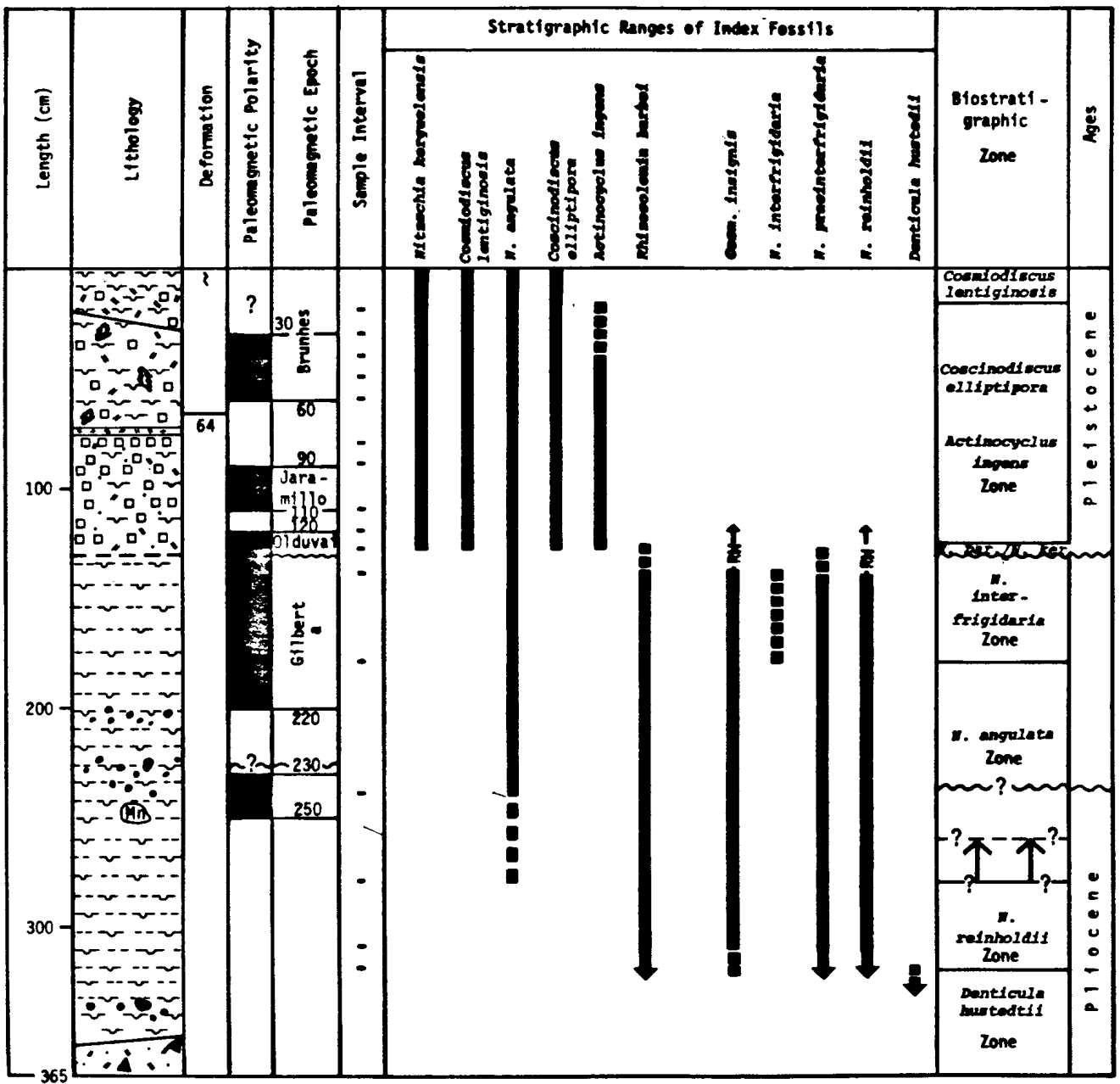
ISLAS ORCADAS 1176-70

Length (cm)			
Lithology			
Deformation			
Paleomagnetic Polarity			
Paleomagnetic Epoch			
Sample Interval			
		Stratigraphic Ranges of Index Fossils	





ISLAS ORCADAS 1176-76



APPENDIX II

The graphic method of correlation used in this study was originally developed by Shaw (1964) to provide a means of correlating portions of a sedimentary sequence with the contemporaneous parts of other sequences. The tops and bases of fossil ranges from the two sections being correlated are plotted as points on a two-axis graph. One axis serves as a numerical reference for the stratigraphic position of the tops and bases of these ranges in one sedimentary sequence and the other axis is a similar reference of the second sequence of the correlation. Figure 30 is an example of a plot of points representing the tops (+) and bases (0) of fossil ranges in two sedimentary sequences. (Shaw has recommended that the positions of these points be measured in physical units of length [feet, centimeters, etc.] from the base of the sedimentary section. In the cores included in this study, however, measurements were made from the core top down to keep with the convention of numbering a core top as 0.) If two or more points are plotted in this manner a line can be fitted to the graph. This line is called the Line of Correlation (LOC).

The graph produced by this procedure is a variation of graphic solutions of motion problems, which employ the equation $D = R \times T$ (Figure 31).

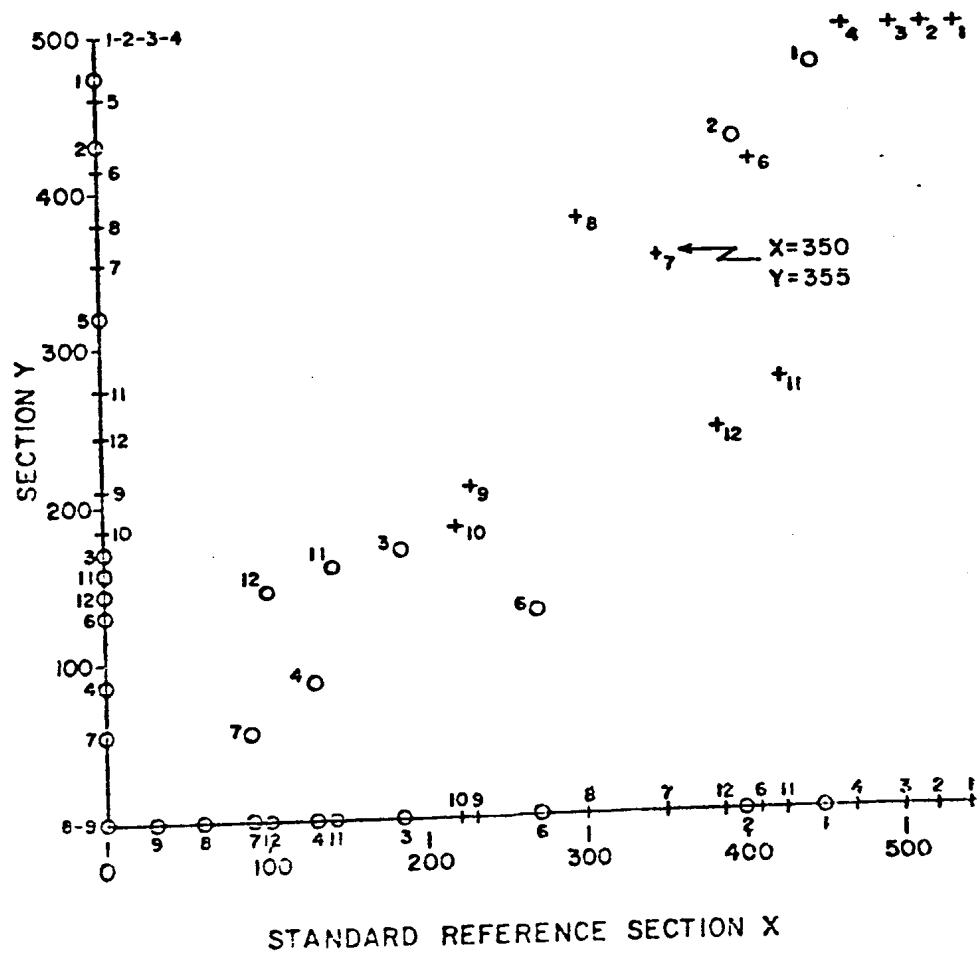


Figure 30. Graphic plot of tops (+) and bases (0) of fossils in a SRS and a sedimentary section. (Miller, 1977.)

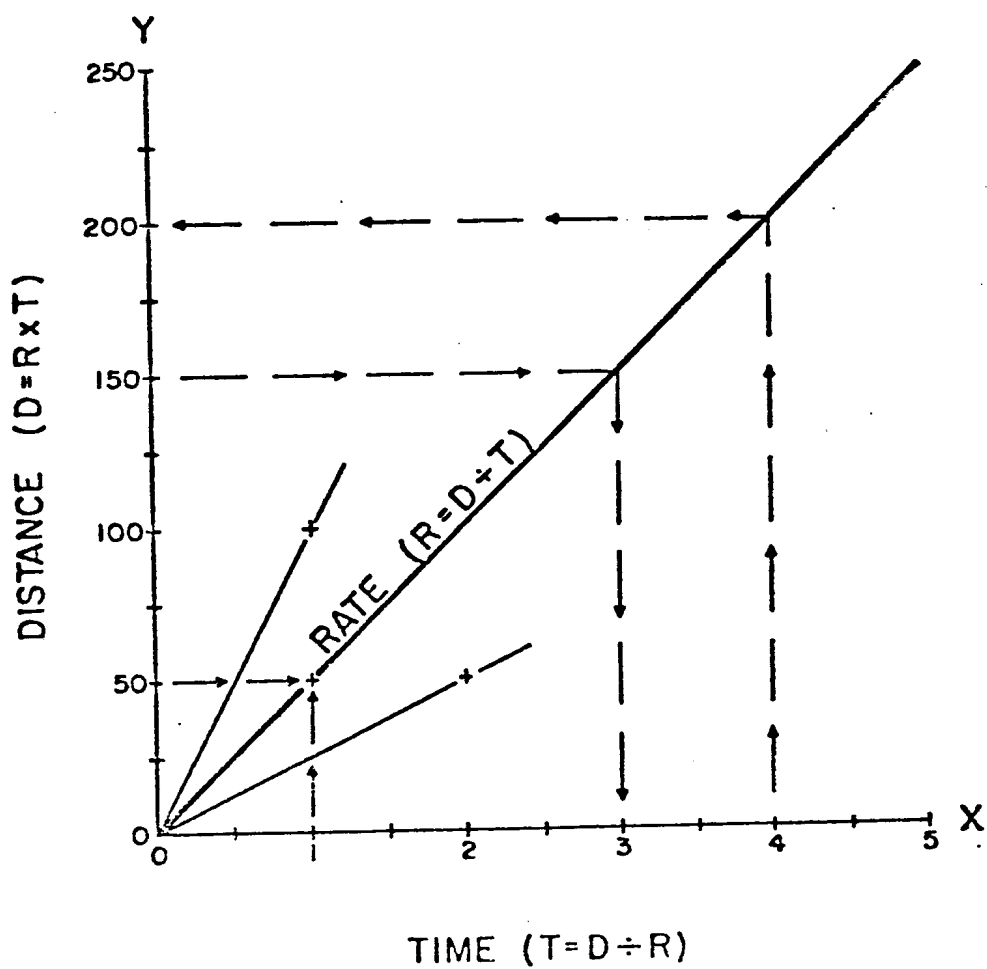


Figure 31. Illustration of the graphic solution to motion problems. (Miller, 1977.)

From one axis (conventionally the X-axis) the pertinent stratigraphic information from the Standard Reference Section (SRS) is derived. The SRS should be the most complete section (unbroken by faults or unconformities if possible) and one whose stratigraphic ranges of fossils most closely approximate the total possible range of those fossils. The ranges contained in the SRS and the chronological scale resulting from those ranges are accurate by definition. A Composite Standard (see below), if developed, is analogous to the time (t) portion of $D = R \times T$ graphs. The other axis (Y-axis) serves as the distance (D) portion of the graph (distances measured as numerical stratigraphic positions of range limits). The LOC represents the rate (R) portion of the graph and enables correlations from the two axes to be made. When the axes represent two individual sections (cores) the rate expressed by the LOC is the relative rate of rock accumulation. If the slope of the LOC is one the rock accumulation rates of the two cores were relatively equal; if the slope is two the rate of sediment accumulation of the core plotted on the Y-axis is twice that of the core plotted on the X-axis, and so on. If the line is a straight line it may represent the average relative rate of sediment accumulation for the time interval. Such a line might actually contain numerous doglegs where changes in slope represent minor fluctuations in the relative rate.

The LOC is fitted to the plotted points in the following manner. The ranges of fossils in the SRS are assumed initially to be those most closely approximating the total possible ranges of the fossils and it is unlikely that these ranges would be as closely approximated in other sections. Since most of the range limits from the two sections are not, therefore, exact time equivalents, they will not fall directly on an accurate LOC. Rather, if in fact the SRS ranges were the closer approximations to the total ranges, plots representing stratigraphic range bases will fall to the left of an accurately placed LOC and plots of tops, to the right (that is only if numbers representing stratigraphic occurrence of these events increase with decreasing age of the section). Later, after the LOC is drawn, correlation of similar events (range limits) will indicate whether or not the ranges in the SRS were closer to the total ranges. Some points may not be confined to the appropriate side of the graph by drawing the LOC as described above. These points represent tops and bases that in the correlated section, are closer to the total range of the fossils than the stratigraphic occurrences in the SRS. Figure 32 is the plot of points seen in Figure 30 with a LOC drawn that confines the majority of bases (0) to the left side of the graph and the majority of tops (+) to the right.

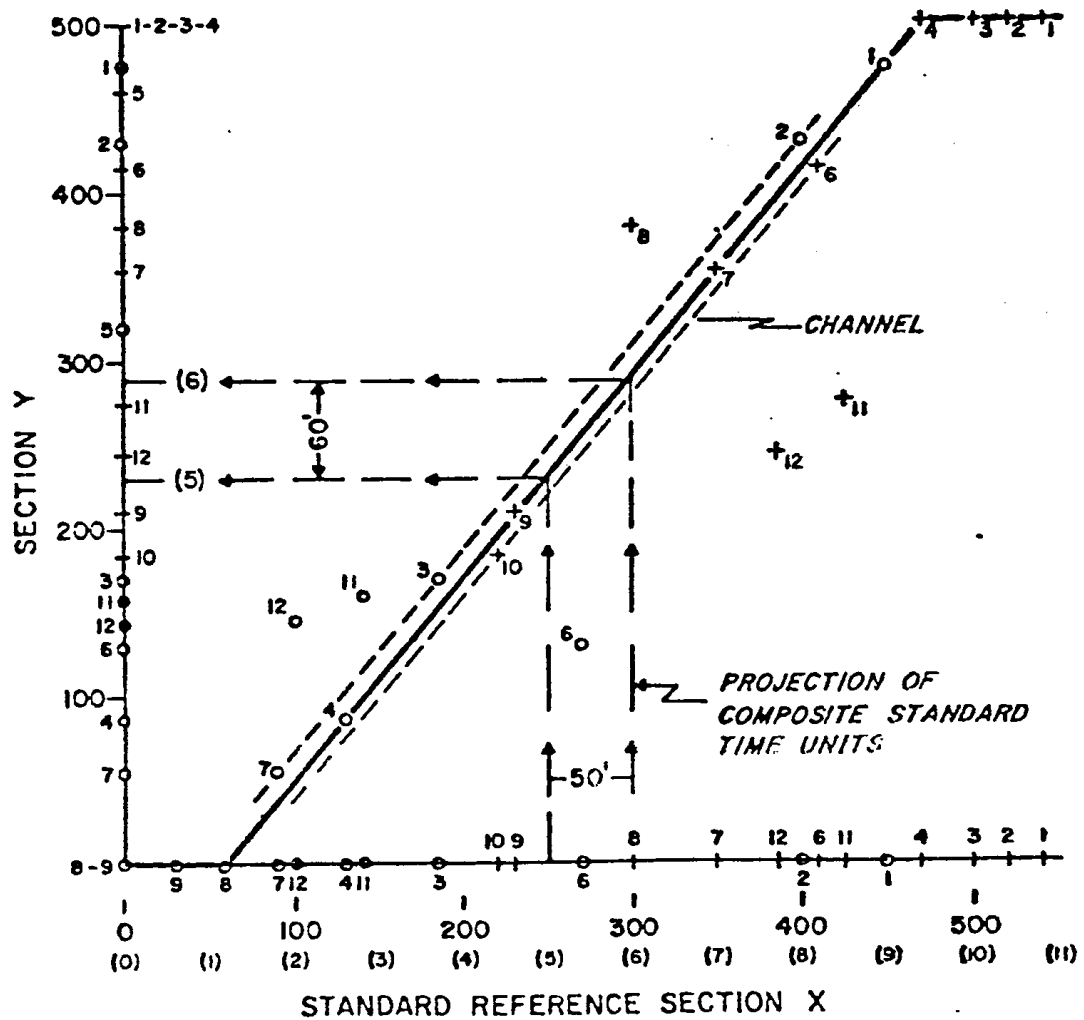


Figure 32. Graphic plot of tops and bases of fossils with a LOC (Miller, 1977).

At this point in the correlation, after plotting the first two sections, the original procedure of the graphic method called for the transfer of information on the Y-axis to the X-axis graphically using the LOC or mathematically using the equation of the LOC. This indicates whether or not the stratigraphic ranges in the SRS were the closest representatives of the total ranges of the index fossils as previously assumed. The compilation of information in this manner creates a Composite Standard (CS) to which information from other sections can be correlated and incorporated. (The ranges of fossils in the Composite Standard are considered the closest approximations to the total ranges of those fossils. New information added to the CS either does not affect those ranges [falls within the previous CS ranges] or lengthens the stratigraphic ranges making them closer approximations of the total ranges.) In this study the development of a Composite Standard was unnecessary. The graphic correlations were made only to determine the accuracy of magnetic assignments of magnetic reversals identified in the core stratigraphies.

When an LOC is fitted to plotted points representing the tops and bases of the stratigraphic ranges of fossils, some points may fall on the LOC itself. These points represent chance "simultaneous" preservations in both sections and, thus, the range limits shown on the graph by these

points have the same time-stratigraphic occurrence in both sections of the correlation.

Like the plots of total stratigraphic ranges of fossils and other points falling on the LOC, plotted points representing any time-significant events, such as the bases of volcanic ash layers or recorded magnetic reversals should fall on the LOC provided they are preserved in both sections being correlated. However, if two different time significant events, such as the base of the Gilbert "a" in one core and Gilbert "b" in another are identified and plotted as the same event (the Gilbert "a", for example) then the point representing this "event" should be well off the LOC. If a LOC is drawn using this point, its slope would appear anomalous. The major drawback to checking magnetic-event assignments in this manner is that should a particular event recorded in two cores be misidentified similarly in both, the subsequent plot of the misidentification would not appear anomalous. Therefore, it is essential to have one core in which magnetic reversals have been identified accurately. The core can then be used for correlation and checking reversal identifications.

In this study the method chosen was to select as an SRS one core with the most complete stratigraphic record and to correlate all other cores to it. This permitted examination of tentative identifications of magnetic events while still

using the control afforded by the plots of biostratigraphic data. The magnetic event assignments could have been checked using an hypothetical core created by assigning a standard magnetic time scale (Figure 14) a constant rate of sediment accumulation (5 cm./1000 yr., for example). However, then if doglegs appeared in the LOC's, they could not have been interpreted exclusively as representing fluctuations in the rate of sediment accumulation. The doglegs could also have indicated a misidentified event sequence and no means of differentiating between the alternatives would have existed. For this reason a core, with the additional advantage of independent biostratigraphic data, was used as the SRS.

Because the cores in this study exhibit a division into two main groups, separated by a regional unconformity, two SRS's were chosen. One was for cores with sediment containing a record of magnetic events identified tentatively as middle Gauss through Brunhes and one to cores with tentative event assignments from middle Gauss to the pliocene/Miocene boundary. Bases of biostratigraphic and magnetostratigraphic events are represented by "." and tops by "+."

For the younger group core I01176-68 was chosen as the SRS. It is complete (unbroken stratigraphically) and

contains the oldest preserved magnetic event (Mammoth event, $t = 3.085-3.0$ m.y. B.P.) of all the portions of cores above the regional unconformity.

I01176-66 served as the SRS for the older (pre-Mammoth) portions of the cores.

The Correlations

Figures 33, 35-45 are the graphic representations of information summarized in Table IV and Table V.

Figure 33 is the graphic correlation of I01176-68 and I01176-52. Unfortunately the biostratigraphic information contained in core -52 is insufficient to verify graphically the accuracy of the Olduvai magnetic event assignment given to the reversal recorded near the base of core -52. Despite this, the assignment of Olduvai is made with confidence. The points T6 (T = top) and B4 (B = base) (see Tables IV and V for number following T or B) occur close enough temporally to the top of the Olduvai and far enough from the top of any other magnetic normal that, provided sedimentation rates are sufficiently high, no problems seem to exist with this identification.

Evident in Figure 33 are the horizontal dashed line at 28 cm. (-52) at of 948 cm. (also -52). Those plateaus, as referred to in the figures, represent sampling inadequacies and unconformities in the stratigraphic record. Could a LOC be fitted to this graph, these

TABLE IV

Paleomagnetic Polarity Changes of Events (cm.'s from core top)

Proposed Paleomagnetic Events (Plotting symbols)	I01176-									
	66	64	67	68	70	71	52	73	76	
Brunhes (B)	T	T-	T-	T-	T-	T-				
	B	1130	250	380	1260	59				
Jaramillo (J)	T		650-	530		219-		72-	90-	
	B		710	560		239		73?	110	
Olduvai (V)	T		1150-	870-			920-		120-	
	B		1228	920			B		130	
Gauss (U)	T			1510-						
	B			1660						
Gauss (M)	T									
	B									
Gauss (L)	T		1228-			399				
	B		1290			939				
Gilbert A (a)	T	24-	1380-		1580-	459-		330-	130-	
	B	134	1490		B	499		525	200	
Gilbert B (b)	T	214-				539-			230-	
	B	434				617			250	
Gilbert C ₁ (C ₁)	T	474-								
	B	504								
Gilbert C ₂ (C ₂)	T	524-								
	B	544								

T = Core top

B = Core base

TABLE V

BIOSTRATIGRAPHIC RANGES (cm.'s from core top)

TAXA		64	67	68	70	71	72	73	76
IO11760									
66									
Nitzschia kerguelensis	T ---	0-	0-	0-	28-	48-	28-	33-	18-
(1)	B	1308	1228	1720	1528	388	948	71	130
Cosmiodiscus lentigenosis	T ---	0-	28-	0-	28-	48-	28-	33-	18-
(2)	B	1308	1228	1700	1528	388	948	71	130
N. angulata	T 68-	0-	28-	0-	28-	48-	28-	33-	18-
(3)	B 268	1308	1588	1767	1608	600	948	591	280
Coscinodiscus elliptipora	T ---	0-	28-	0-	28-	48-	28-	33-	18-
(4)	B	1308	1168	850	1528	388	928	71	130
Actinocyclus ingens	T ---	1128-	208-	200-	618-	48-	28-	33-	20-
(5)	B	1308	1228	1300	1528	388	948	84	130
Rhizosolenia barthei	T 28-	---	1168-	850-	1538-	408-	928-	84-	128-
(6)	B 828	---	1588	1767	1608	638	948	591	320
Cosmiodiscus insignis	T ---	---	1248-	1400-	1538-	408-	---	84-	138-
(8)	B	---	1588	1767	1608	590	---	591	320
N. interfrigidaria	T 28-	---	1248-	---	---	408-	---	84-	138-
(9)	B 50	---	1428	---	---	448	---	388	180
N. praeinterfrigidaria	T 68-	---	1428-	---	1538-	468-	---	348-	138-
(10)	B 668	---	1588	---	1608	638	---	591	320
N. reinholdii	T 68-	---	---	---	1538-	468-	---	84-	238-
(11)	B 688	---	---	---	1608	638	---	591	320
Denticula hustedtii	T 468-	---	---	---	---	758	---	---	320
(12)	B 828	---	---	---	---	---	---	---	---
Cosc. kolbei	T ---	---	---	900-	---	---	---	---	---
(7)	B	---	---	1520	---	---	---	---	---

T = core top
B = core base

lines would be locations of shifts in the horizontal position of the LOC (see Figure 34 as an example of this). The plateaus in Figure 33 represent contributions causing the inability to fit a LOC to this graph.

Figure 35 is the correlation of 101176-64 with the SRS. As in Figure 30, no LOC could be accurately fitted to the points. Nonetheless, the Brunhes assignment to the magnetic normals at the tops of both cores is probably correct because of the unreasonably high rates of sediment accumulation that would be necessary if a magnetic event other than Brunhes were identified.

The coincident points T1, T2, T3, and T4 represent the tops of the ranges of fossils 1-4, which occur stratigraphically together in all the cores (with sediment of appropriate age). These diatoms are extant in the Southern Ocean and because of this the tops of their observed stratigraphic occurrences are controlled by either deposition or sampling and have no time significance. For this reason they have not been considered in any fit of an LOC.

The correlation of 101176-67 with the SRS (Figure 36) contains enough biostratigraphic information to support the magnetic identifications. The slope of the LOC, which is drawn through Tj, Bj and TV, is similar to that which would be expected from an LOC based on biostratigraphic

points T5 and the coincident points (⊕) B6 and B4. Some problem arises in explaining the position of the Brunhes (B) base plot although the accuracy of this magnetic event assignment is acceptable (the Brunhes is the only magnetic normal since the Jaramillo). The only alternative is that the normal interval identified as the Brunhes in core -67 is actually part of the Jaramillo but includes a section of magnetically reversed sediment. The extremely high sediment accumulation rates resulting from such an explanation would be difficult to explain (14.2 cm/1000 yr.). The possible alternatives that remain include the acceptance of the event as Brunhes and these explanations are: (1) the position of the Brunhes base has been misidentified slightly in one or both cores or (2) something has caused the rate of sediment accumulation in core -67 between the Brunhes and Jaramillo events to increase relative the rate in core -68.

The correlation of cores I01176-70 and the SRS (Figure 37) has probably not yielded an accurate LOC. Confidence in the identification of the base of the Brunhes magnetic event is still high considering biostratigraphic problems and the very high rates of sediment accumulation that would accompany alternative assignments.

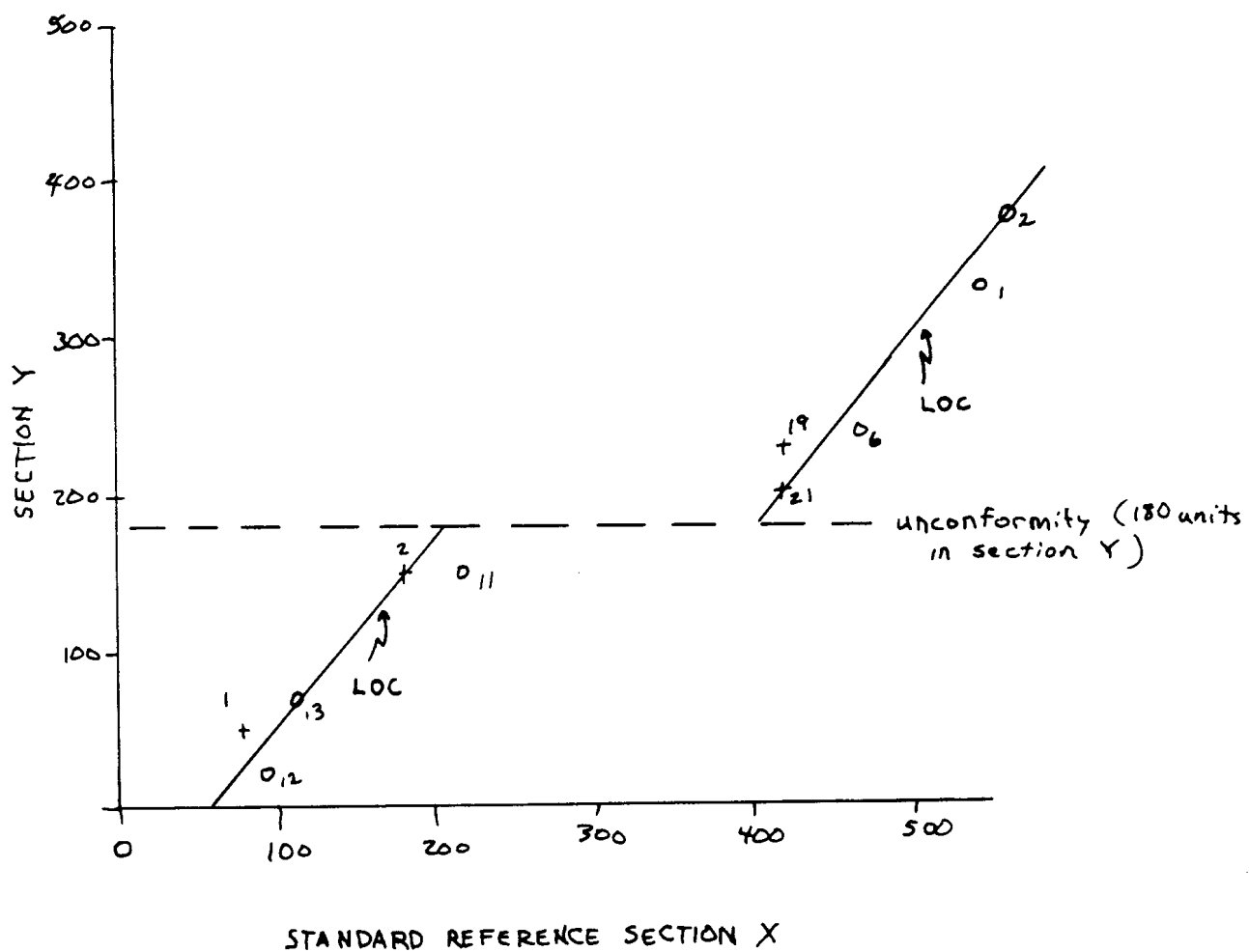


Figure 34 Graphic plot of stratigraphic events and a LOC exhibiting the "plateau" effect due to omission of strata or inadequacy of the sampling coverage.

Although, as in Figure 36, the correlation of I01176-71 and the SRS (Figure 38) does not provide enough accompanying biostratigraphic evidence to confirm graphically the identification of magnetic-event assignments, the alternatives have biostratigraphic problems and questionably high rates of sediment accumulation.

The correlation of I01176-73 with the SRS (Figure 39) has no magnetic reversals plotted (none occurs above the zone of reworking from 71 to 84 cm. in core -73). This graph was included to provide another example of the effect of sampling inadequacies and unconformities on the distribution of points.

The correlation of I01176-76 with I01176-68 (Figure 40) exhibits the dogleg form of the LOC mentioned above and represents fluctuations in the relative rates of sediment accumulation in the two cores. As in most other previous examples, alternatives to the assigned magnetic event present difficulties. In this graph the LOC is not substantiated by plots of biostratigraphic information. An alternative LOC, represented by the dashed line, takes better account of biostratigraphic points.

Figure 41 is the first figure of correlations involving core sediment tentatively identified as stratigraphically below the regional unconformity and is a correlation between I01176-66 (the SRS) and I01176-67. The graphic correlation does not support the tentative

identification of the Gilbert "a" event in I01176-67. Therefore, the sole basis for this assignment is the correlation between the stratigraphic record of magnetic reversals and the assigned biostratigraphic zones (cf. Appendix I).

Figure 42, the correlation of I01176-70 with the SRS, contains only one point of interest (the top of the Gilbert "a") and does not confirm the accuracy of that tentative identification. As with I01176-67, the identification of this magnetic event is based on biostratigraphic correlation alone.

Figure 43 is the correlation of I01176-71 to the SRS. The LOC drawn through points Ta, Tb, Ba and Bb appears well supported by points B9, T10 and T11 which occur very close to the LOC and substantiate the assignment of magnetic event names.

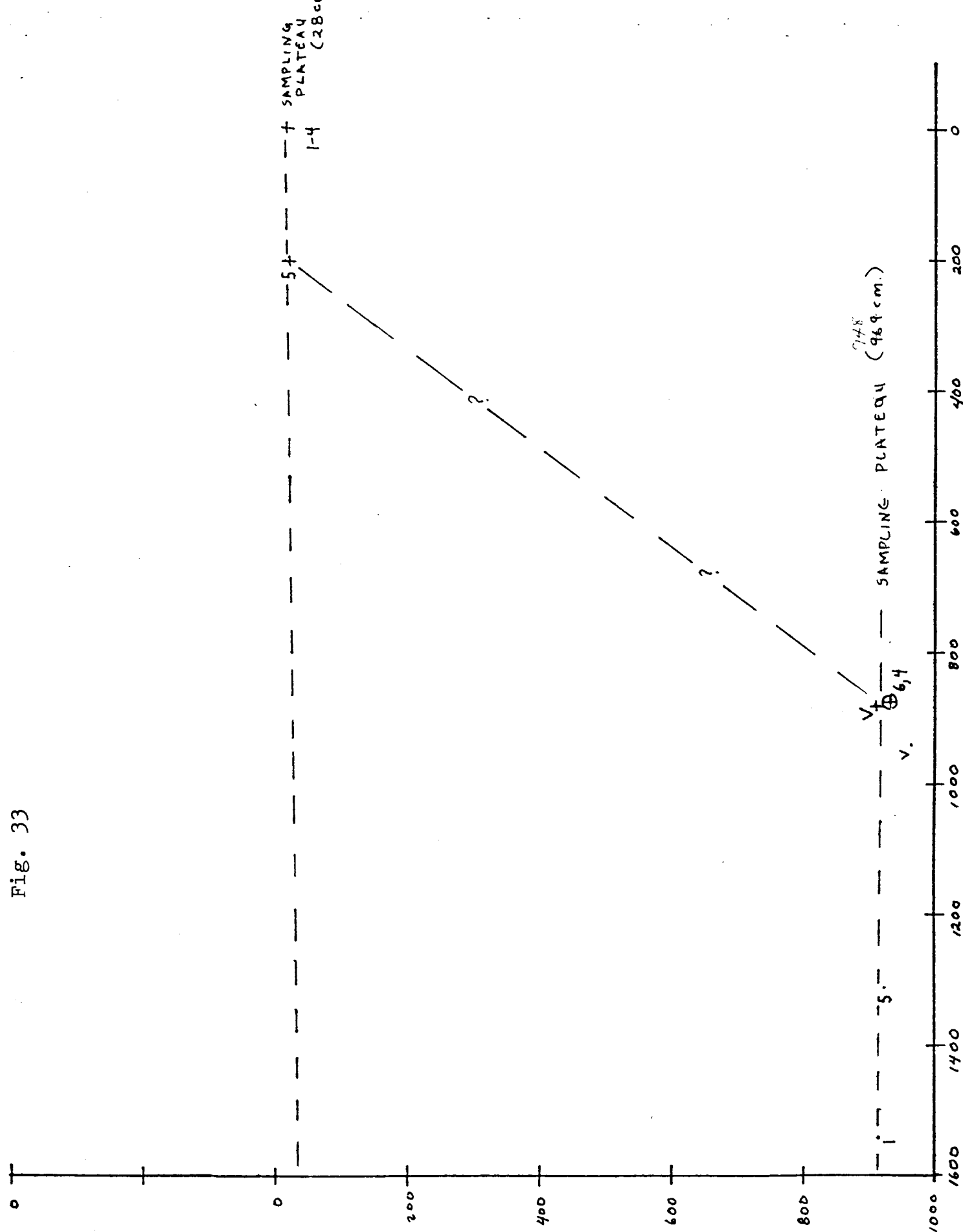
In the graphic correlation of I01176-73 to the SRS (Figure 44) the position of points B9 and T10 do not necessarily support the position of the LOC or the identification of the magnetic event Gilbert "a."

Figure 45 is the final graphic correlation discussed here and is between I01176-76 and the SRS. The distribution of most biostratigraphic points seems to support the position of the LOC (and the magnetic assignments). The

position of B3 is difficult to explain. Transferring the point to the SRS (by means of the LOC) would place this stratigraphic event far below the position of the range base in the SRS. A number of explanations including misidentification of the range base, contamination of lower (stratigraphically) samples and slides, reworking downward of sediment containing the fossil (N. angulata), a change in the slope of the LOC to the right of point Bb and, finally, the actual time-stratigraphic occurrence of N. angulata low in the sedimentary record might account for the position of B3.

Another explanation of the apparently anomolous relationship is that the LOC in Figure 45 and also in Figure 43 has been drawn through points misidentified as Bb and Tb. Alternatives to the LOCs in these figures drawn through B3 and Ba in 45 and B9 and B3 in Figure 43 are dashed lines and suggest the Gilbert "b" magnetic event in -66 was misidentified.

Fig. 33



IO1176-52

Fig. 33

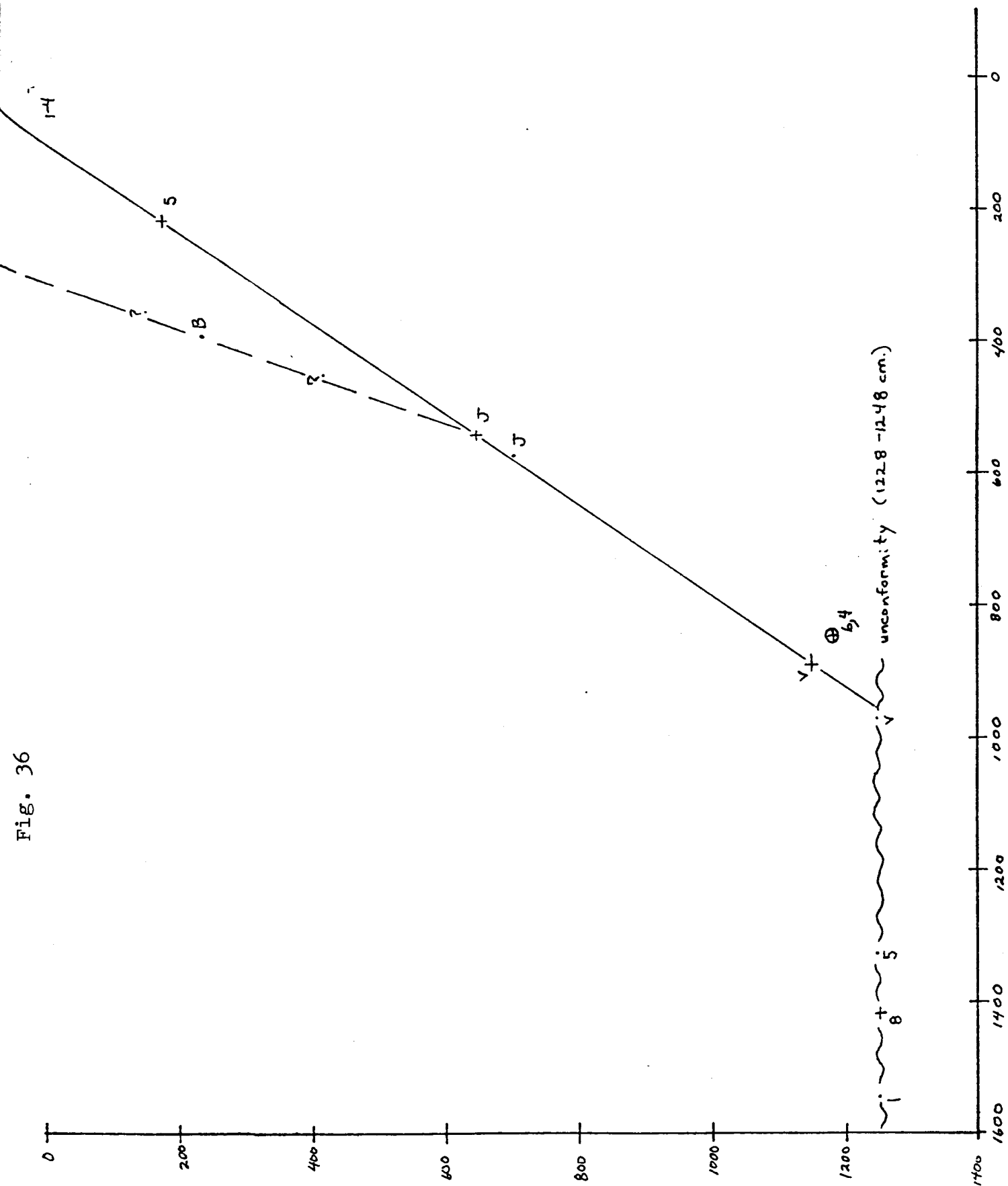
IO1176-68

1-4
+



IO1176-68

Fig. 36



IO1176-67

IO1176-68

Fig. 37

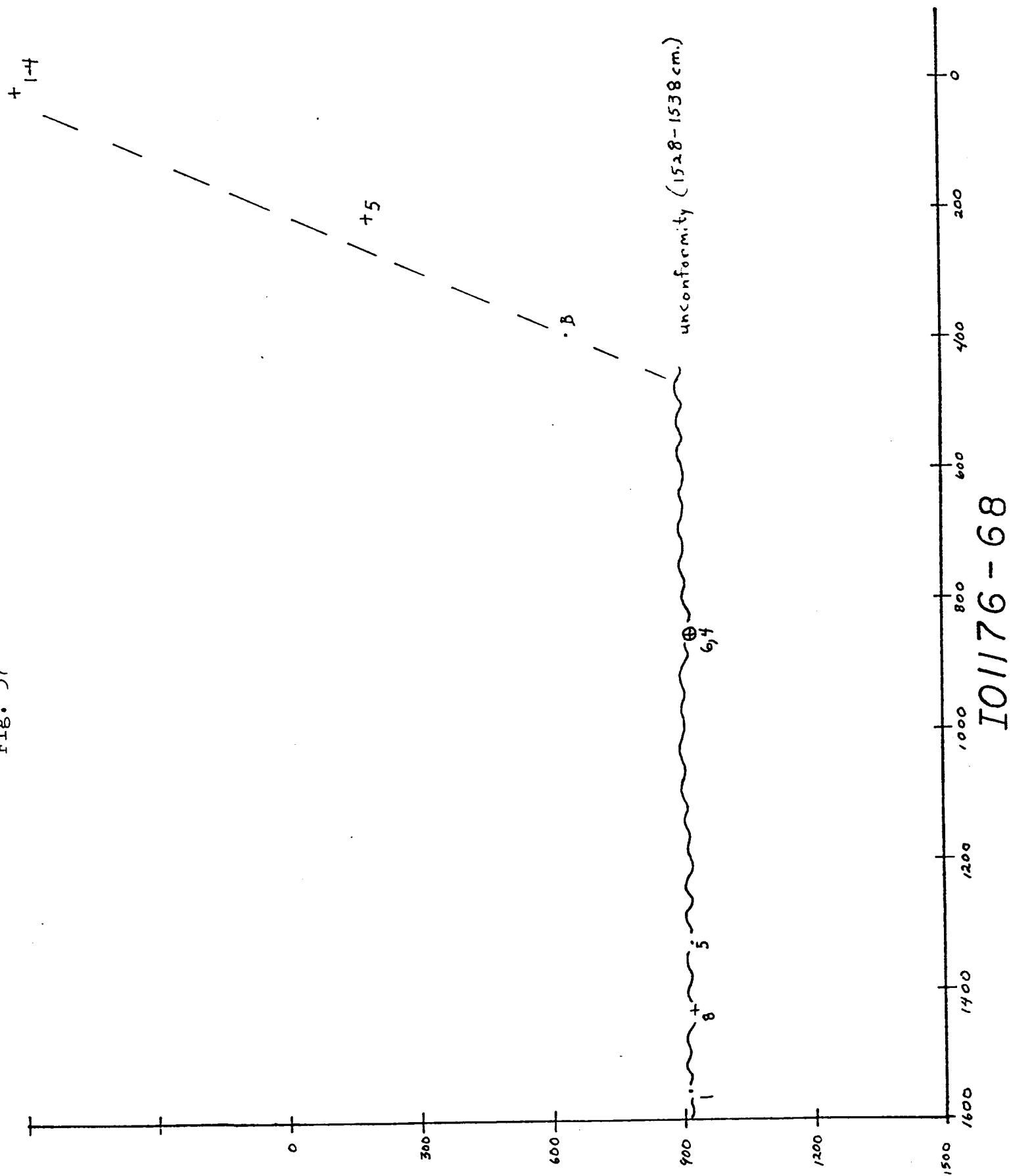
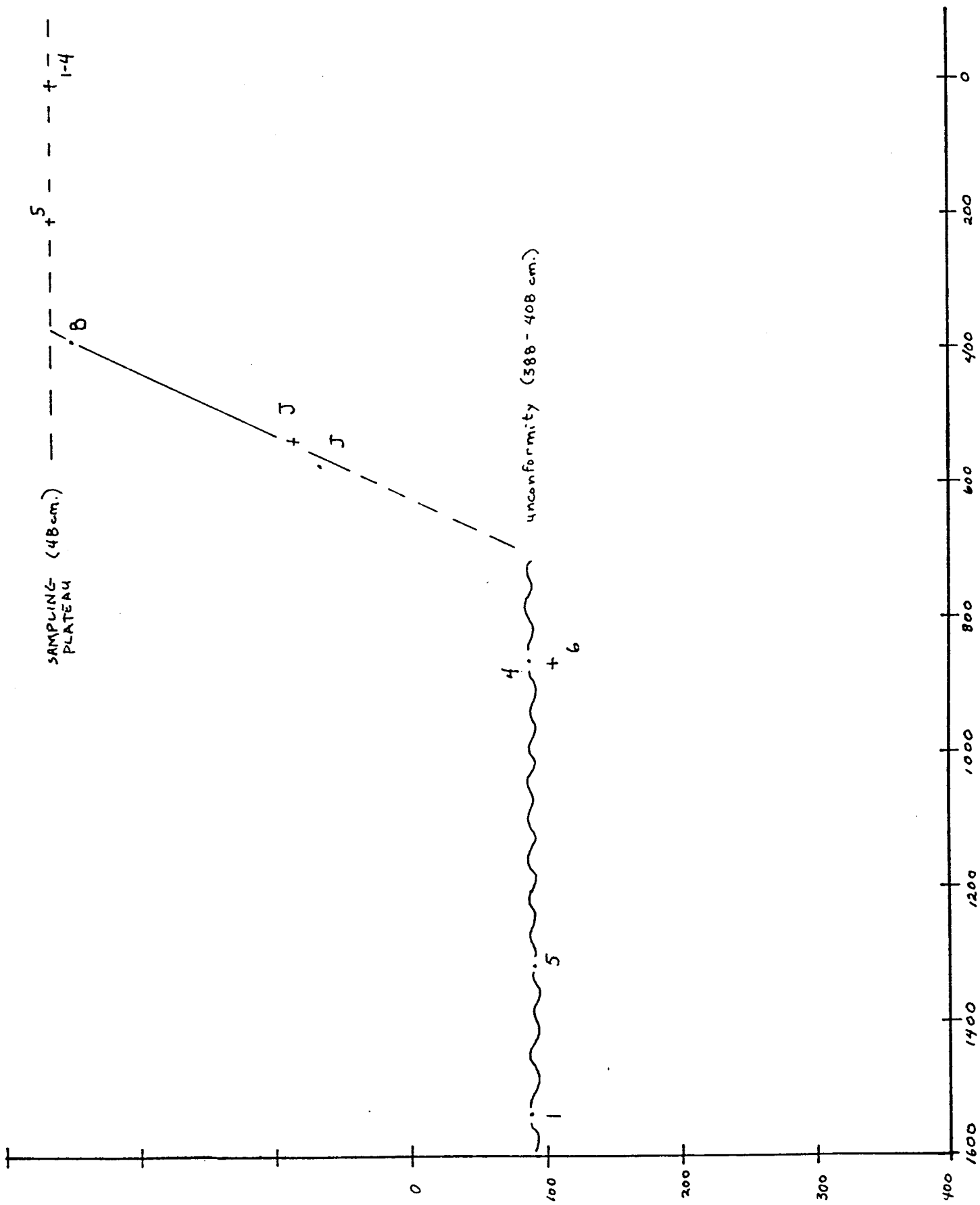


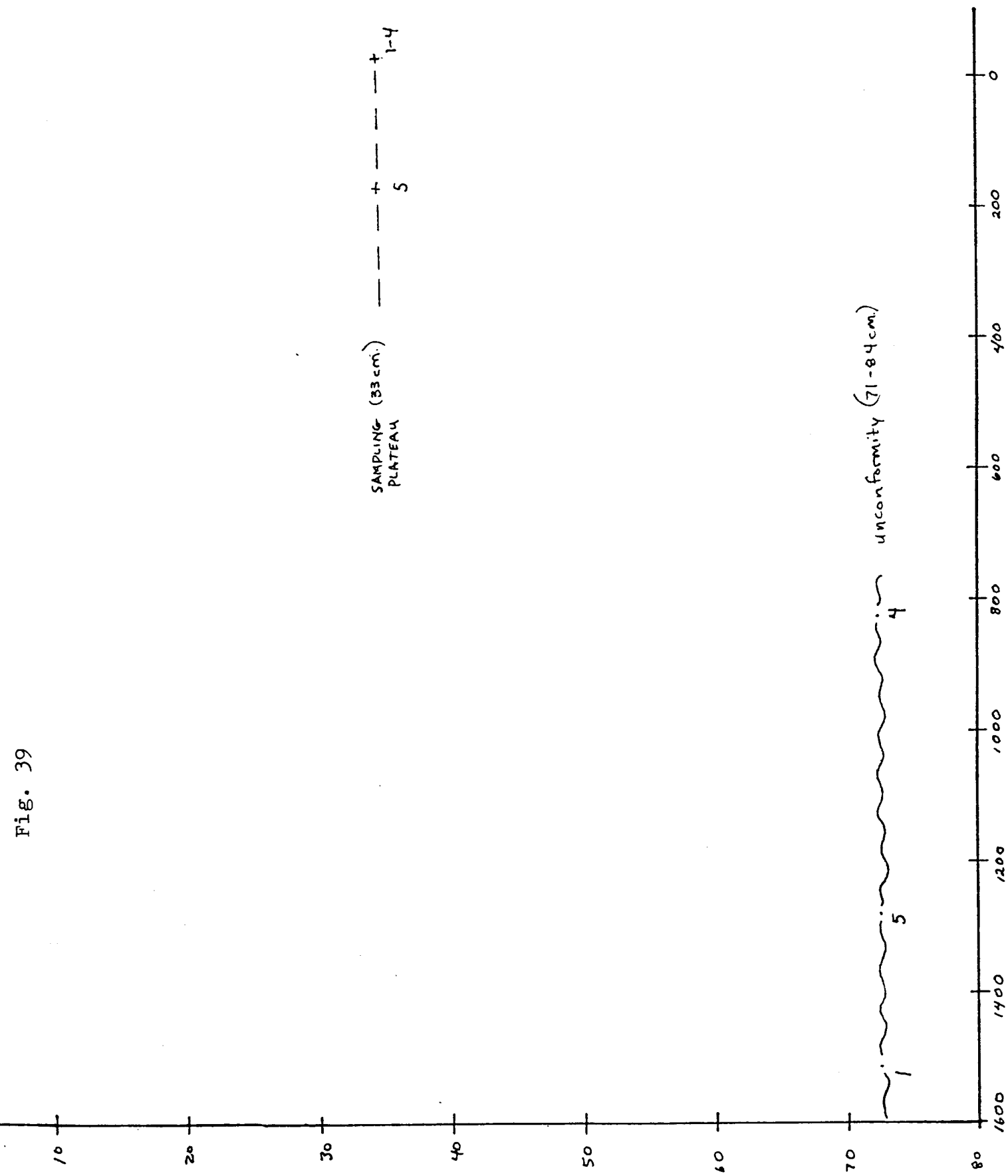
Fig. 38



IO1176-71

IO1176-68

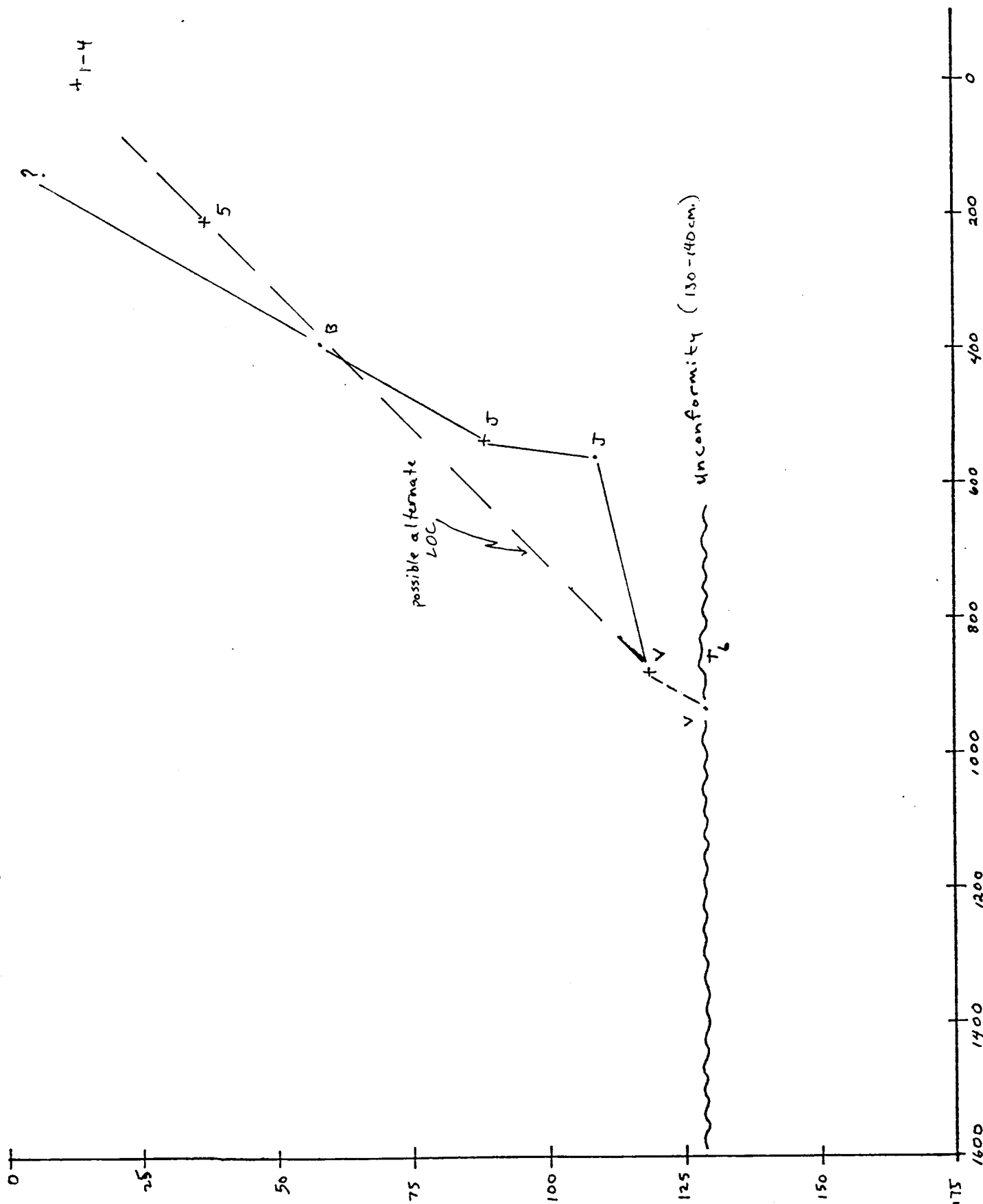
Fig. 39



IO1176-73

IO1176-68

Fig. 40



IO1176-76

IO1176-68

Fig. 41.

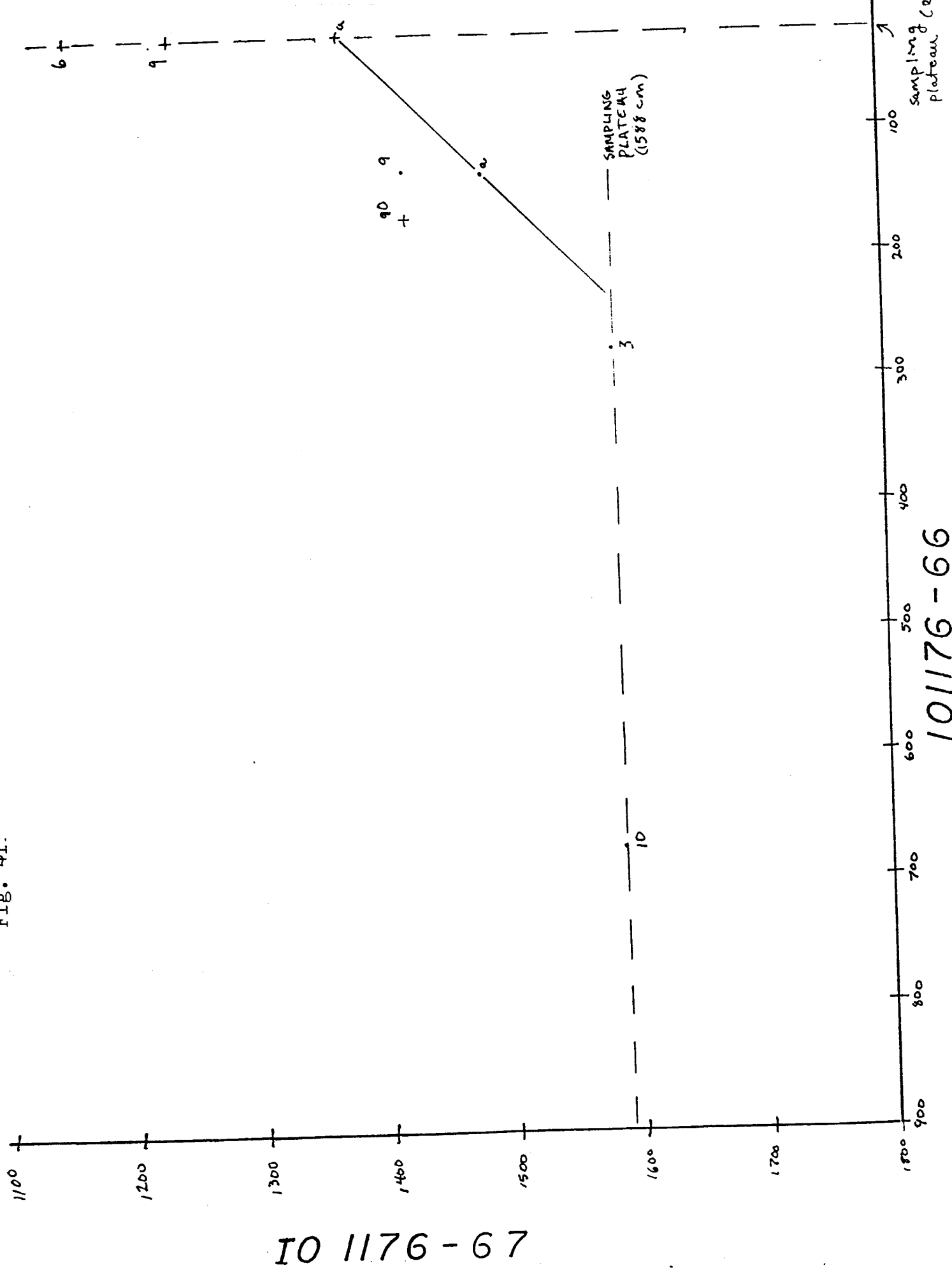
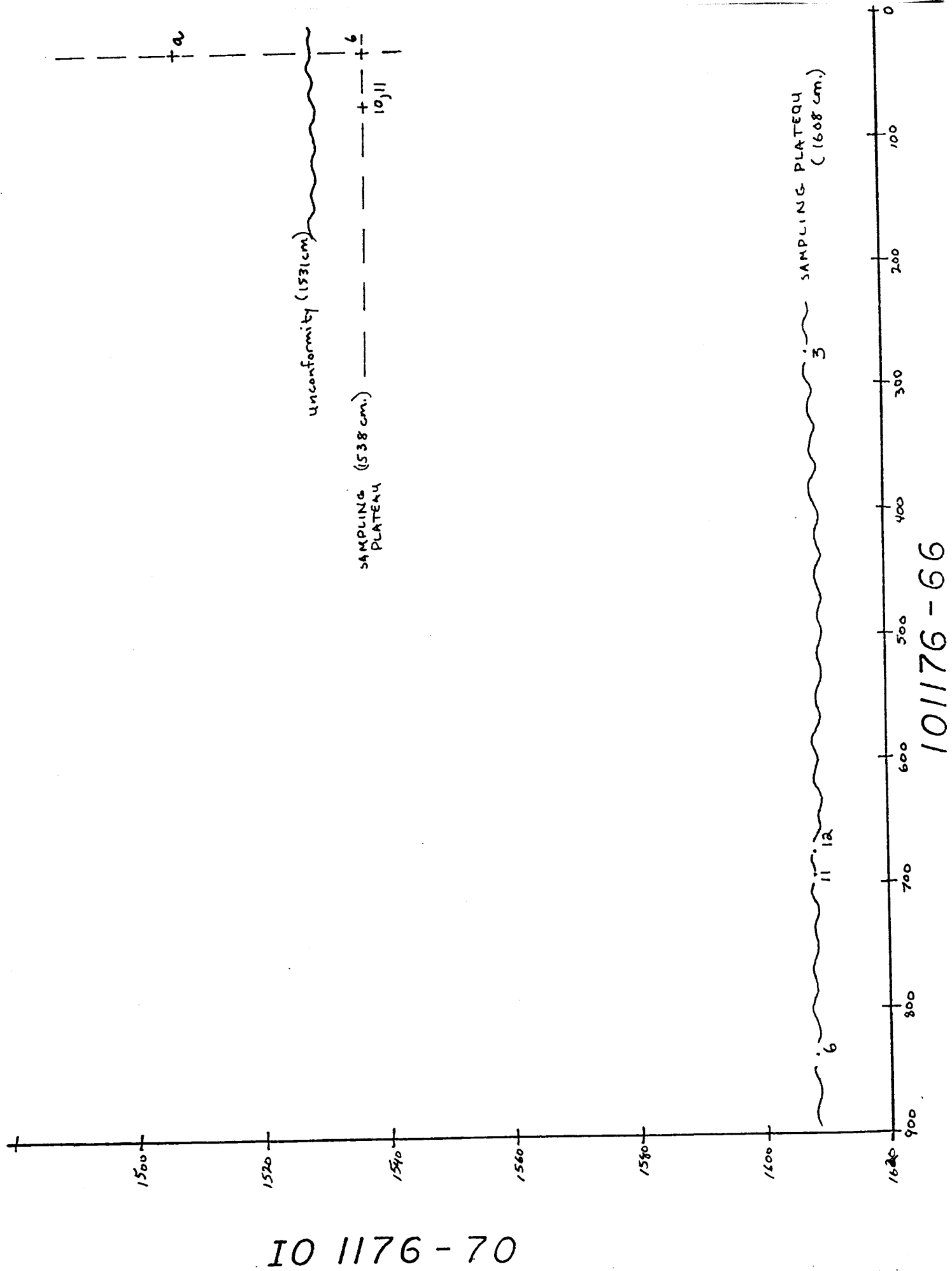


fig. 42

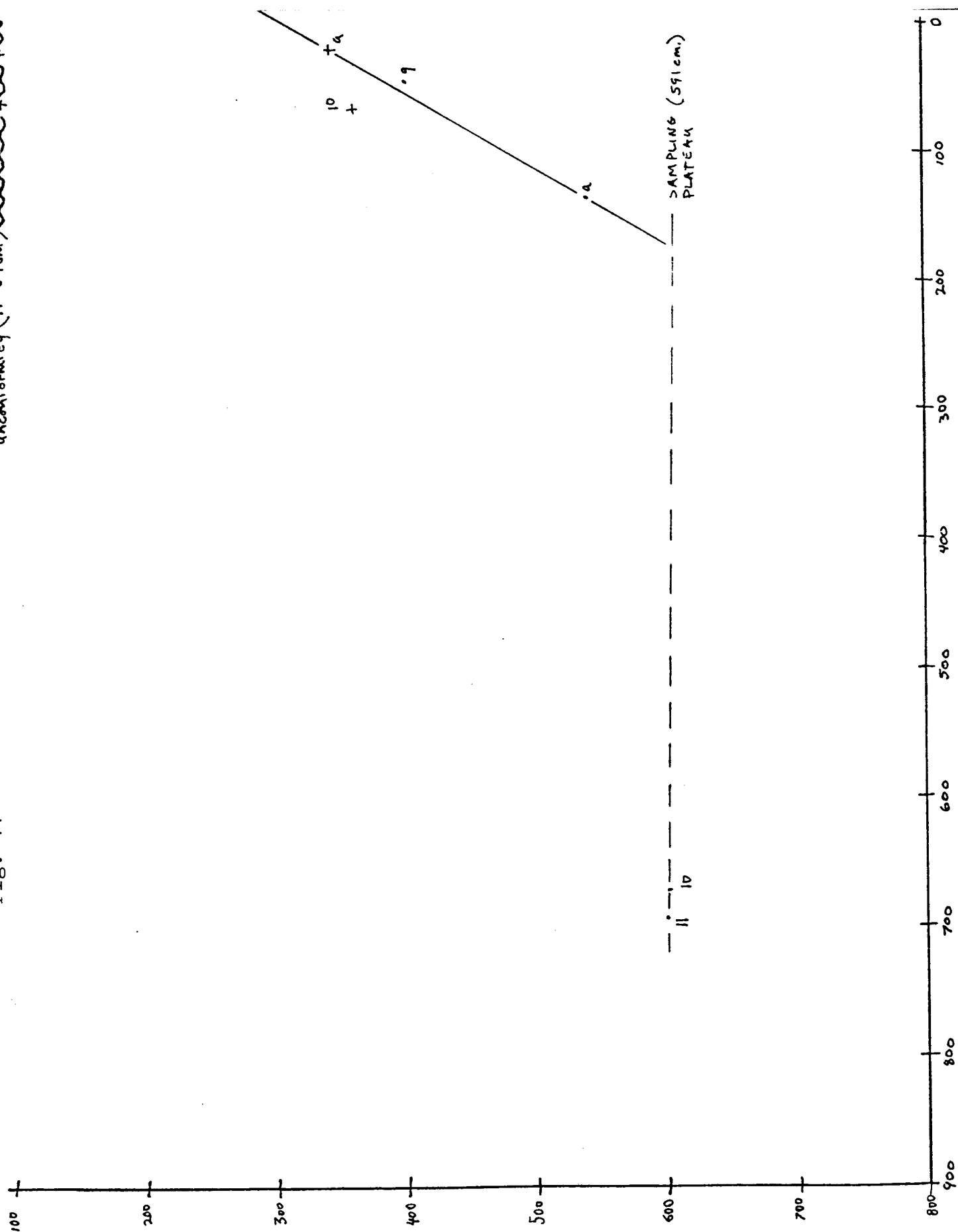


IO 1176-71



Fig. 44

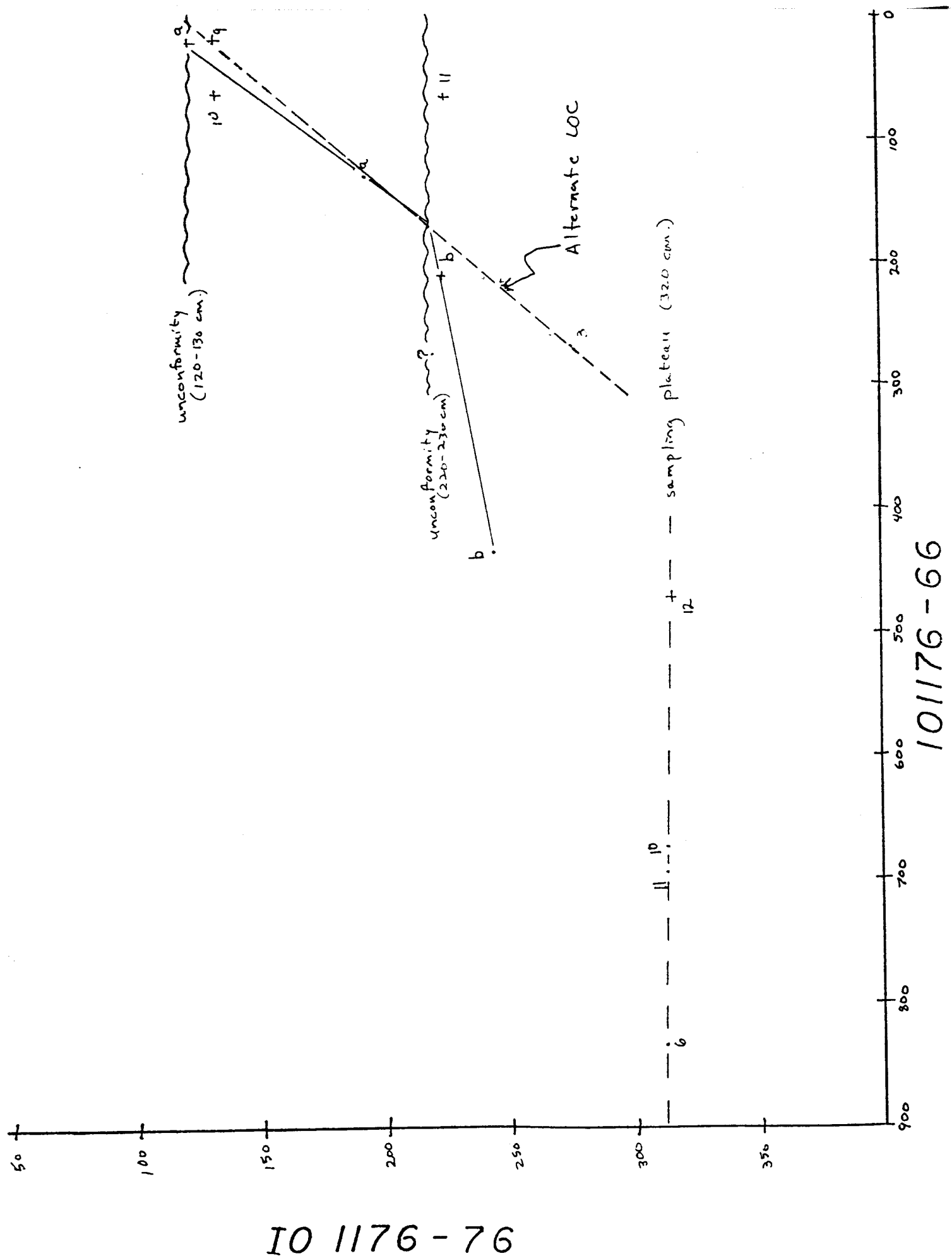
unconformity (71-84 cm) 11 + 6.9



IO 1176 - 73

101176-66

Fig. 45



Bibliography

- Anderson, John B., Clark H.c., and Weaver, Fred M., 1977, Sediments and Sedimentary Processes on High Latitude Continental Shelves, Offshore Technology Conference, Houston, p. 91-93.
- Chapuis, Ralph A., 1974, Sediment Response to Climatic Change as Recorded in Deep Sea Piston Cores from the Southern Ocean, Department of Geology, Florida State University, Contribution No. 38, p. 25-28, 33-36, 39-42.
- Ciesielski, Paul F., 1974, Silicoflagellate Paleotemperature Curve for the Southern Ocean, Antarctic Journal, v. IX, no. 5, p. 269-270.
- _____, and Weaver, Fred M., 1975, Southern Ocean Pliocene Paleotemperatures Based on Silicoflagellates from Deep Sea Cores, Antarctic Journal, Sept. - Oct., p. 295-296.
- _____, _____, 1974, Early Pliocene Temperture Changes in the Antarctic Seas, Geology, October, p. 511-515.
- Fisher, Victor A., 1968, The Southern Ocean 700,000 Years Ago, Department of Geology, Florida State University, Contribution No. 28, p. 1-6, 18-25.
- Goodell, H.G. et.al., 1973, Marine Sediments of the Southern Ocean, Antarctic Map Folio Serice, American Geographical Society, New York, pp. 1-7.
- Goodell, H.G., Watkins, N.D., Mather, T.T. and Koster, S., 1968, The Antarctic Glacial History Recorded in Sediments of the Southern Ocean: Paleogeography, Paleoclimatology, Paleoecology, v. 5, p. 41-62.
- Gordon, Arnold L., 1971, Recent Physical Oceanographic Studies of Antarctic Waters, Research in the Antarctic, pp. 609 - 627.
- _____, 1973, Physical Oceanography, Antarctic Journal, v. VIII, no. 3, pp. 62 - 68.
- Hays, James D., 1965, Radiolaria and Late Tertiary and Quaternary History of Antarctic Seas, Biology of the Antarctic Seas II, Antarctic Research Series 5, p. 125.
- Kennett, J.P. and Fillion, R.H., 1970, Micropaleontological and Associated Studies of Southern Ocean Deep Sea Cores, Antarctic Journal, v. V., no. 5, p. 181.
- Kurtz, D.D., et. al., 1979, Glacial Marine Sedimentation: Relationship to the Distribution of Sediment Geotechnical Properties of High Latitude Continental Margins, offshore Technical Conference, Houston, p. 685.

Bibliography (cont.)

- Ledbetter, Michael T., and Watkins, Norman D., 1978, Separation of Primary Ice-Rafter Debris from Lag Deposits Utilizing Manganese Micronodule Accumulation Rates in Abyssal Sediments of the Southern Ocean, GSA Bull., v. 89, p. 1619.
- Lisitzin, Alexander P., 1972, Sedimentation in the World Ocean, Society of Economic Paleontologist and Mineralogists, Special Publication no. 17, pp. 108 - 109, 135 - 163.
- McCollum, D.W., 1975, Diatom Stratigraphy of the Southern Ocean, DSDP Leg 28, pp. 516 0 519 and 530.
- Miller, F.X., 1977, The Graphic Correlation Method in Biostratigraphy. - Dowdan, Hutchinson and Ross, pp. 165 - 186, Stroudsburg.
- Opdyke, Neil D., 1966, Paleomagnetic Study of Antarctic Deep Sea Cores, Science, v. 154, no. 3748, pp. 349 - 357.
- , 1972, Paleomagnetism of Deep Sea Cores, Reviews of Geophysics and Space Science, v. 10, No. 1, pp. 213-249.
- Sclater, John G., et al., 1977, Islas Orcadas Cruise 11, Buenos Aires to Cape Town, Antarctic Journal, October 1977, pp. 62 - 65.
- Shaw, Alan B., 1964, Time in Stratigraphy, McGraw - Hill Book Company, New York, p. 119 - 154.
- Sweet, Walter C., 1979, Late Ordovician Conodonts and Biostratigraphy of the Western Midcontinent Province, Birgham Young University Geology Studies, v. 26, no. 305, pp. 50 - 54.
- Warnke, Detlef A., 1970, Glacial Erosion, Ice Rafting, and Glacial - Marine Sediments: Antarctica and the Southern Ocean, American Journal of Science, vol. 269, October, pp. 276 - 294.
- Watkins, Norman D., Keany, John, Ledbetter, Michael T., and Ter-Chien Huang, 1974, Antarctic - Glacial History from Analysis of Ice - Rafter Deposits in Marine Sediments: New Model and Initial Tests, Science, v. 186, pp. 533 - 534.
- , and Kennett, J.P., 1970, Paleomagnetic and Associated Studies of Eltanin Deep-Sea Sedimentary Cores, Antarctic Journal, v. 5, no. 5, p. 183.
- Weaver, Fred M., 1973, Pliocene Paleoclimatic and Paleoglacial History of East Antarctica Recorded in Deep Sea Piston Cores, Department of Geology, Florida State University, Contribution No., 35, pp. 19 - 31.

Bibliography (cont.)

_____, and Ciesielski, Paul F., 1974, Pliocene
Paleotemperatures and Regional Correlations Southern Ocean,
Antarctic Journal, v. IX, no. 5, pp. 251 - 253.

_____, 1976, Pliocene Diatom Biostratigraphy, pp.
40 - 42.